Results of Life Sciences DSOs Conducted Aboard the Space Shuttle 1988-1990

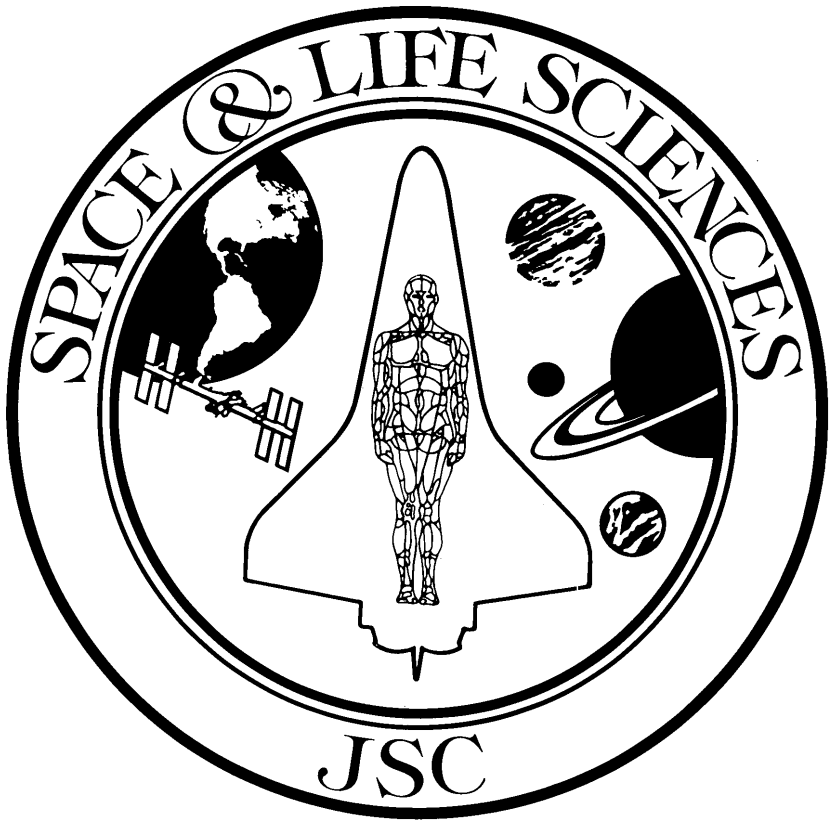

January 1991

Table of Contents

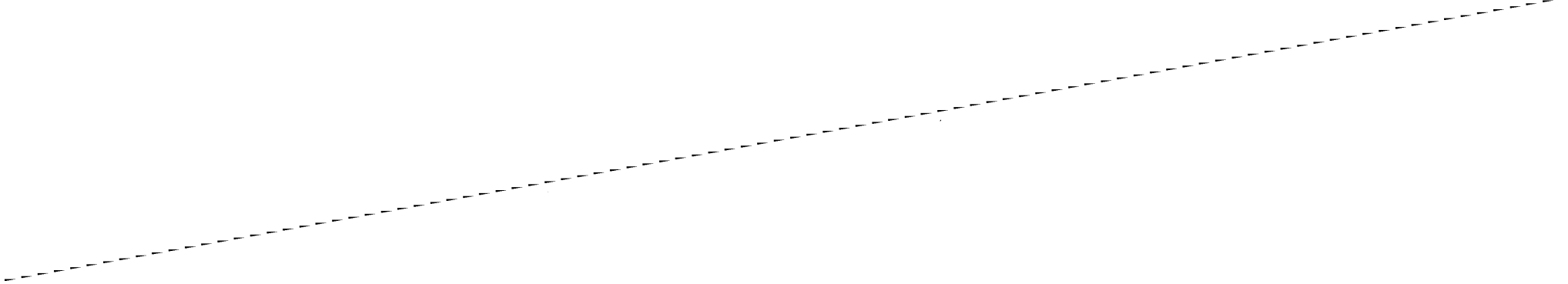

Introduction

BIOMEDICAL DETAILED SUPPLEMENTARY OBJECTIVES

On September 29, 1988, NASA returned to flight with the launch of *Discovery*, STS-26. On this flight and on subsequent missions, several biomedical Detailed Supplementary Objective (DSO) investigations were completed. This document reports the results of these investigations.

Characterizing the physiological consequences of space flight is the mandate of two branches of the Medical Sciences Division. The Space Biomedical Research Institute (SBRI) and the Biomedical Operations and Research Branch are dedicated to the development of operational countermeasures that protect crew health and performance. Early investigations focused on adaptation to microgravity and specifically space motion sickness, continuing the studies begun during the Apollo and Skylab programs. More recently, investigations have been expanded to include determinations of the extent of cardiovascular deconditioning, muscle loss, changes in coordination and balance strategies, radiation exposure, and changes in the body's biochemistry and pharmacokinetics. These and other investigations will increase our understanding of how humans adapt to the space environment.

The Medical Sciences Flight Projects Office implements investigations through the DSO process. DSO investigations are supplementary to the primary Shuttle payload, performed voluntarily by the crew and designed to require minimal crew time, power, and stowage. Biomedical DSOs focus on operational concerns and involve data collection before, during, and after flight. Ground-based studies, sometimes including bedrest simulations of microgravity, precede in-flight research to make optimal use of valuable crew time. Various biomedical DSOs have been manifested on every Shuttle mission to date.

In February 1989 biomedical DSOs received a new focus and increased priority with the creation of the Extended Duration Orbiter (EDO) Program. This program was established by the Shuttle Program Office to extend Shuttle missions to provide more time for microgravity experiments and for construction of Space Station *Freedom*. Level I PRCB Directive H50504 authorized modifications to *Columbia* for missions of up to 16 days and scars to *Endeavour* for missions of up to 28 days. The longest Shuttle mission to date was the 11-day flight of STS-32 *Columbia*, made in January 1990.

Shuttle missions of 13-28 days are predicted to present a new challenge to human physiology. Although Skylab astronauts flew missions of up to 84 days, they were not required to pilot and land the spacecraft. Extended duration Shuttle missions necessitate immediate readaptation to a gravity environment such that the crew can safely land the Orbiter and egress rapidly if necessary.

The Extended Duration Orbiter Medical Project (EDOMP) was developed to address the physiological concerns raised by extending Shuttle mission duration. EDOMP investigations focus on orthostatic intolerance, disequilibrium, and inhibited muscle performance that may occur postflight. The EDOMP will provide recommendations to the Shuttle Program about the severity of these problems, proposed countermeasures, and recommendations for the maintenance of a habitable environment on the Shuttle.

Note: The DSOs completed before September 1988 are described in NASA Technical Memorandum 58280. Appendix A provides a complete listing of biomedical DSO numbers and titles.

Section One: Orthostatic Function

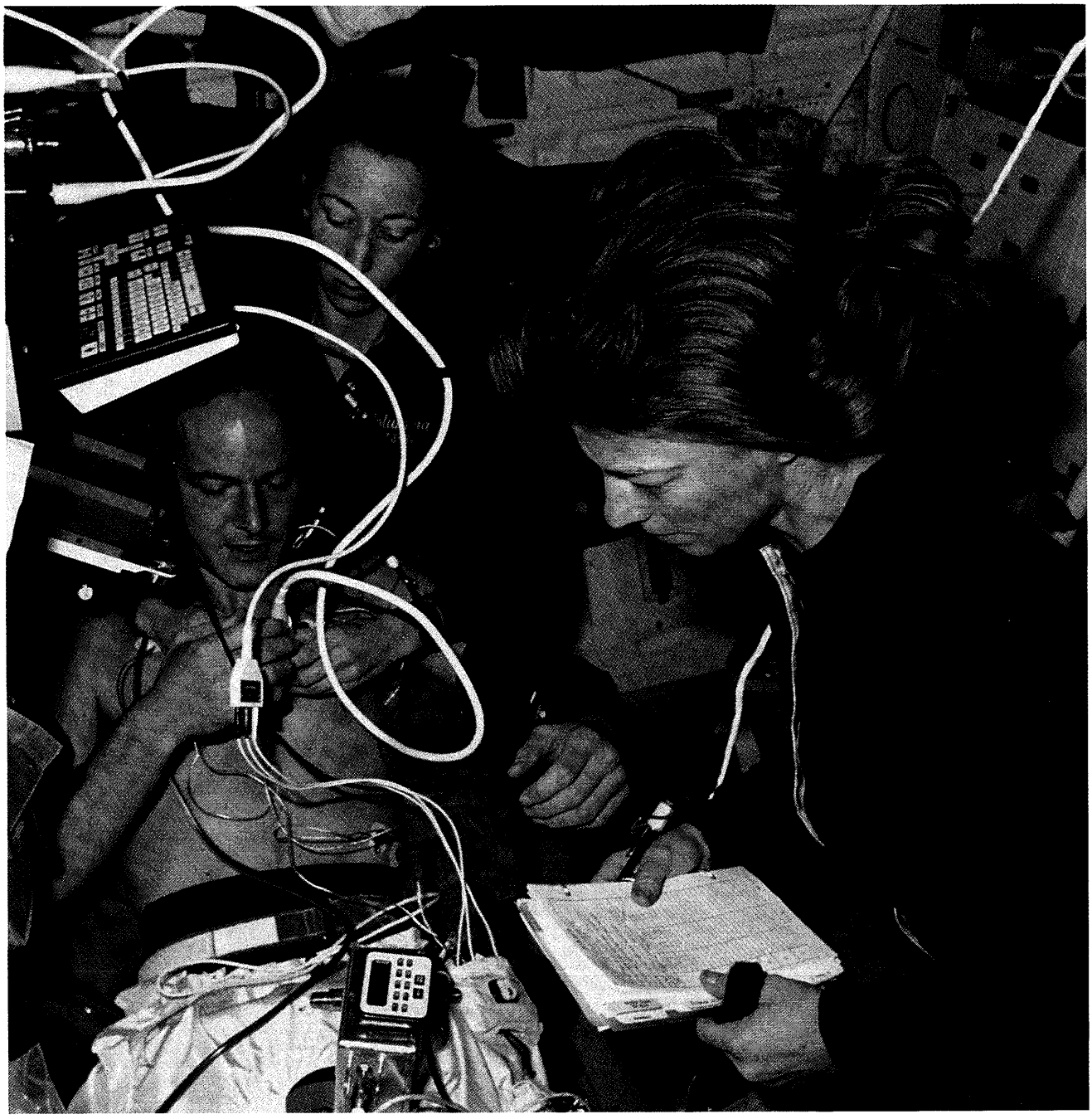

Lower Body Negative Pressure (LBNP). Orthostatic intolerance following space flight causes many crewmembers to feel dizzy or to faint when they stand. LBNP is being tested for its efficacy in counteracting orthostatic intolerance. This picture shows crewmembers from STS-32 monitoring heart rate and blood pressure and performing echocardiography during LBNP.

DSO 460: Changes in Total Body Water During Space Flight

Investigators: Carolyn S. Leach, Ph.D.; L. Daniel Inners, Ph.D.; John B. Charles, Ph.D.

INTRODUCTION

This investigation was designed to measure, by means of direct in-flight assessment, the changes in total body water (TBW) occurring in humans as a consequence of several days' exposure to microgravity on the Space Shuttle. TBW measurements provide important data for several cardiovascular and fluid/electrolyte experiments making up the science payload for the dedicated life sciences missions (SLS-1 and SLS-2). According to several models, changes in TBW are predicted to parallel fluid shifts. Therefore, changes in TBW can be used as a convenient indicator of the time course of adaptation to weightlessness. Because of its ease of measurement, TBW was the method of choice to verify in flight the timing proposed for fluid compartment measurements planned for SLS-1, thus increasing the investigators' confidence in the protocol for a core experiment in a complex and costly scientific payload.

The investigators of this study hypothesize that TBW decreases by 1.5-2.0 liters within the first three days of weightlessness and is maintained at that level for the duration of the exposure.

Fluid shifts and transient increases in central venous pressure occurring during the first few hours of weightlessness have been identified as the probable causes of early adaptive responses of the human cardiovascular and renal/endocrine systems (Greenleaf, 1986; Leach et al., 1970; Nixon et al., 1979). Fluid shifts have also been implicated as possible contributory factors in altered vestibular function. Despite this role in triggering the response of major pathways of adaptation, the timing and extent of the exchanges of water and electrolytes between compartments have not been studied.

Although exposure to weightlessness has long been known to affect the distribution of body fluids, previous measurements of TBW have been confined to preflight and postflight periods. Leach and Rambaut (1977) measured TBW pre- and postflight on Skylab missions 2, 3, and 4 on a total of nine subjects, using tritiated water as the tracer. Comparison of pre- and postflight measurements indicated a mean decrease of 1.7% in postflight TBW relative to preflight.

Many of the changes that are observed after prolonged bedrest mimic those observed after exposure to microgravity. TBW has been measured in a number of bedrest studies. In recent work, Fortney et al. (1991) observed a progressive decrease in TBW during four weeks of bedrest. The average loss by the fourth week was 3.2%.

Schoeller et al. (1980) have developed an isotope dilution technique for TBW based on water labeled with a stable isotope of oxygen, ^{18}O, as the tracer. The precision of the method as measured by the coefficient of variation is reported as approximately 2% (Schoeller et al., 1980). This method offers a number of advantages which make it nearly ideal for space-flight applications. For instance, ^{18}O does not exchange appreciably with oxygen in biological macromolecules. Also, since ^{18}O is a stable isotope, its use does not expose the crew to additional radiation, and ^{18}O has virtually no physiological effect in the dosages employed for TBW determinations.

Macromolecular exchange would be detected as an effective dilution of the ^{18}O and would result in an overestimation of TBW. Indeed, measurements made with deuterated or tritiated water are typically about 3% higher than those made with ^{18}O-labeled water (Schoeller et al., 1980). For this reason, measurements made with ^{18}O are generally regarded as providing a more accurate estimate of TBW than that provided by isotopes of hydrogen.

With the development of noninvasive techniques employing stable isotopes and using saliva (Schoeller, 1982) instead of urine or plasma samples, it is now possible to make direct, precise measurements of TBW at almost any time during a mission while

Accepted for publ. by *J. Clin. Pharm.*

making very minor demands on crew and spacecraft resources. These newer methods preserve the 3- to 6-hour resolution of the earlier techniques based on ^{2}H or ^{3}H labeled water.

PROCEDURES

Subjects

The subjects for this experiment were five male crewmembers of Space Shuttle missions STS-61C and STS-26. Height, age, percent body fat, and postflight body mass are summarized in Figure 1 below.

Height (cm)	Body Mass (kg)	% Body Fat	Age
178.5	80.6	14.7	39
170.0	67.1	14.2	35
177.7	70.8	14.4	43
181.4	70.0	14.4	43
179.3	71.9	6.3	40

Figure 1. Subject profiles. Tabulated are height, body mass, percent body fat, and age for the five male subjects who participated in this experiment. All data except body mass were recorded as part of the previous annual physical examination for each crewman. Body mass was taken from R+0 postflight data.

Protocol

The nominal schedule of the study is summarized below in Figure 2. The design included no special control group or control experiment. Instead, all in-flight and postflight data were compared to preflight baseline data. Because of a delay in the launch of STS 61-C and the unavailability of some crewmembers during the immediate pre- and postflight periods, the first preflight measurements were at L-31 to L-30, while some measurements were missed entirely. The actual schedule of measurements is indicated in Figure 3.

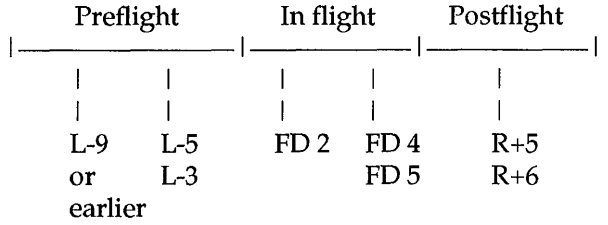

Figure 2. Nominal schedule of experimental sessions for measurement of TBW.

Subject	Hour	L-31 L-30 L-9	L-3 L-5	FD 2	FD 4 FD 5	R+5 R+6
1	3	41.6	43.1	39.0	40.7	43.5
	5		43.4	38.5		
2	3	41.9	43.2	45.3	40.9	43.1
	5	43.8	44.6	43.6	45.3	
3	3	47.0		43.3	46.1	
	5	46.9		43.7	45.2	
4	3	42.4	42.3	40.6	41.3	43.5
	5	42.7	44.6	40.7	42.5	45.5
5	3	47.3	46.9	49.4	47.3	
	5	49.1	48.7	49.3	47.6	48.8

Figure 3. TBW measurements, STS-61C and STS-26, adjusted to 70 kg body mass. TBW (kg) was measured for five crewmen on the mission days indicated. This is the unbalanced data matrix used for the maximum likelihood analysis (BMDP3V).

TBW was measured by the isotope dilution technique utilizing ^{18}O-labeled water as the tracer. Briefly, this method requires the ingestion of a known mass of ^{18}O water followed by sampling of representative body fluids such as urine or saliva over a period of several hours following the administration of the tracer. The protocol for a typical measurement is shown in Figure 4.

The measurements were initiated immediately after a sleep cycle with the crewmember in a fasted state. After the collection of background samples, the dose was consumed, followed by at least 50 ml of fruit juice or galley water. The subject was allowed to consume a light breakfast 30 minutes after dose administration and was requested to abstain from caffeine-containing

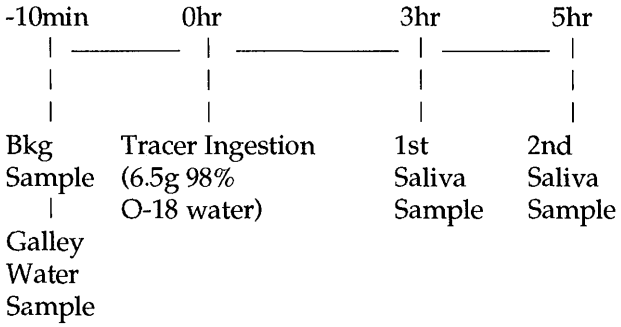

Figure 4. Schematic representation of a typical in-flight experiment session.

beverages for the duration of the experiment. All food consumed during the experiment was recorded on a log sheet.

Samples of galley water were collected on Flight Day 2 (FD) and FD 4/FD 5. The experimental design called for galley water sampling on all days on which TBW was measured because water sampled from the galley on several occasions, including STS-51D, was found to be enriched in ^{18}O.

Dental cotton rolls were used for saliva collection. All cotton used in the experiment was from one batch, and all were packaged individually in vapor-tight, 10-ml glass lyophilization vials (Wheaton) in a single operation lasting about 30 minutes. Once closed, the sample vials were opened only for sample collection and sample removal. The sample collection vials were packaged in a Nomex kit similar to that shown in Figure 5 for in-flight stowage.

The ^{18}O water (95-98%) was purchased from Mound Laboratories, Miamisburg, OH. The dose was approximately 6.5 g. The labeled water was filtered directly into a sealed, sterile syringe vial through a nonsterile 13-mm Millipore Type HA filter (0.45 µm pore) using a disposable filter holder. The syringe used was a two-piece disposable type manufactured by IMS (El Monte, CA), consisting of a glass vial containing the dose and a separate plastic injector with a lavage tip (Figure 5a,b). This syringe was weighed three times: empty, filled with the labeled water, and after use to determine the dose delivered and the amount remaining in the syringe (usually about 0.3 ml). Syringes were stowed in a Nomex kit. To ingest the dose, a crewmember removed the protective caps, assembled the syringe, and delivered the contents directly into his mouth. Used dose syringes

(a) Beverage containers, saliva sample vials, and tracer kit components with tracer syringe in stowed configuration

(b) Assembled tracer syringe containing approximately 6.5g ^{18}O water ready for administration

Figures 5a and b. The illustrations show a kit constructed of Nomex fabric, a dose syringe with lavage tip, syringe cap, two saliva sample vials, and two beverage containers used to collect Shuttle galley water samples. A similar, separate kit was used for stowing the saliva sample vials.

were left assembled with the tips capped and stowed in an empty food locker to minimize the chance of contamination of the samples by highly-enriched ^{18}O water vapor.

Test subjects collected saliva by placing a dental cotton roll under the tongue for several minutes and then replacing the saturated cotton in the vial. It was determined in supporting studies that samples could be stored for more than a week at ambient temperature without affecting isotope content, provided they were protected from evaporation. Sample vials were replaced in the original kit and stowed in a middeck

locker different from the one for used dose syringes. As mentioned above, this precaution was taken to minimize the possibility of accidental contamination of the sample vial contents. The samples were frozen at -70° C after being returned to the laboratory.

Oxygen-18 Analysis

Analyses of the samples were carried out in ground-based facilities of the USDA/ARS Children's Nutrition Research Center, Department of Pediatrics, Baylor College of Medicine and Texas Children's Hospital, Houston, TX. Two methods of analysis were used because of the advance in technology between the two missions on which data were gathered.

STS-61C: Frozen samples were thawed, and approximately 0.3-0.5 g were transferred to preweighed 20-ml Vacutainer serum tubes using disposable plastic tuberculin syringes. The tubes were reweighed to determine the mass of the sample. The tubes were then filled with 5% carbon dioxide, 95% nitrogen and equilibrated for 48-72 hours at 25° C. The cryogenically purified carbon dioxide was analyzed using a Model 3-60 Gas Isotope Ratio Mass Spectrometer (Nuclide Corp., University Park, PA). Details of the analytic procedure and calculation are found in Schoeller et al. (1980, 1982).

STS-26: Samples were analyzed using a microchemical technique requiring only 100 µL of sample (Wong et al., 1987). The method employed a modified ISOPREP-18 (VG Isogas Ltd., Cheshire, England) in which 100 µL of the aqueous sample was equilibrated with carbon dioxide for 10 h at 25° C, 300 mbar. The carbon dioxide was cryogenically purified and introduced into a VG SIRA-12 gas-isotope-ratio mass spectrometer (VG Isogas Ltd.) for determination of ^{18}O to ^{16}O ratio.

RESULTS

TBW measurements adjusted to 70 kg body mass are summarized in Figure 3. Body mass at R+0 (Figure 1) was used as a "normalizing" factor. The gaps in the data represent missing saliva samples, late samples, and several values which were unexpectedly high, perhaps owing to inadvertent dilution of the saliva prior to collection. The data for the five subjects have been grouped into five mission periods: (1) data collected at L-9 or earlier, (2) data collected just before launch at L-5 to L-3, (3) data for Flight Day 2 (approximately 22-26 hours Mission Elapsed Time (MET)), (4) data from FD 4 to 5 (68-96 hours MET), and (5) data collected 5-6 days after landing. The values in the exhibit were not corrected for fluid intake. Because there was no means of measuring body mass in flight on either mission, the ratio of TBW to body mass could not be analyzed.

Figure 3 data were analyzed without further reduction according to the general mixed model analysis of variance, utilizing BMDP module BMDP3V (BMDP Statistical Software, Los Angeles, CA). Subject was treated as a random variable, while mission day and sample time (i.e., 3-hour or 5-hour) were regarded as fixed variables. In this, as well as subsequent analyses, mission day was regarded as a fixed treatment effect, and the null hypothesis was formulated to test mission period as the source of variance. BMDP3V was chosen for the initial analysis because it can accept data from unbalanced models of essentially arbitrary form (Jennrich and Sampson, 1985).

An examination of Figure 3 will reveal that complete data were available for four of the subjects. This data set is presented in Figure 6, in which TBW entries for 3 hr and 5 hr, where both were available, have been averaged to construct a balanced layout. These data were analyzed by conventional repeated measures analysis of variance (Winer, 1971). Also presented in Figure 6 are the means, unbiased variances, and standard errors of the mean for TBW measurements made during each of the five observation periods. In Figure 7, mean TBW has been plotted against time, represented by the five mission periods. The error brackets delineate the standard error of the mean for each mission period.

It is clear from Figures 6 and 7 that the variability on FD 2 is much greater than on any other day. Since homogeneity of variance is one of the requirements for valid application of ANOVA, the data were tested for homoscedasticity. Both the F-max test (Sokal and Rohlf, 1981) and Bartlett's test (Ostle and Malone, 1988) indicate that the variance on FD 2 is not significantly different from that observed on other mission days.

The results of all analyses are summarized in Figure 8. The results of both the maximum likelihood approach and the repeated measures analysis of variance indicate differences significant at the 10% level when all mission periods are included. If FD 2

Subject	L-9 L-30 L-31	L-3 L-5	FD 2	FD 4 FD 5	R+5 R+6
1	41.6	43.2	38.7	40.7	43.5
2	42.9	43.9	44.5	40.9	44.2
4	42.5	43.5	40.7	41.9	44.5
5	48.2	47.8	49.3	47.4	48.8
Mean	43.8	44.6	43.3	42.7	45.2
Unbiased Var.	8.89	4.64	21.84	10.22	5.88
Std. Error	1.49	1.08	2.34	1.60	1.21

Figure 6. TBW measurements for four subjects with complete data. Values at 3 hr and 5 hr have been averaged and adjusted to a body mass of 70 kg. All values are in kg except the variance.

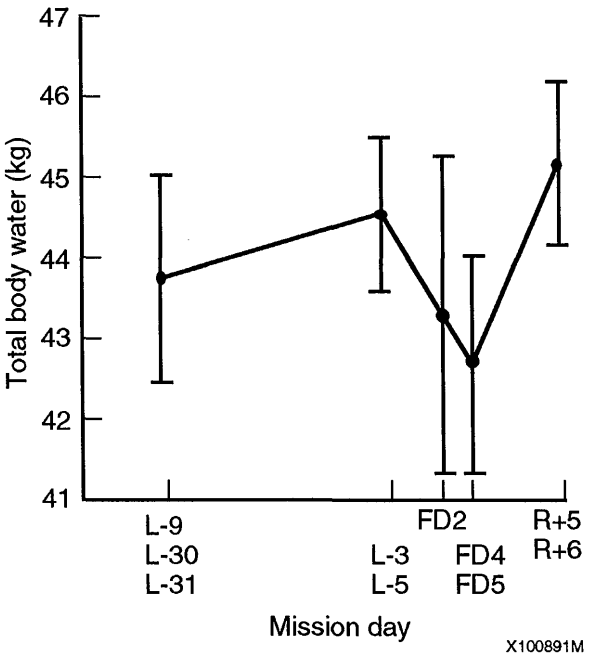

Figure 7. Mean TBW during space flight. Data are adjusted to 70 kg body mass. The error bars represent the standard error of the mean of the four observations on each of the five mission periods.

Data Set	Analytical Method	Test Statistic	df	UTP
5 Subjects 5 Days 2 Hours	Likelihood Ratio Test (BMDP 3V) Statistic: Chi-Square	8.59	4	0.072
5 Subjects 4 Days 2 Hours	Likelihood Ratio Test (BMDP 3V) Statistic: Chi-Square	19.57	3	0.0002
4 Subjects 5 Days	Repeated Measures Analysis of Variance Statistic: F	2.63	4,12	0.087
4 Subjects 4 Days	Repeated Measures Analysis of Variance Statistic: F	15.07	3,9	0.0007

Figure 8. Statistical analysis of TBW data. UTP is the upper tail probability for the statistic indicated. All measurements were adjusted to 70 kg body mass. The second and fourth entries list the result when FD 2 measurements are dropped from the data set.

is dropped from the analysis, the differences are significant at the 0.1% level.

In order to identify the differences, the method of orthogonal contrasts (Hicks, 1982) was used. This method requires all contrasts to be independent and to be formulated prior to examination of the data. A uniform approach was adopted to formulate these contrasts: (1) ground-based observations (preflight and postflight) contrasted with observations performed in flight, (2) in-flight observations contrasted with one another, and (3) preflight observations contrasted with postflight measurements. This approach is detailed in Figure 9, which shows the contrast matrix. The sums of squares for each contrast, the F-statistic, and the upper tail probabilities (UTPF) are tabulated in Figure 10. It is clear from this exhibit that only the difference between the ground-based means and the in-flight means are statistically significant.

	Preflight		In-flight		Postflight
Contrast 1	2	2	-3	-3	2
Contrast 2	0	0	-1	1	0
Contrast 3	1	1	0	0	-2

Contrast 1: Pre- and postflight vs. in-flight values
Contrast 2: In-flight FD 2 vs. FD 4/FD 5 values
Contrast 3: Preflight vs. postflight values

Figure 9. Matrix for orthogonal contrasts.

Contrast	SSC	F(1, 12)	UTPF
1	11.21	7.34	0.019
2	0.70	0.46	0.510
3	2.83	1.85	0.199

SSC: sum of squares for the contrast. UTPF: upper tail probability for the F statistic. The contrast number is identical to that in Figure 9.

Figure 10. Orthogonal contrasts of TBW data for the 4 subjects with complete data.

DISCUSSION

The analysis summarized in Figure 8 is based on the assumption that the day of measurement, i.e., the phase of the mission, is a fixed treatment effect. Under the null hypothesis that this treatment has no effect, the resulting ratio of variances would be observed with a probability of 0.07, implicating day of observation as a significant factor in explaining the observed variance. The decision to reject the null hypothesis is borderline at this probability, but the probability is sufficiently small to warrant further comparison of the means.

From Figure 10 it is apparent that the preflight and postflight mean TBW values are significantly different from the in-flight mean values. On the other hand, the preflight and postflight values are not significantly different, nor do the in-flight means on FD 2 and FD 4/FD 5 differ appreciably from one another. To calculate the change in TBW resulting from exposure to microgravity, the mean of the preflight and postflight values presented in Figure 6 was compared with the mean of the in-flight values. The former is 44.5 kg and the latter is 43.0, a decrease of 1.5 liters or 3.4%.

The high variability of the measurements on FD 2 suggests that individuals may differ in the rate at which they respond to the weightless environment. The difference in response may be intrinsic or may be related to some other factor such as the nausea induced by space motion sickness (SMS).

Returning flight crews rate their incidence of SMS on a scale of 0 to 3, where 0 represents no symptoms and 3 represents severe symptoms including three or more episodes of vomiting (Davis et al., 1988). It is reasonable to assume that astronauts who are experiencing even mild nausea would limit their consumption of water and other liquids and would therefore experience some degree of dehydration.

It was noted that, of the three crewmen who reported an SMS index of 0 for the missions in question, two had not experienced a decrease of TBW by the time of the FD 2 measurement, i.e., approximately 24 hours after launch. On the other hand, the two crewmen who reported either 1 or 2 for SMS had experienced a decrease of several kg by this time. This observation suggests that decreased water intake may be an important factor influencing the rate of TBW decrease.

In agreement with previous observations, the galley water was found to be enriched in ^{18}O; e.g., on STS-26 the enrichment was 57 parts per thousand relative to the standard, Vienna Standard Mean Ocean Water (V-SMOW). The actual ratio of ^{18}O to ^{16}O in galley water was 0.00212 (both at 19 and at 65 hours MET). This value may be compared with the ratio observed in V-SMOW 0.0020052 (Wong et al., 1987). The source of this enrichment seems likely attributable to the design of the Shuttle galley water system, which makes use of the water produced in the fuel cells. Enhanced evaporation of the lighter isotope during storage of the liquid oxygen may account for its enrichment in the heavier ^{18}O.

This level of enrichment of the crew's drinking water is not regarded as a source of error in the measurement of TBW. The measurement takes place over a period which is short enough that a small intake of slightly enriched water would not be expected to confound the measurement.

SUMMARY

This study represents the first time that it has been possible to measure a body fluid compartment by direct means during space flight. Based on the results observed in the five crewmembers, it is concluded that TBW decreases by 3.4% after one to three days of exposure to microgravity in the Space Shuttle. Some individuals appear to undergo this decrease within 24 hours. This effect may be enhanced by decreased water intake due to nausea associated with SMS.

REFERENCES

Davis, J. R.; Vanderploeg, J. M.; Santy, P. A.; Jennings, R. T.; Stewart, D. F. Space motion sickness during 24 flights of the Space Shuttle. Aviat. Space Environ. Med. 59: 1185-1189, 1988.

Fortney, S. M.; Hyatt, K. H.; Davis, J. E.; Vogel, J. M. Changes in body fluid compartments during a 28-day bedrest. Aviat. Space Environ. Med. 62:97-104, 1991.

Greenleaf, J. E. Mechanism for negative water balance during weightlessness: An hypothesis. J. Appl. Physiol. 60: 60-62, 1986.

Hicks, C. R. Fundamental Concepts in the Design of Experiments, 3rd Edition. New York: Holt, Rinehart & Winston, 1982.

Jennrich, R.; Sampson, P. General mixed model analysis of variance. In BMDP Statistical Software Manual. Berkeley, CA: University of California Press, 1985.

Leach, C. S.; Alexander, W. C.; Fischer, C. L. Compensatory changes during adaptation to the weightlessness environment. The Physiologist 13:246, 1970.

Leach, C. S.; Rambaut, P. C. Biochemical responses of the Skylab crewmen: An overview. In Biomedical Results from Skylab, edited by R. S. Johnston, and L. F. Dietlein. Scientific and Technical Information Office, NASA, Washington, DC, 1977.

Nixon, J. V.; Murray, R. G.; Bryant, C.; Johnson, R. L., Jr.; Mitchell, J. H.; Holland, O.B.; Gomez-Sanchez, C.; Vergne-Marini, P.; Blomqvist, C. G. Early cardiovascular adaptation to simulated zero gravity. J. Appl. Physiol.: Respirat. Environ. Exercise Physiol. 46: 541-548, 1979.

Ostle, B.; Malone, L.C. Statistics in Research, 4th Edition. Ames, IA: Iowa State Univ. Press, 1988.

Schoeller, D. A.; van Santen, E.; Peterson, D. W.; Dietz, W.; Jaspan, J.; Klein, P. D. Total body water measurement in humans with 18-O and 2-H labeled water. Am. J. Clin. Nutr. 33:2686-2693, 1980.

Schoeller, D. A.; Dietz, W.; van Santen, E.; Klein, P. D. Validation of saliva sampling for total body water determination by 18-O water dilution. Am. J. Clin. Nutr. 35: 591-594, 1982.

Sokal, R. R.; Rohlf, F. J. Biometry, 2nd Edition. San Francisco, CA: W. H. Freeman, 1981.

Winer, B. J. Statistical Principles in Experimental Design, 2nd Edition. New York: McGraw-Hill, 1971.

Wong, W. W.; Lee L. S.; Klein, P. D. Deuterium and oxygen-18 measurements on microliter samples of urine, plasma, saliva, and human milk. Am. J. Clin. Nutr. 45: 905-913, 1987.

ACKNOWLEDGMENTS

The authors wish to thank Dr. Peter D. Klein, Dr. Tom Boutton, and Dr. William W. Wong of the USDA/ ARS Children's Nutrition Research Center, Dept. of Pediatrics, Baylor College of Medicine and Texas Children's Hospital, and Dr. Karl Lin, KRUG Life Sciences, for their expert assistance. We also wish to thank the crews of STS-61C and STS-26, whose cooperative spirit assured the success of this study.

DSO 466: Pre- and Postflight Cardiovascular Assessment/Interim Report

Investigators: J. B. Charles, Ph.D.; M. W. Bungo, M.D.; S. L. Mulvagh, M.D.

INTRODUCTION

Previous observations from Soviet and U.S. space programs have indicated that exposure to weightlessness, even for short periods, induces significant changes in the cardiovascular system. These changes are proposed to be secondary to headward fluid shifts, subsequent plasma volume contraction, and ensuing adaptations in cardioregulatory function. This results in a cardiovascular state appropriate to space flight and is manifested by the clinical findings of tachycardia (rapid heart rate), decreased exercise capacity, and orthostatic intolerance demonstrated by symptoms of dizziness and/or loss of consciousness on return to Earth.

These findings have led to operational concerns during the Space Shuttle program, which have become especially pertinent to the Extended Duration Orbiter program, with flights of longer duration anticipated. The need for full mental and physical functioning as a prerequisite for safe return of the orbiter has underscored the danger of potential syncopal symptoms upon reentry, landing, and egress. Defining the extent and nature of this potential concern aids in the design and evaluation of countermeasures such as salt and fluid loading, G-suits, and lower body negative pressure to avoid complications resulting from microgravity-induced cardiovascular changes. Echocardiography provides an effective noninvasive technique to evaluate cardiac function before, during, and after space flight.

Thus, DSO 466, the Pre- and Postflight Cardiovascular Assessment, was designed to investigate the following hypotheses:

- The microgravity environment induces changes in the cardiovascular system that may have potential adverse effects on crew function.
- Certain countermeasures may be devised to prevent or diminish the negative operational effects.

Specific objectives included:

1. Studying the magnitude and direction of changes in cardiac size, volume, mass, and function in crewmembers experiencing varying periods of weightlessness.
2. Determining the time course required for postflight recovery of such changes.
3. Defining the basis for implementation of countermeasures to prevent or diminish the untoward effects of such changes.

PROCEDURES

Three basic sets of echocardiographic data were collected:

DSO 402:
- STS flights from 1982-83: 2-dimensional
- STS flights from 1983-85: 2-dimensional and M-mode

DSO 466:
- STS flights from 1988-89: 2-dimensional, M-mode and some Doppler

The revision and modification of collection methods for each data set depended upon results of previous data and acting operational constraints.

In total, from 1982 through 1989, 54 crewmembers from 16 missions participated. The basic protocol involved incorporation of the echocardiographic data collection into the existing operational Stand Test. Preflight baseline studies were done approximately 10 days and, since 1988, 5 days before launch. Postflight, landing day, and several recovery day data collections were acquired to a maximum of 14 days. Many crewmembers reported motion sickness symptoms early in flight, and most used some degree

of oral saline loading countermeasures prior to landing.

Continuous echocardiographic recordings were made during the traditional 5-minute supine and 5-minute standing test with coordinate electrocardiographic recording and blood pressure monitoring. The variables collected for analysis were 1) heart rate (HR), 2) systolic and diastolic blood pressure (SBP and DBP), 3) left ventricular diastolic and systolic dimensions, 4) left ventricular wall thicknesses, 5) right ventricular dimensions, 6) left atrial and aortic dimensions, 7) velocity of circumferential fiber shortening (VCF is a measure of left ventricular contractibility), and 8) left ventricular inflow and outflow velocities. Hemodynamic parameters derived from these measurements included 1) mean arterial and pulse pressures (MAP and PP), 2) left ventricular end-diastolic, 3) end-systolic and stroke volume indexes (LVEDVI, LVESVI, LVSI), 4) ejection fraction (EF), 5) cardiac index (CI), and 6) total peripheral vascular resistance index (TPRI). The use of hemodynamic indexes normalizes for differences in body surface area between crewmembers.

RESULTS

I. ECHOCARDIOGRAPH

STS: 1982 - 1985

2-Dimensional Echocardiographic Studies: (Missions 5, 6, 7, 8)

These results have been published (J. Appl. Physiol. 62(1):278-283, 1987). In brief, these four missions were of 5 to 8 days' duration and involved 17 crewmembers. All had one preflight and one post-landing day data collection (R+7 through R+14), but only seven had landing day (R+0) data collection. Studies were done only in the supine (left lateral decubitus) position. On R+0, there were increases in heart rate (HR), mean arterial pressure (MAP), and total peripheral vascular resistance (TPR), and a 25% decrease in left ventricular diastolic volume (LVEDV). During the recovery phase, MAP and TPR quickly normalized, while HR and LVEDV appeared to slowly return toward baseline.

Problems with drawing far-reaching conclusions from this study included the relatively small number of subjects studied, the wide range of post-landing recovery data collection times, and methodological limitations of calculating left ventricular volumes from 2-dimensional images taken from the parasternal window.

2-Dimensional-Guided M-Mode Echocardiographic Studies: (Missions 8, 41-B, 41-C, 41-D, 51-D, 51-G)

Twenty-four crewmembers of six missions lasting 6 to 8 days had sufficient participation to enable data analysis. All had supine (left lateral decubitus) echocardiographic data collection on one occasion preflight, and 15 had data collection on Landing Day. Post-landing (recovery) data collection was variable with four crewmembers having two recovery studies at R+1, and R+4, one having three recovery studies at R+1, R+3, and R+4 and seventeen having one recovery study at either day R+5, R+7, or R+9.

Results of the 1982-1985 missions are summarized below and are illustrated in Figures 1-4.

Landing day: Relative increases occurred in HR, SBP, DBP, and MAP; relative decreases occurred in LVEDVI and LVSI.

Post-Landing Days (Recovery): There was a trend to return to preflight baseline values within several days of recovery for HR, SBP, DBP and MAP, but noticeable overshoot and variability were observed in LVEDVI and LVSI.

Variability in preflight values (e.g., differences in data collected on L-10 versus L-5) and variability in time of postflight collection introduced problems in interpretation of this data set.

STS: 1988 - 1989

2-Dimensional-Guided M-Mode Echocardiographic Studies: (Missions 26, 27, 29, 30, 28, 34, 33)

Twenty-four crewmembers of seven missions of 4 to 5 days' duration participated. All had supine 2-dimensional and M-mode echocardiograms; 14 had technically adequate standing 2-dimensional and M-mode echocardiograms. Crewmembers having data collection at the following times included all at preflight (L-10 and L-5), landing day (R+0), +2, +3, and +7-10, and 19 at R+4-6.

Figures 1-4. Pre- and postflight echo results (1982-1985) STS-8, 41-B, 41-C, 41-D, 51-D, and 51-G.

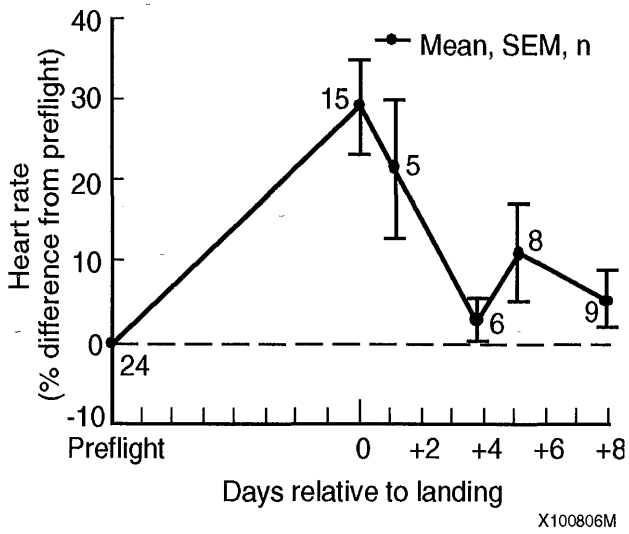

Figure 1. Heart rate (supine).

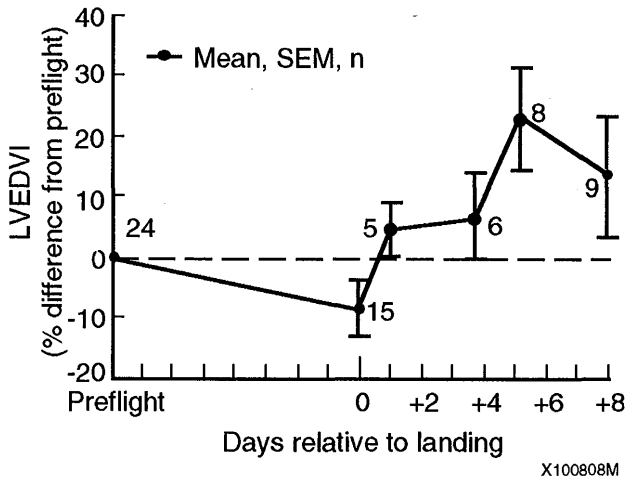

Figure 3. Left ventricular end-diastolic volume index (supine).

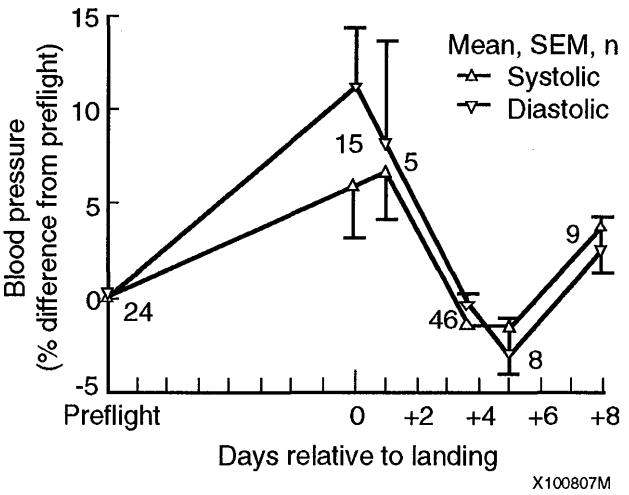

Figure 2. Blood pressure (supine).

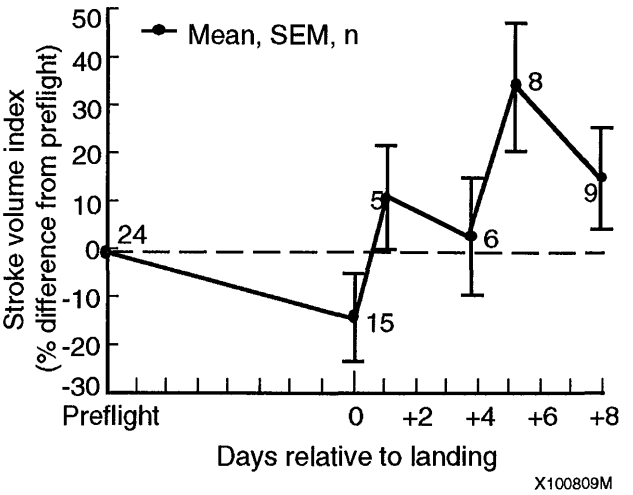

Figure 4. Stroke volume index (supine).

Statistical analysis of observed changes in the described parameters with respect to flight day, position, and/or orthostatic response (standing value minus supine value) by repeated measures analysis of variance and/or paired t-testing was done. Due to a methodologic change in echocardiographic data acquisition that resulted in missing data points, standing ultrasound data was often unable to be completely statistically analyzed.

Results of the 1988-89 missions are summarized below and are illustrated in Figures 5 to 18.

Overall: HR, SBP, DBP, and MAP were significantly increased in the standing compared to the supine position. PP, LVEDVI and LVSI were significantly decreased in the standing compared to the supine position for all test days.

Preflight (L-10, -5): No significant differences between the two preflight data collections on L-10 and L-5 were seen, with the exception of increases in standing SBP ($p < .04$) and supine VCF ($p < .04$) on L-5 when compared to L-10.

Landing Day (R+0): Supine heart rate was significantly increased by 23% ($p < .0005$) on R+0, compared to preflight; similarly, standing heart rate was significantly increased by 35% ($p < .0001$). The orthostatic response in HR was increased on R+0 compared to preflight ($p < .0001$). The 11% increase in supine DBP on R+0 compared to preflight approached, but did not achieve, significance ($p < .063$). The orthostatic response in DBP was decreased on R+0 compared to preflight ($p < .01$). The 10 and 12% decreases in supine and standing PP, respectively, on R+0 compared to preflight approached, but did not achieve, significance ($p < .058$). No significant differences in supine or standing SBP and MAP were noted on R+0 compared to preflight.

Supine LVEDVI and LVSI were significantly decreased by 11.4% ($p < .04$) and 16.6% ($p < .006$) on landing day compared to preflight. Standing LVEDVI and LVSI had similar trends to the supine data, but could not be statistically analyzed. TPRI was significantly greater in the standing position, compared to the supine, on all test days except for R+0 ($p < .03$). The orthostatic response in TPRI was decreased on R+0 compared to preflight ($p < .03$), as was the orthostatic response in DBP (see above). Landing day LVESVI, LVCI, LVEF, LV mass, LV wall thickness, and VCF showed no significant changes when compared to preflight values.

Post-Landing Days (R+2, +3, +4-6, +7-10): By R+2, the hemodynamic perturbations noted above on landing day had all returned to within the baseline preflight range.

II. DOPPLER

Nine crewmembers of three missions (STS-28, 34, 33) of 4 to 5 days' duration had Doppler echocardiographic studies preflight and on R+0, +2, +3, +4, and +7-9.

Results are pending data analysis.

Figure 5-17. Pre- and postflight results STS 26, 27, 29, 30, 28, 34, and 33.

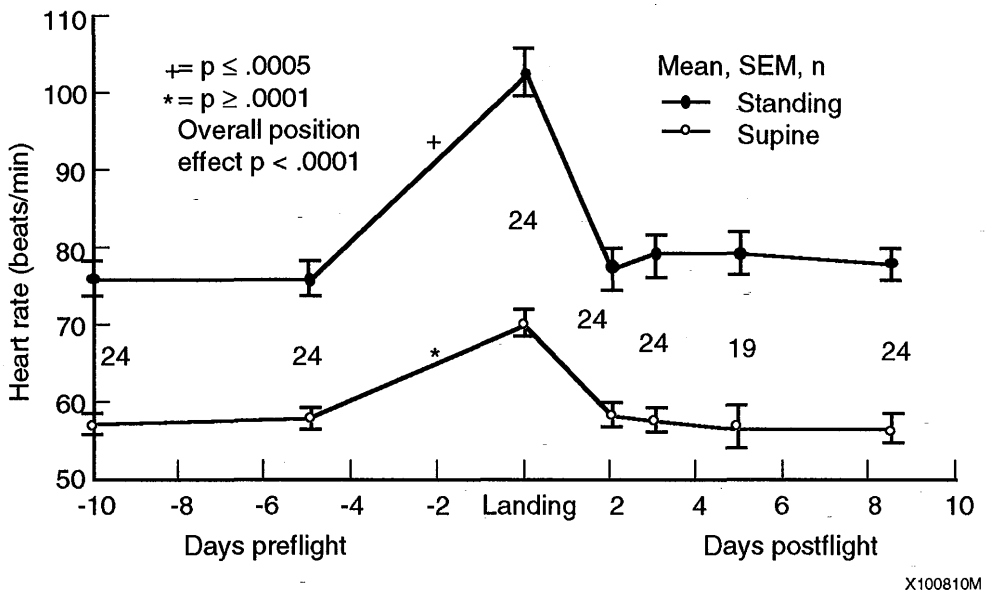

Figure 5. Heart rate.

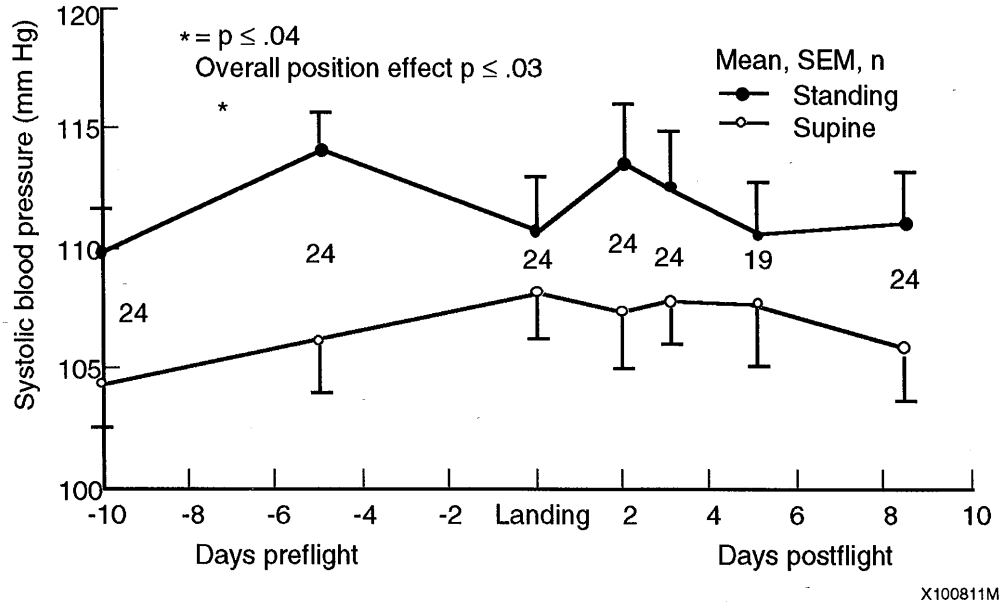

Figure 6. Systolic blood pressure.

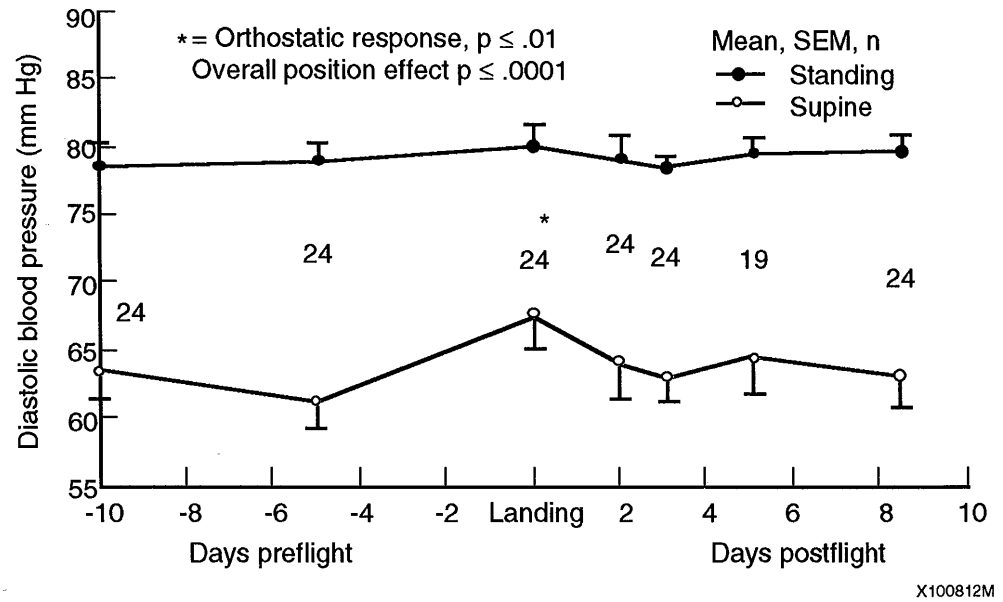

Figure 7. Diastolic blood pressure.

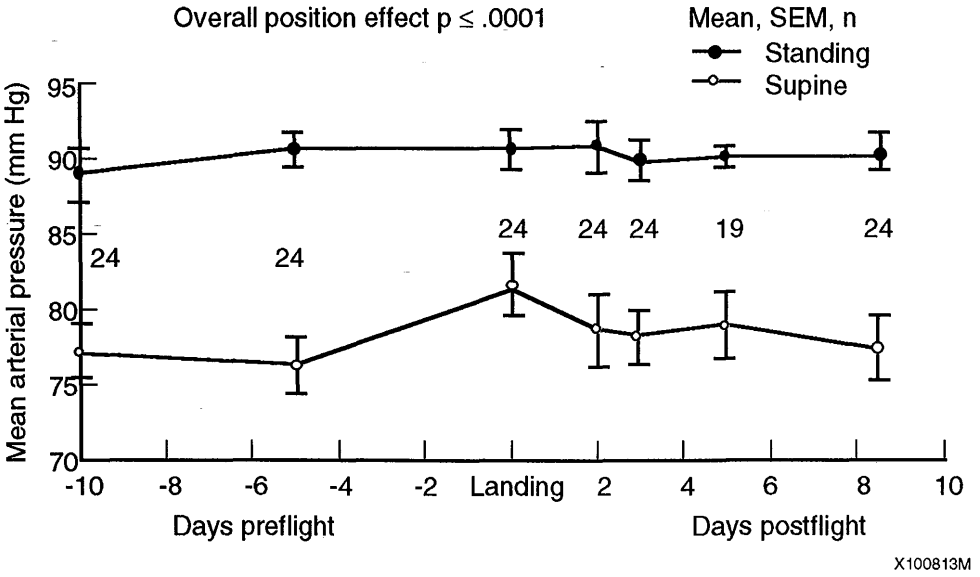

Figure 8. Mean arterial blood pressure.

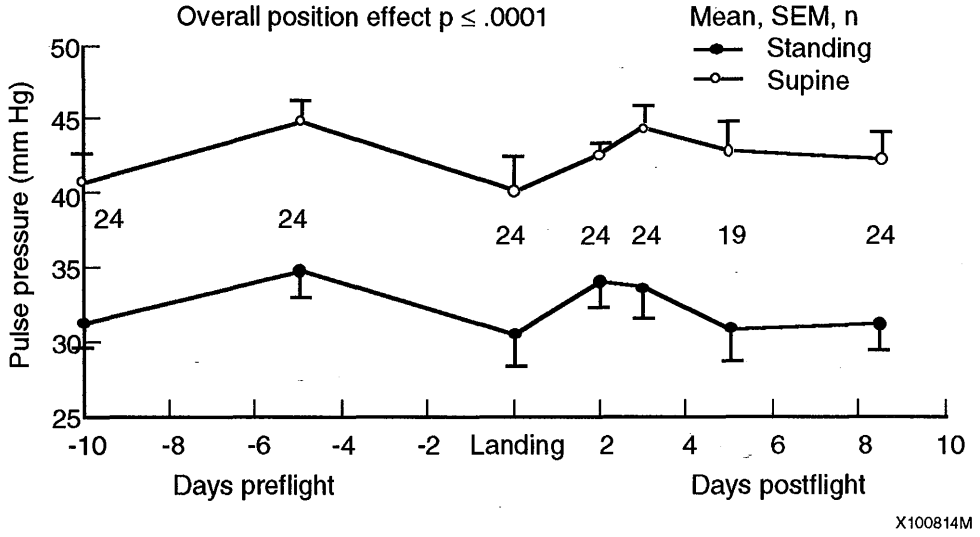

Figure 9. Arterial pulse pressure.

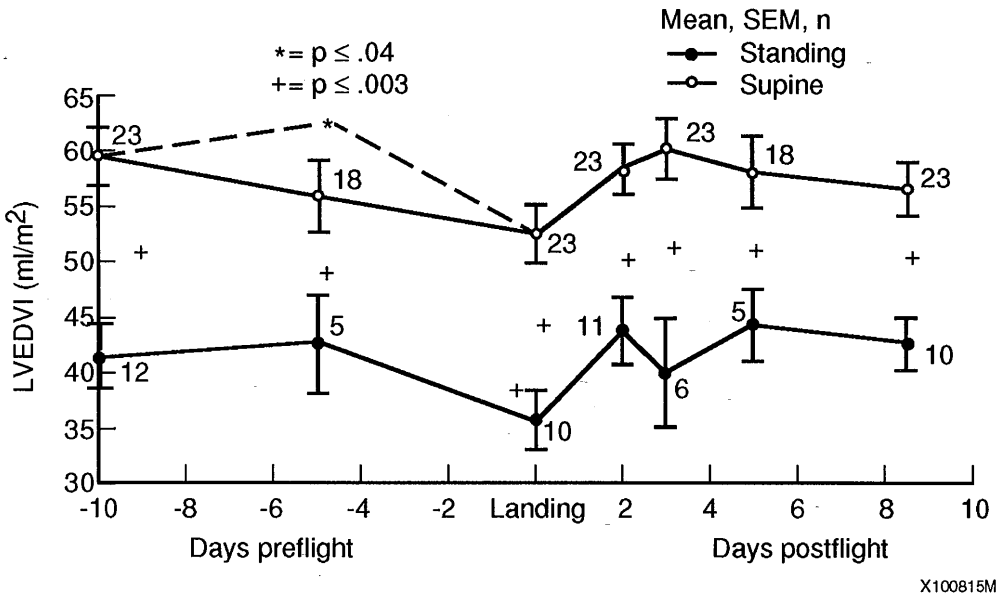

Figure 10. Left ventricular end-diastolic volume index.

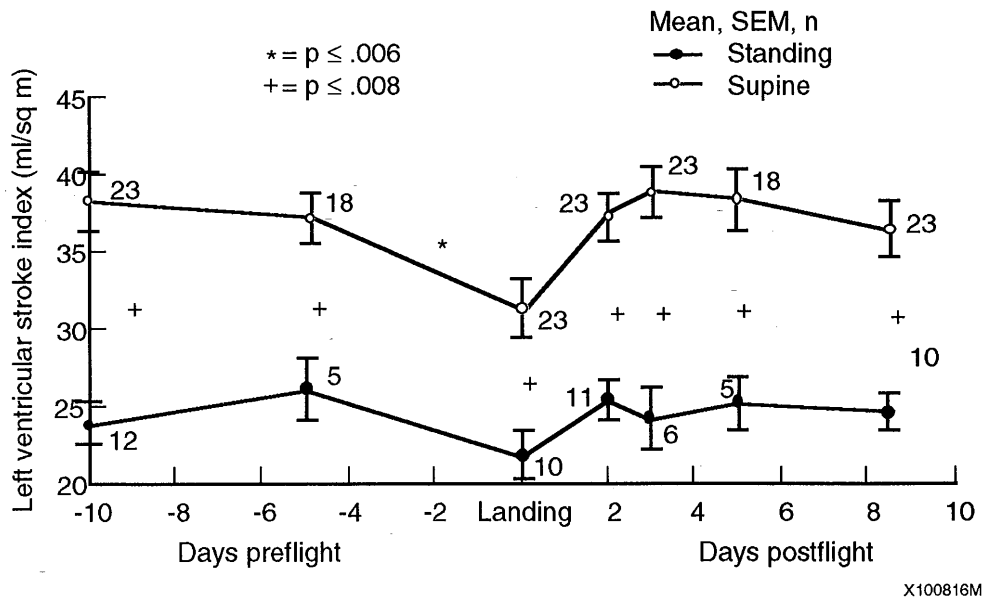

Figure 11. Left ventricular stroke volume index.

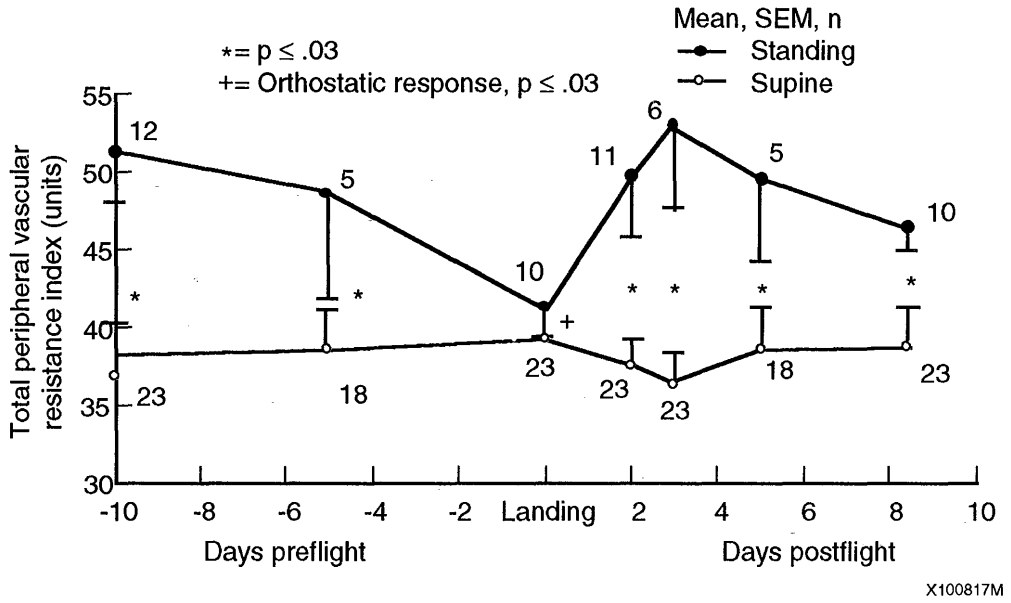

Figure 12. Total peripheral vascular resistance index.

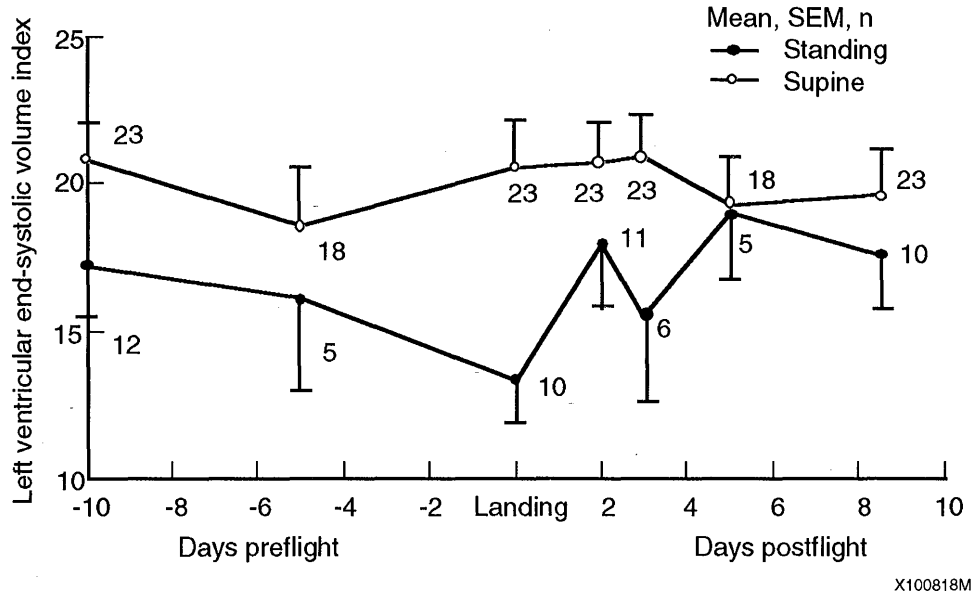

Figure 13. Left ventricular end-systolic volume index.

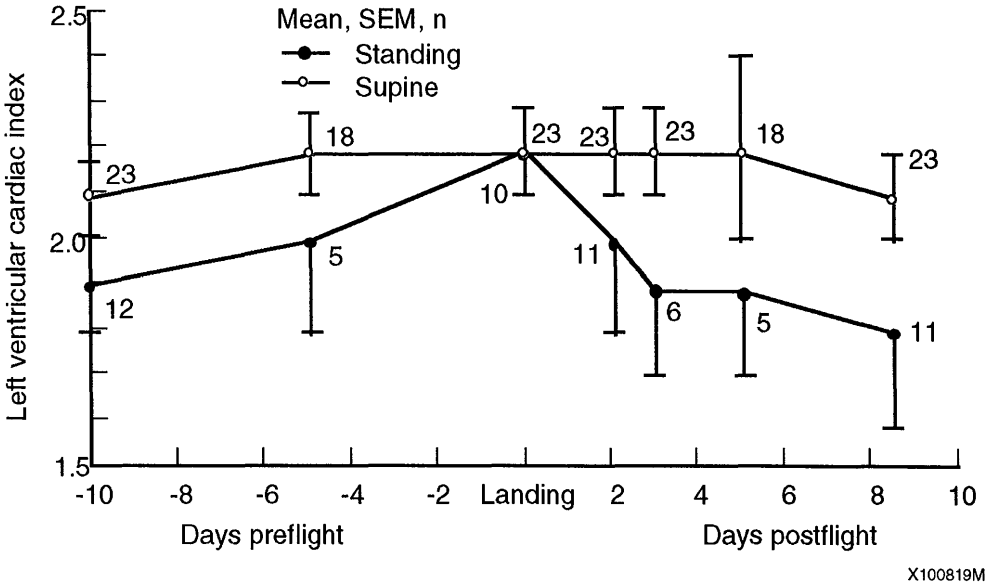

Figure 14. Left ventricular cardiac index.

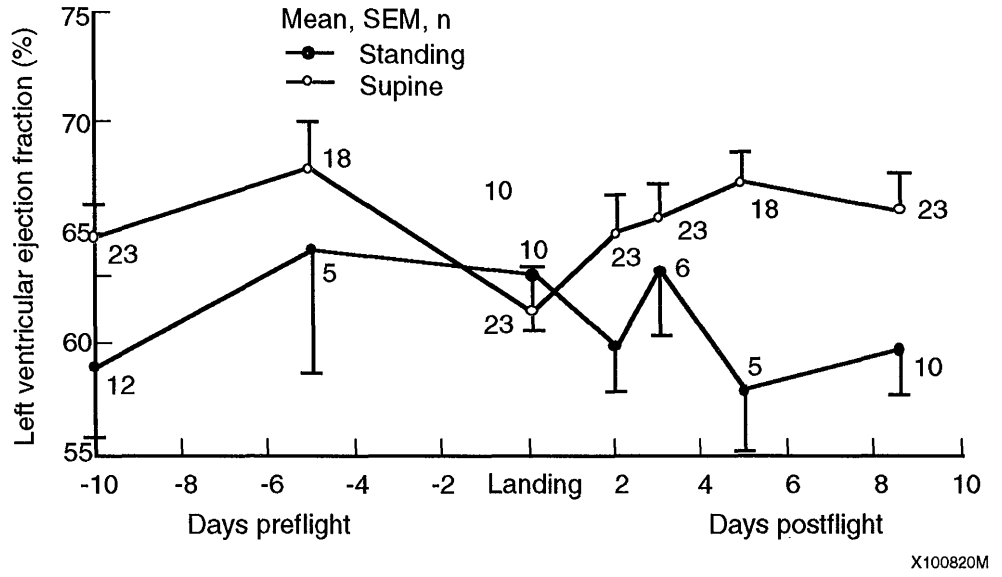

Figure 15. Left ventricular ejection fraction.

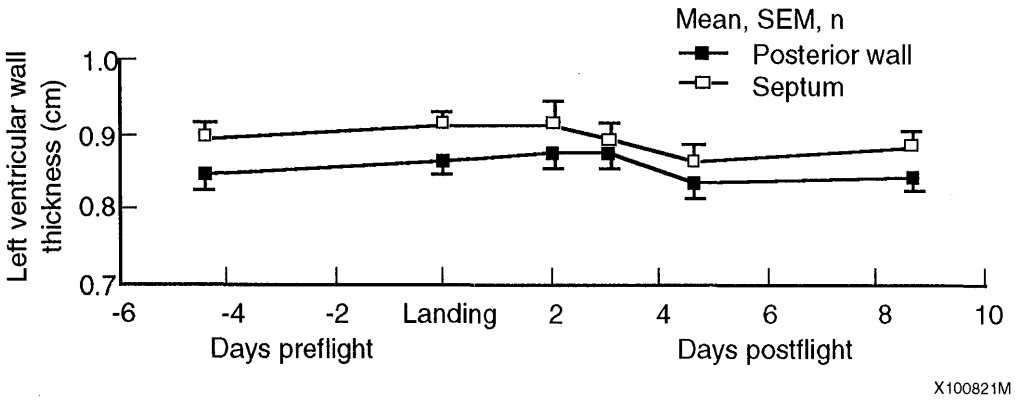

Figure 16. Left ventricular wall stress.

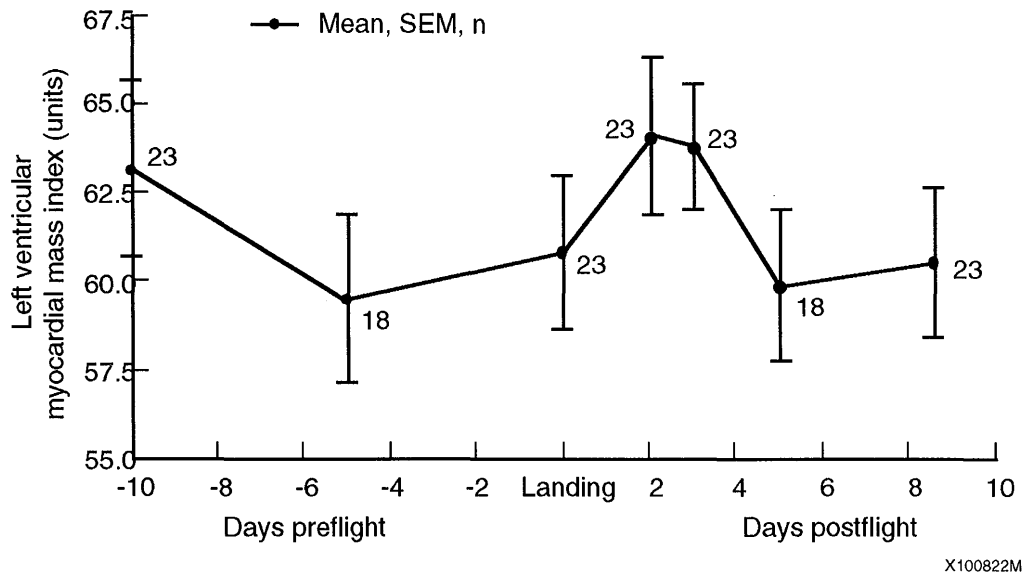

Figure 17. Left ventricular myocardial mass index.

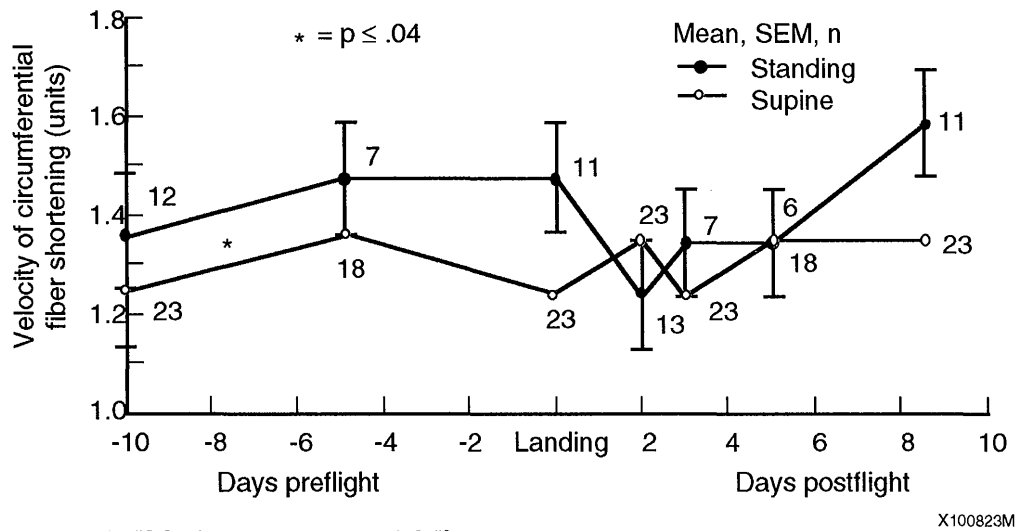

Figure 18. Velocity of circumferential fiber shortening.

DISCUSSION

Cardiovascular physiological changes induced by short duration (4-5 day) missions include decreases in left ventricular end-diastolic volume and stroke volume indexes commensurate with compensatory increases in heart rate, resulting in the maintenance of constant cardiac output. Diminished left ventricular filling volumes seen at landing may result from the recognized alterations in fluid shifts that occur early in the course of space flight. It is of concern that despite pre-landing fluid loading attempts by individual crewmembers, these hemodynamic changes were still observed. This suggests that more intensive countermeasure efforts are required and justifies the evaluation of in-flight LBNP and various fluid loading protocols currently under investigation.

The observed changes in TPRI and DBP support coincident observations from DSO 467 (Changes in Baroreceptor Reflex Function After Space Flight) of autonomic nervous system dysfunction on return to 1-g after exposure to microgravity environment. Further evaluation of this interesting phenomenon, indicating a resetting of the cardioregulatory autonomic tone and decrement in compensatory vascular reserve, is warranted.

It is reassuring, at least in the setting of short duration missions, that a compromise of left ventricular contractility or left ventricular mass after exposure to space flight does not appear. However, an evaluation of cardiac function and mass during and after longer duration flights will be necessary.

The interpretation of data collected to date must take into consideration the relatively small sample size and non-uniformity of collection. However, the postflight variability seen after the 1982-1985 missions is not present in the later cohort from 1988-1989. Explanations for this observed difference with respect to the earlier cohort may be the effect of variable and increased mission durations (up to 8 days), the different times of single-point post-landing day data acquisition, non-uniformity of countermeasure usage and/or recent improvements in technical applications.

The need for standardized data collection regimens and schedules is emphasized by the difficulty in developing meaningful conclusions in heterogeneous populations. Detailed fluid intake/output, body weight, and exercise information before every data collection is essential in order to ensure comparability of pre- and postflight data.

As there is minimal data collection information beyond 7 days after landing, any delayed hemodynamic changes cannot be excluded from this data base.

There is evidence of hemodynamic differences between 10 days and 5 days before launch. Given the lack of control over — and insight into — this period, these changes remain a topic for future research.

Longer duration missions (>9 days) will require similar ongoing evaluation of cardiovascular function to delineate the effects of the anticipated physiological changes and to evaluate countermeasures to orthostatic intolerance with the ultimate goal of ensuring crew safety.

CONCLUSIONS

Cardiovascular Physiology

Short duration (4-5 days) space flight results in diminished cardiac volumes which are compensated for by elevated heart rates on return to the 1-g environment. These alterations in cardiovascular physiology appear to resolve within 48 hours.

Operational Relevance

A full understanding of the effects of exposure to microgravity on the cardiovascular physiological state is especially imperative in order to assess fitness for nominal and emergency duties during entry, landing, and egress. Such information provides the background necessary for the evaluation of effective countermeasures to resultant orthostatic intolerance postflight, the potential for which appears to increase with prolonged duration of space flight.

DSO 467: Influence of Weightlessness of Baroreflex Function

Investigators: Janice M. Fritsch, M.S.; John B. Charles, Ph.D.; Barbara S. Bennett, M.S.; Michele M. Jones; and Dwain L. Eckberg, M.D.

ABSTRACT

Orthostatic intolerance is a predictable but poorly understood consequence of space travel. Because arterial baroreceptors modulate abrupt pressure transients, including those provoked by standing, the hypothesis that space flight impairs baroreflex mechanisms was tested. Vagally-mediated carotid baroreceptor-cardiac reflex responses (provoked by neck pressure changes) in the supine position and heart rate and blood pressure in the supine and standing positions were studied in 16 U.S. astronauts before and after 4- to 5-day Space Shuttle missions. On landing day, astronauts' resting R-R intervals and standard deviations, and the slope, range, and position of their resting R-R intervals on the carotid transmural pressure-sinus node response relation (operational point) all were reduced relative to preflight values. Reductions of operational points (indicating reduced hypotensive buffering capacity) were related directly and significantly to reductions of postflight systolic pressure responses to standing. After landing day, baroreflex slopes and ranges were subnormal and remained so for the duration of the study (8 to 10 days). These results suggest that short-duration space flight leads to significant, functionally relevant impairment of human baroreflex mechanisms.

INTRODUCTION

Exposure to weightlessness alters postflight cardiovascular responses to exercise and standing. Although these changes are probably initiated during flight, they are not known to impair cardiovascular performance in space (Dietlein, 1977). However, functional problems become apparent upon landing, when most astronauts have reduced exercise capacity and orthostatic tolerance (Bungo and Johnson, 1983). The cause of orthostatic intolerance is unclear. Loss of plasma volume during weightlessness (Johnson et al., 1977) may be partly responsible. However, acute comparable blood volume reductions usually do not provoke orthostatic hypotension (Murray et al., 1967), and repletion of blood volume after simulated weightlessness does not completely prevent orthostatic hypotension (Blomqvist et al., 1980).

This study explores a possibility suggested by ground-based research that impairment of normal baroreflex mechanisms contributes to post-weightlessness orthostatic intolerance. Head-down tilt, a widely used simulation of weightlessness (Kakurin et al., 1976), reduces R-R interval responses to carotid baroreceptor stimulation (Convertino et al., 1990; Eckberg and Fritsch, 1990); in one study (Convertino et al., 1990), such reductions were related directly to the magnitude of post-bedrest blood pressure reductions during standing.

This study investigated vagally-mediated baroreceptor-cardiac reflex responses of U.S. astronauts before and after Space Shuttle missions lasting 4 to 5 days and correlated baroreflex responses with blood pressure and heart rate responses to standing. The results suggest that space flight reduces baseline levels of vagal-cardiac outflow and vagal responses to changes of arterial baroreceptor input. Further, the data suggest that these changes are related to postflight reductions of astronauts' ability to maintain standing arterial pressures.

PROCEDURES

Subjects and Protocol

Sixteen astronauts (15 male and 1 female), whose average ($\pm$ SE) age was 43 $\pm$ 4 (range 36 - 54) years, were studied before and after Space Shuttle missions lasting 4 to 5 days. The protocol was approved by the Johnson Space Center Human Research Policies and Procedures Committee and the human research committees of the Hunter Holmes McGuire Department of Veterans Affairs Medical Center and the Medical College of Virginia. Preflight studies were performed nominally 10 and 5 days before launch; in practice, preflight data were collected between 13 and

Accepted for publ. by *J. Appl. Phys.*

7 days, and again between 7 and 5 days before launch. Acceptable postflight data were collected on landing day (n = 11), on R+2 and +3 (n = 16), and again on R+8, +9, or +10 (n = 12).

The electrocardiogram, respiration (abdominal bellows connected to a strain-gauge pressure transducer), and neck chamber pressure were recorded by FM tape and strip chart recorders. The electrocardiogram and respiration were recorded during the last 5 minutes of a 20-minute rest period prior to any intervention. Resting vagal-cardiac activity was estimated from average R-R intervals and their standard deviations (Eckberg, 1984; Katona and Jih, 1975). Blood pressure was measured manually with a sphygmomanometer before baroreceptor testing.

Several aspects of this experiment were beyond the investigators' control. Eight crewmembers shifted their sleep/wake cycles in preparation for flight and took sleeping medications [flurazepam HCl (Roche) or temazepam (Sandoz)] the night before the second preflight measurement (about 5 days before launch); three crewmembers took temazepam within 24 hours before landing. Data obtained on days after these medications were taken were discarded. For all other subjects, measurements made nominally 10 and 5 days before launch were averaged to obtain control values. Data could not be collected from two subjects on landing day because of equipment malfunction.

Baroreflex Stimuli

After the rest period, a tightly sealing Silastic chamber was strapped to the anterior neck (Sprenkle et al., 1986) (Figure 1). A computer-controlled, stepping motor-driven bellows delivered a fixed sequence of pressure and suction steps to the chamber during held expiration, as follows: Pressure was increased to about 40 mmHg for about 5 seconds, reduced by approximately 15 mmHg decrements after each of the next seven R-waves, to about -65 mmHg, and then returned to ambient levels. Responses from seven successful repetitions of this stimulus sequence during each experimental session were averaged. R-R intervals were plotted against carotid distending pressures (taken to be systolic minus neck chamber pressures). Earlier studies have shown that these stimuli and baroreflex responses are highly reproducible (Eckberg, Convertino, Fritsch, and Doerr, unpublished).

Prior studies (Fritsch et al., 1989; Kasting et al., 1987) also have shown that when data from such baroreflex stimuli are fitted to a four-parameter logistic equation, confidence limits are so large that derived equations do not describe the data accurately. Therefore, in this study baroreflex response relations were reduced to other parameters for analysis including minimum, maximum, and range of R-R interval responses; carotid distending pressures at minimum and maximum R-R intervals; maximum slopes; and operational points. Maximum slopes were identified with linear regression analyses applied to each set of three consecutive pairs of data on the stimulus-response relation. Operational points were defined as [(R-R intervals at 0 mmHg neck pressure minus minimum R-R intervals)/R-R interval range] x 100%. The operational point is a measure of the relative baroreflex buffering capacity for pressures above and below resting levels. (Thus, when operational points are low, there is less relative buffering capacity for hypotensive stimuli, and when operational points are high, there is less relative buffering capacity for hypertensive stimuli.)

R-R intervals were used in these analyses because the relation between changes of R-R intervals and changes of vagal-cardiac traffic is linear (Katona et al., 1970). The relation between heart rate and vagal-cardiac traffic is curvilinear; this makes comparisons before and after interventions difficult if baseline heart rate has changed. Figure 2 is an original record showing a neck pressure sequence and responses of one subject (A) and a plot of that subject's average responses to seven stimulus sequences (B).

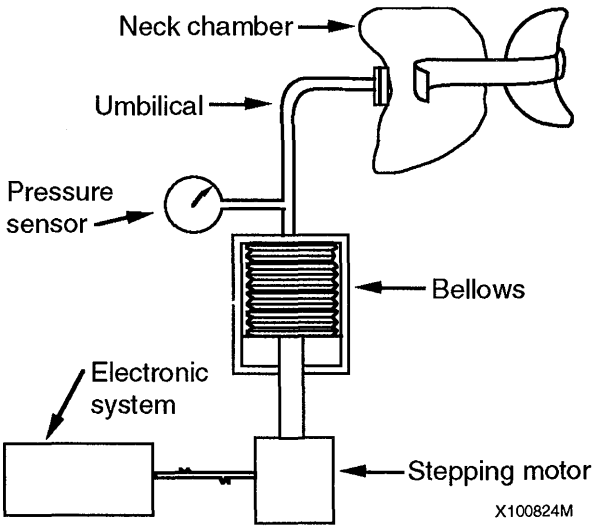

Figure 1. Schematic diagram of all elements in the baroreflex measurement system.

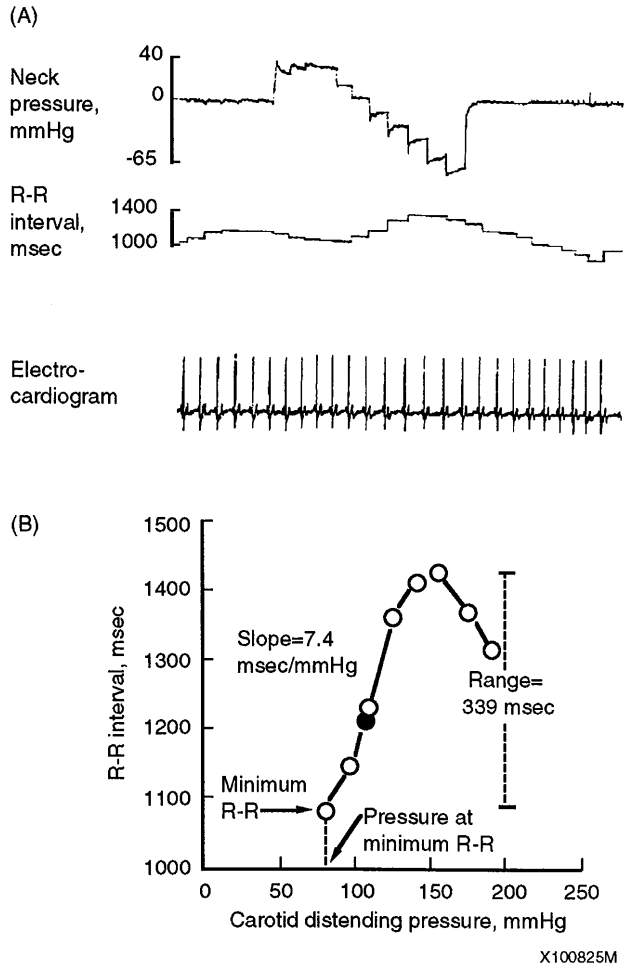

Figure 2. Original record showing a neck pressure sequence and responses of one subject (A) and a plot of that subject's average responses to seven stimulus sequences (B). The filled circle denotes operational point.

Stand Test

Routine stand tests were performed on all subjects 10 days before launch, on landing day, and 3 days after landing. Blood pressure and heart rate were measured every minute for 10 consecutive minutes (five during supine rest, one immediately after standing, and four during standing with subjects leaning against a wall with their heels 6 inches from the wall). Cardiac responses to standing are presented both as heart rate increases and as R-R interval decreases. Heart rates are presented because they are hemodynamically more relevant than R-R intervals.

Statistics

Because some measured variables were not distributed normally (Lilliefors, 1967), nonparametric statistical tests were used. The Wilcoxon signed-rank test (Snedecor and Cochran, 1967) was used to identify differences among results obtained during experimental sessions, and the Spearman test (Gibbons, 1976) was used to identify correlations among measurements. Cluster analysis (Anderberg, 1973) identified groups according to blood pressure responses on landing day. Forward selection, backward elimination, and stepwise regression modeling methods (Draper and Smith, 1981) were used to predict changes of standing minus supine systolic pressure on landing day. The following factors were entered into the model as independent variables: maximum baroreflex slope and R-R interval range, operational point, and body weight. The entry level significance for these independent variables was set at $P = 0.25$. Results from forward selection and backward elimination methods were similar, and therefore, only results from backward elimination analyses are presented. $\underline{P}$ values < 0.05 were considered to be significant.

RESULTS

Control Measurements

Average baseline measurements for all subjects are given in the table on the following page. Baseline arterial pressure did not change throughout the study. Resting R-R intervals, their standard deviations, and body weight were all significantly reduced, but on landing day only.

Baroreflex Responses

Average R-R interval responses to carotid baroreceptor stimuli for all subjects are presented in the table, and responses measured on landing and subsequent days are shown in Figures 3-5. Average slopes and ranges were reduced insignificantly on landing day and significantly postflight on days R+2 through +10. On landing day (Figure 3), the response relation was lower on the R-R interval axis (as reflected by minimum and maximum R-R intervals) but at the same position on the pressure axis (as reflected by carotid distending pressures at minimum and maximum R-R intervals).

TABLE 1. AVERAGE BASELINE MEASUREMENTS FOR ALL SUBJECTS

	Preflight	Landing day			Postflight day
			R+2	R+3	R+8 to 10 (n=12)
Systolic pressure, mmHg	116 ± 2	116 ± 2	117 ± 2	116 ± 2	116 ± 2
Diastolic pressure, mmHg	75 ± 1	73 ± 2	72 ± 2	73 + 2	74 ± 2
R-R interval, msec	1123 ± 42	965 ± 25*	1069 ± 38	1134 ± 39	1069 + 31
Standard deviation of R-R, msec	62 ± 6	40 ± 4*	58 ± 6	55 + 5	47 ± 5
Body weight, kg	75.6 ± 4.0	74.4 ± 2.4*	75.2 ± 2.4	75.3 ± 2.4	75.4 ± 2.1
Baroreflex measurements					
Maximum slope, msec/mmHg	5.0 ± 1.0	3.4 ± 0.5	3.6 + 0.6*	3.9 ± 0.6*	3.9 ± 0.6*
R-R range, msec	243 ± 47	182 ± 25	177 ± 20*	192 + 102*	189 ± 27*
Operational point, %	48.9 ± 3.5	29.4 ± 4.2**	39.8 ± 3.6	52.4 ± 4.7	42.4 ± 6.0
Minimum R-R, msec	1081 ± 43	923 + 30*	1036 ± 39	1084 ± 35	1037 ± 31
Maximum R-R, msec	1324 + 68	1104 ± 31*	1213 ± 41*	1275 ±43	1226 ± 38*
Carotid distending pressure at minimum R-R, mmHg	80 ± 4	83 ± 4	92 ± 9	82 ± 7	75 ± 2
Carotid distending pressure at maximum R-R, mmHg	153 ± 8	172 ± 4	160 ± 6	157 + 7	161 + 5

* = $\underline{P} < 0.05$; ** = $\underline{P} < 0.01$

Also on landing day, maximum slopes and ranges were reduced in about half of the subjects, and the position of the operational point was reduced in 86% of them.

By R+2 (Table and Figure 4), the average baroreflex slope and range were significantly reduced, but the operational point had returned to the preflight level. Compared with preflight levels 60% of subjects had reduced slopes on R+2, 75% had reduced ranges, and 69% had lower operational points. The average minimum, but not maximum, R-R intervals had returned toward a higher point on the R-R interval axis. The position of the response relation on the pressure axis still was not different from preflight.

On R+3 and thereafter (Table and Figure 5) the average R-R interval slope and range remained significantly reduced. The average maximum R-R interval was reduced on day "8-10." All other parameters were comparable to preflight values.

Stand Tests

Changes of systolic and diastolic pressures and heart rates upon standing are shown in Figure 6. Preflight increases of systolic and diastolic pressures with standing were 11 + 3 (107 ± 3 to 118 ± 1), and 15 ± 3 (68 ± 2 to 83 ± 1) mmHg. The preflight maximum increase of heart rate with standing was 16 ± 1 (55 ± 2 to 71 ± 1) beats/min. On landing day, average increases of systolic and diastolic pressure were 5 ± 3 (115 ± 3 to 120 ± 3, $\underline{P} = 0.04$ from preflight), and 12 ± 2 (76 ± 3 to 88 ± 2, $\underline{P} = 0.13$) mmHg. Heart rate increases from supine to standing positions averaged 31 ± 3 (65 ± 7 to

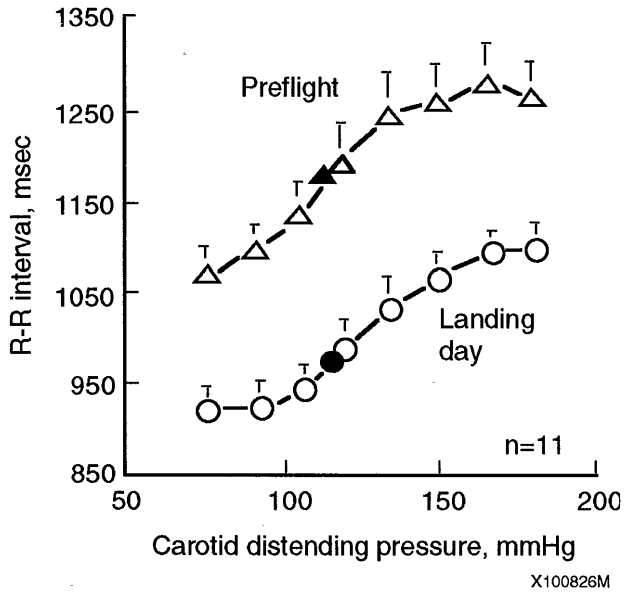

Figure 3. Carotid baroreceptor vagal-cardiac reflex responses before flight and on landing day. Filled symbols represent the position of operational points. Average operational point was reduced significantly on landing day, but slope and range were not.

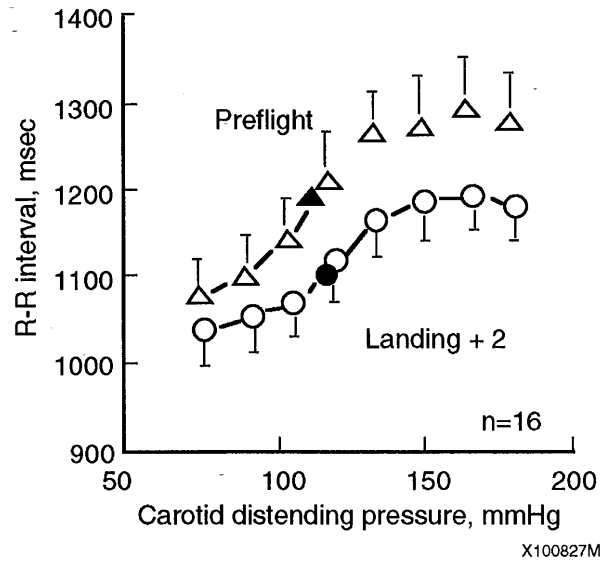

Figure 4. Carotid baroreceptor vagal-cardiac reflex responses before flight and 2 days after landing. Average slope and range were significantly reduced, and operational point (filled symbols) was not.

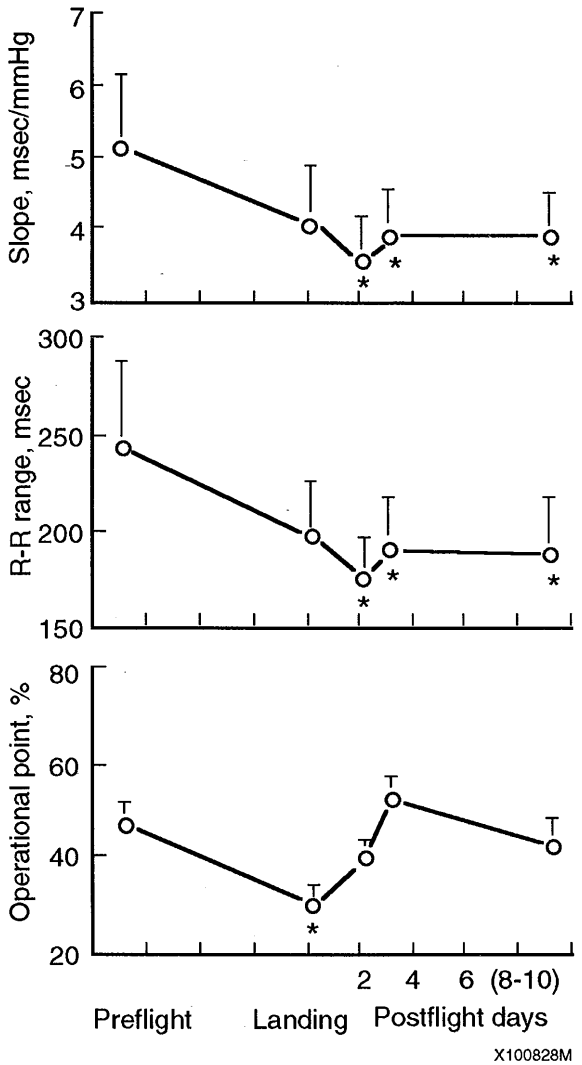

*Figure 5. Average slopes, ranges, and operational points throughout the study. * = $P < 0.05$; ** = $P < 0.01$.*

96 ± 4, P = 0.0008, from preflight) beats/min on landing day and were significantly larger than preflight values. Heart rate responses also were converted to R-R intervals for analysis. Decreases of R-R intervals with standing averaged 254 ± 32 (1113 ± 35 to 859 ± 30) before launch, and 293 ± 29 (933 ± 29 to 640 ± 28) msec on landing day (P = 0.052 from preflight).

Correlations Among Stand Tests With Baroreflex Data

Systolic pressure responses to standing varied among subjects on landing day. Cluster analysis of these

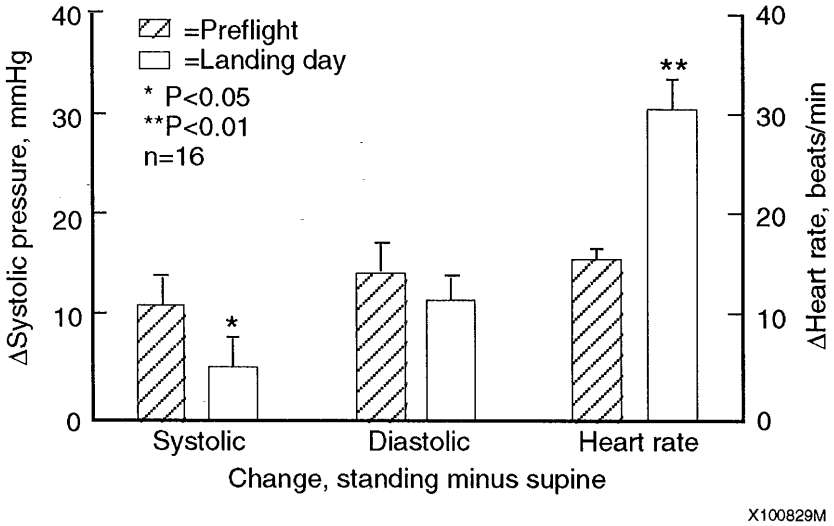

Figure 6. Preflight and postflight differences of standing minus supine systolic and diastolic pressures and heart rate.

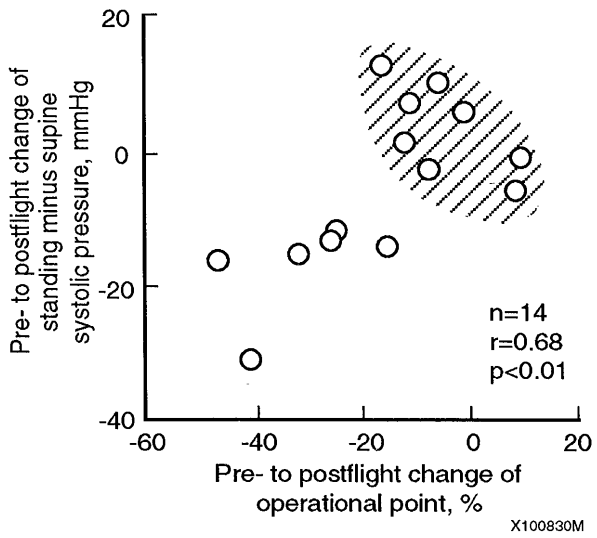

Figure 7. Pre- to postflight (landing day) changes of operational points and systolic pressure responses to standing. Linear regression correlation coefficients are for all data. Cluster analysis (see methods) of these data identified two distinct groups, which have been termed less and more resistant to postural change. The cross-hatched area identifies the more resistant group.

changes identified two groups of astronauts ($r = 0.88$, $P < 0.05$). Figure 7 illustrates the results of this analysis. One group (cross-hatched area) maintained standing systolic pressures well, and the other did not. Responses of these two groups to standing are shown in Figure 8. In subjects who maintained systolic pressure well, the average increase of systolic pressure with standing was 3 ± 2 mmHg greater on landing day than it was before flight (systolic pressure increased from 110 to 121 mmHg before flight and from 110 to 124 on landing day). In subjects who did not maintain systolic pressure well, the average increase of systolic pressure with standing was actually 17 ± 3 mmHg less on landing day than it was before flight. This difference between groups was significant ($\underline{P} = 0.0001$). The two groups also differed significantly in preflight to postflight standing minus supine reductions of diastolic pressure (-0.9 ± 3.9 vs. -9.3 ± 4.6 mmHg, $\underline{P} = 0.031$); preflight to postflight reductions of their operational points (-6.9 ± 3.0 vs. -30.8 ± 4.7 %, $\underline{P} = 0.0005$); and weight lost during the flight (-0.79 ± 1.3 vs. -1.44 ± 0.5 kg, $\underline{P} = 0.0001$).

Results from backward elimination analysis showed that preflight to postflight changes of standing minus supine systolic pressures on landing day were predicted primarily by preflight to postflight changes of operational point ($P = 0.0041$) and preflight to postflight changes of body weight ($\underline{P} = 0.034$). The $\underline{R}$ value for the model was 0.64 $\underline{P} = 0.0034$). No other variables (preflight or postflight) contributed to the model.

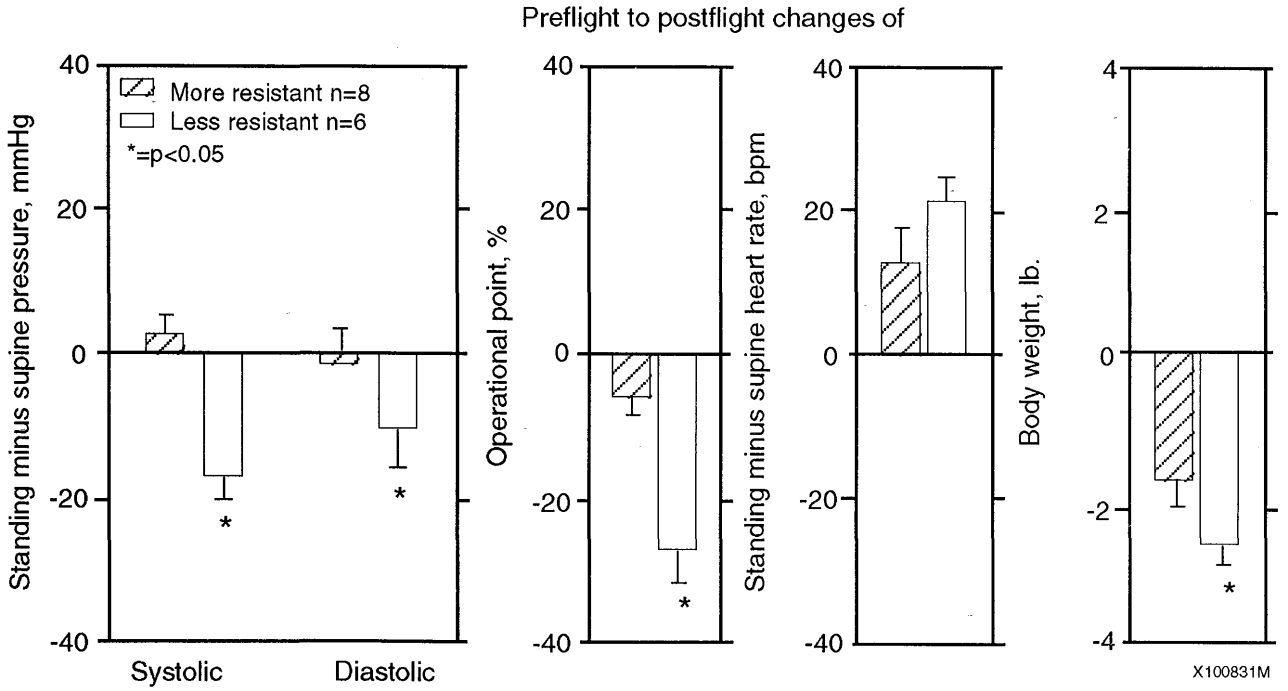

Figure 8. Comparisons between landing day measurements from the two groups identified by cluster analysis depicted in Figure 7.

On landing day, baseline, minimum, and maximum R-R intervals correlated directly with heart rate responses to standing (P = 0.003, 0.050, and 0.005). Slopes and ranges did not correlate with any variable measured during the stand test.

By R+3, stand test responses were not different from preflight values. Heart rate increases with standing averaged 18 + 2 (55 ± 2 to 73 ± 3, P = 0.014) beats/min, and systolic and diastolic increases with standing averaged 5 ± 2 (112 ± 2 to 117 ± 2, P = 0.78), and 12 ± 2 (69 ± 2 to 81 ± 1, P = 0.95) mmHg. The average R-R interval was reduced 287 ± 25 (1131 ± 50 to 844 ± 38) msec upon standing on this day. The group differences noted on landing day were no longer evident.

DISCUSSION

A profile of neck pressure and suction changes was delivered to 16 U.S. astronauts before and after brief (4- to 5-day) Space Shuttle missions to test the hypothesis that space travel impairs human baroreflex control mechanisms. Significant abnormalities of carotid baroreceptor-cardiac reflex were documented functions that on landing day were related to impairment of arterial pressure responses to standing. First, there was a reduction of estimated baseline vagal-cardiac traffic on landing day. Second, there was a reduction of cardiac responses to carotid baroreceptor stimuli; this change was insignificant on landing day, but was significant thereafter and persisted until the last measurements were obtained ten days after landing. Third, there was a reduction of standing minus supine systolic pressure increases on landing day that was predicted by preflight to postflight changes of baroreflex operational points and body weight. Fourth, cluster analysis identified two distinct groups of subjects on the basis of their landing day abilities to maintain standing systolic pressures; these groups were also different in their reductions of operational points, and their losses of body weight during flight.

Vagal Responses on Landing Day

Several measurements point toward reductions of baseline vagal-cardiac traffic and vagal responses to changes of baroreceptor input on landing day. Reductions of average baseline R-R intervals and their standard deviations reflect reduced levels of resting vagal-cardiac nerve traffic (Eckberg, 1983; Eckberg et al., 1988; Katona and Juh, 1975). R-R intervals were

evaluated because they provide linear estimates of vagal-cardiac nerve traffic (Katona et al., 1970; Parker et al., 1984). Reductions of R-R intervals were nearly significant on landing day ($P = 0.052$), and increases of baseline heart rate (a reciprocal of R-R interval which is a more important hemodynamic variable) over preflight levels were highly significant ($\underline{P} = 0.0008$). Reduced average slopes and ranges of baroreceptor stimulus-sinus node response relations (although not significant) reflected a trend toward reduction of vagal responsiveness to beat-to-beat arterial pressure changes. It is possible that the lack of significance on landing day is a beta-statistical error resulting from the reduction of sample size from 16 to 11. Reductions of the operational point positions (which were significant) reflect a proportionally greater loss of hypotensive than hypertensive buffering capacity.

It should be emphasized that although most of the changes documented were significant, they also were subtle and seemed not to impair crew performance during or following these very brief flights. Despite reductions of vagal responsiveness suggested by these measurements, crewmembers were asymptomatic. No subject reported difficulty exiting the Space Shuttle, and no subject exhibited syncope or presyncope during postflight stand tests. However, all subjects had exaggerated speeding of heart rate during standing (orthostatic tachycardia) after flight. Because our data document reduced capacity to increase heart rate by withdrawal of vagal outflow, exaggerated cardio-acceleration during standing probably was due to increased sympathetic-cardiac responses to standing. This interpretation is supported by a study which shows that rats experience significantly increased adrenomedullary responses to stress after space flight (Kvetnansky et al., 1981). Responses of astronauts are reminiscent of those of a patient reported by Rosen and Cryer (1982) who had chronic, unexplained hypovolemia associated with exaggerated increases of plasma norepinephrine and cardioacceleration with standing.

Persistence of Reduction of Vagal Responses

Impairment of R-R interval responses to carotid baroreceptor stimuli persisted for the duration of the period of data collection (8 to 10 days). Our documentation of protracted impairment of baroreflex function is not without precedent; there is substantial evidence that readaptation after weightlessness or simulated weightlessness to a gravity environment is a prolonged process. Following the 140-day Salyut-6 mission, cosmonauts had higher plasma catecholamine levels on the eighth day after flight than on landing day (Tigranian et al., 1980); following the 237-day Salyut-7 mission, cosmonauts' plasma catecholamines remained elevated for 25 days after landing (Kvetnansky et al., 1988); and following the 84-day Skylab-4 mission, astronauts' responses to lower body negative pressure did not return to preflight levels until 5 to 11 days after landing (Johnson et al., 1977). After 30 days of head-down bedrest, subjects' baroreflex function did not return to normal until after 5 days of ambulation (Convertino et al., 1990).

The orthostatic hypotension that occurs after longer space missions may be due in part to impairment of baroreflex function. Humans with arterial baroreceptor denervation (arguably the most severe baroreceptor impairment possible) may have orthostatic hypotension (Holton and Wood, 1965; Kochar et al., 1984). Importantly, conscious dogs with chronic baroreceptor denervation also have severe orthostatic hypotension (Cowley et al., 1973; Persson et at., 1988).

Correlations Between Carotid Baroreflex Function and Stand Tests

Astronauts in the group with reduced increases of systolic pressure during standing appeared to have two factors working against them. First, their postflight operational points were much lower than those of the more resistant group. Thus, they had less capacity for early heart rate speeding with standing, secondary to vagal withdrawal. Second, this group also had significantly greater losses of body weight (perhaps reflecting greater losses of plasma volume) after flight. Thus, impairment of blood pressure responses to standing on landing day in this group may have resulted from greater average blood volume reductions. Curiously, this group's impaired ability to maintain systolic pressure upon standing occurred despite an insignificantly greater cardioacceleration than that of the resistant group. This suggests that greater impairment of standing blood pressure responses may have resulted from factors unrelated to heart rate. Another study (Mulvagh et al., 1990) of astronauts' hemodynamic function before and after Space Shuttle flights (which included some of the same subjects as in this study) showed that increases of total peripheral resistance with standing are markedly reduced on landing day from preflight levels.

Mechanisms That May Contribute to Postflight Baroreflex Malfunction

There is no sure explanation for these findings; it seems unlikely that baroreflex impairment was caused simply by the blood volume reductions that occur after space missions (Johnson et al., 1977). Baroreflex abnormalities caused by prolonged head-down bedrest develop days after blood volume reductions occur and persist for days after blood volume returns to normal (Convertino et al., 1990).

The working hypothesis proposed by the investigators is that post-space flight baroreflex impairment results in some way from autonomic neural plasticity (Milgram et al., 1987) provoked by altered autonomic sensory input. In space, afferent neural traffic is probably altered in several ways. Changes of arterial and venous pressures (Hoffler et al., 1974; Kirsch et al., 1984) probably alter arterial and cardiopulmonary baroreceptor input, and decreases of left ventricular volume (Blomqvist and Stone, 1983; Winter, 1979) probably alter left ventricular receptor firing. Moreover, the usual disparity that exists between aortic and carotid pressures in sitting and upright positions is not present during weightlessness.

Limitations

This study was more difficult to conduct than usual studies involving human subjects because measurements were made before and after Space Shuttle missions. Changes of sleep/wake cycles, personal exercise regimens, quantity and quality of sleep, and diet (including fluid intake) before and during flights could not be controlled. Other factors, including launch and landing delays, equipment transport difficulties, and competition for subjects' time also conspired against orderly prosecution of this research. Landing day data are particularly difficult to obtain and interpret; these data are included, however, because of their potentially large practical importance.

In conclusion, vagally-mediated carotid baroreceptor-cardiac reflex responses were studied before and after short Space Shuttle missions. Subtle, but functionally relevant impairment of baroreflex responses that became more marked several days after landing and did not recover by 8 to 10 days after landing were found. This study reports the first evidence that baroreflex mechanisms are impaired after space flight.

ACKNOWLEDGMENTS

First and foremost, we are grateful to the 16 astronauts who donated their valuable time to this effort. They enthusiastically volunteered for this study which was conducted at times when they had extraordinary mission responsibilities. Without their cooperation this research could not have been done. We also thank Douglas T.F. Simmons for his statistical support, Debra F. Lanehart for her technical support, and Jay C. Buckey for loan of his equipment. This research was supported by NASA contracts NAS9-17720 and NAS9-16038, and NASA grant NAG2-408.

REFERENCES

Anderberg, M. R. Cluster Analysis for Applications. New York: Academic Press, 1973.

Blomqvist, C. G.; Nixon, J. V.; Johnson, R. L., Jr.; Mitchell, J. H. Early cardiovascular adaptation to zero gravity simulated by head-down tilt. Acta Astronautica 7: 543-553, 1980.

Blomqvist, C. G.; Stone, H. L. Cardiovascular adjustments to gravitational stress. In: Handbook of Physiology. Section 2: The Cardiovascular System. Volume III. Peripheral Circulation and Organ Blood Flow, Part 2, edited by J.T. Shepherd and F.M. Abboud. Bethesda, Maryland: American Physiological Society, 1983, p. 1025-1063.

Bungo, M. W.; Johnson, P. C., Jr. Cardiovascular examinations and observations of deconditioning during the space shuttle orbital flight test program. Aviat. Space Environ. Med. 54: 1001-1004, 1983.

Convertino, V. A.; Doerr, D. F.; Eckberg, D. L.; Fritsch, J. M.; Vernikos-Danellis, J. Head-down bed rest impairs vagal baroreflex responses and provokes orthostatic hypotension. J. Appl. Physiol. 68: 1458-1464, 1990.

Cowley, A. W., Jr.; Liard, J. F.; Guyton, A. C. Role of the baroreceptor reflex in daily control of arterial blood pressure and other variables in dogs. Circ. Res. 32: 564-576, 1973

Dietlein, L. F. Skylab: A beginning. In: Biomedical Results from Skylab, edited by R.S. Johnston and L.F. Dietlein. Washington, D.C.: National Aeronautics and Space Administration, 1977, p. 408-418.

Draper, N. R.; Smith, H. Applied Regression Analysis. New York: John Wiley & Sons, 1981, p. 294-352.

Eckberg, D. L. Human sinus arrhythmia as an index of vagal cardiac outflow. J. Appl. Physiol. 54: 961-966, 1983.

Eckberg, D. L. Respiratory sinus arrhythmia: a window on central autonomic regulation in man. In: The Peripheral Circulation, edited by S. Hunyor, J. Ludbrook, J. Shaw, and M. McGrath. Amsterdam: Elsevier, 1984, p. 267-274.

Eckberg, D. L.; Fritsch, J. M. Carotid baroreceptor ardiac-vagal responses during 10 days of head-down tilt (Abstract). Physiologist. 33(Suppl. 1): S177, 1990.

Eckberg, D. L.; Rea, R. F.; Andersson, O. K.; Hedner, T.; Pernow, J.; Lundberg, J. M.; Wallin, B. G. Baroreflex modulation of sympathetic activity and sympathetic neurotransmitters in humans. Acta Physiol. Scand. 133: 221-231, 1988.

Fritsch, J. M.; Rea, R. F.; Eckberg, D. L. Carotid baroreflex resetting during drug-induced arterial pressure changes in humans. Am. J. Physiol. 256 (Regulatory Integrative Comp. Physiol. 25): R549-R553, 1989.

Gibbons, J. D. Nonparametric Methods for Quantitative Analysis. New York: Holt, Rinehart and Winston, 1976.

Hoffler, G. W.; Wolthuis, R. A.; Johnson, R. L. Apollo space crew cardiovascular evaluations. Aerospace Med. 45: 807-820, 1974.

Holton, P.; Wood, J. B. The effects of bilateral removal of the carotid bodies and denervation of the carotid sinuses in two human subjects. J. Physiol. Lond. 181: 365-378, 1965.

Johnson, P. C.; Driscoll, T. B.; LeBlanc, A .D. Blood volume changes. In: Biomedical Results from Skylab, edited by R.S. Johnston and L.F. Dietlein. Washington, D.C.: National Aeronautics and Space Administration, 1977, p. 235-241.

Johnson, R. L.; Hoffler, G. W.; Nicogossian, A. E.; Bergman, S. A., Jr.; Jackson, M. M. Lower body negative pressure: third manned Skylab mission. In: Biomedical Results from Skylab, edited by R.S. Johnston and L.F. Dietlein. Washington, D.C.: National Aeronautics and Space Administration, 1977, p. 284-312.

Kakurin, L. I; Lobachik, V. I.; Mikhailovk, V. M.; Senkevich, Y. A. Antiorthostatic hypokinesia as a method of weightlessness simulation. Aviat. Space Environ. Med. 47: 1083-1086, 1976.

Kasting, G. A.; Eckberg, D. L.; Fritsch, J. M.; Birkett, C. L. Continuous resetting of the human carotid baroreceptor-cardiac reflex. Am. J. Physiol. 252 (Regulatory Integrative Comp. Physiol. 21): R732-R736, 1987.

Katona, P.G.; Jih, F. Respiratory sinus arrhythmia: noninvasive measure of parasympathetic cardiac control. J. Appl. Physiol. 39: 801-8051975.

Katona, P. G.; Poitras, J. W.; Barnett, G. O.; Terry, B.S. Cardiac vagal efferent activity and heart period in the carotid sinus reflex. Am. J. Physiol. 218: 1030-1037, 1970.

Kirsch, K. A.; Rzcker, L.; Gauer, O. H.; Krause, R.; Leach, C.; Wicke, H. J.; Landry, R. Venous pressure in man during weightlessness. Science. 225: 218-219, 1984.

Kochar, M. S.; Ebert, T. J.; Kotrly, K.J. Primary dysfunction of the afferent limb of the arterial baroreceptor reflex system in a patient with severe supine hypertension and orthostatic hypotension. J. Am. Col. Cardiol. 4: 802-805, 1984.

Kvetnansky, R.; Davydova, N. A.; Noskov, V. B.; Vigas, M.; Popova, I. A.; Usakov, A. C.; Macho, L.; Grigoriev, A. I. Plasma and urine catecholamine levels in cosmonauts during long-term stay on space sation Salyut-7. Acta Astronautica 17: 181-186, 1988.

Kvetnansky, R.; Torda, T.; Macho, L.; Tigranian, R. A.; Serova, L.; Genin, A. M. Effect of weightlessness on sympathetic-adrenomedullary activity of rats. Acta Astronautica 8: 469-481, 1981.

Lilliefors, H. W. On the Kolmogorov-Smirnov test for normality with mean and variance unknown. J. Am. Statist. Assn. 62: 399-402, 1967.

Milgram, N. W.; MacLeod, C. M.; Petit, T. L. Neuroplasticity, learning and memory. In: Neuroplasticity, Learning, and Memory, edited by N.W. Milgram, C.M. MacLeod, and T.L. Petit. New York: Alan R. Liss, Inc., 1987, p. 1-16.

Mulvagh, S. L.; Charles, J. B.; Fortney, S. M.; Bungo, M. W. Changes in peripheral vascular resistance may

account for orthostatic intolerance after space flight (Abstract). Circulation 82 (Suppl. III): III-515, 1990.

Murray, R. H; Krog, J.; Carlson, L. D.; Bowers, J. A. Cumulative effects of venesection and lower body negative pressure. Aerospace Med. 38: 243-247, 1967.

Parker, P.; Celler, B. G.; Potter, E. K.; McCloskey, D. I. Vagal stimulation and cardiac slowing. J. Autonom. Nerv. Syst. 11: 226-231, 1984.

Persson, P.; Ehmke, H.; Kirchheim, H.; Seller, H. Effect of sino-aortic denervation in comparison to cardiopulmonary deafferentiation on long-term blood pressure in conscious dogs. Pfluegers Arch. 411: 160-166, 1988.

Rosen, S. G.; Cryer, P. E. Postural tachycardia syndrome. Reversal of sympathetic hyperresponsiveness and clinical improvement during sodium loading. Am. J. Med. 72: 847-850, 1982.

Snedecor, G. W.; Cochran, W. G. Statistical Methods. Sixth edition. Ames, Iowa: Iowa State University Press, 1967.

Sprenkle, J. M.; Eckberg, D. L.; Goble, R. L.; Schlehorn, J. J.; Halliday, H.C. Device for rapid quantification of human carotid baroreceptor-cardiac reflex responses. J. Appl. Physiol. 60: 727-732, 1986.

Tigranian, R. A.; Kvetnansky, R.; Kalita, N. F.; Davydova, N. A.; Pavlova, E. A.; Voronin, L. I. Effect of space flight stress factors on the activity of the sympathetic adrenomedullary and the pituitary-adrenocortical systems. In: Catecholamines and Stress: Recent Advances, edited by E. Usdin, R. Kvetnansky, and I.J. Kopin. New York: Elsevier/North-Holland, Inc., 1980, p. 409-421.

Winter, D. L. Weightlessness and gravitational physiology. Fed. Proc. 36: 1667-1671, 1979.

Section Two: Neurophysiology

After-image ocular counterrolling goggles. With the crewmember's head stabilized by a dental bite, he viewed an inverted "T" that appeared as an after-image on the retina. Measurement of eye torsion was accomplished by then matching the retinal image with a reference target. The OCR goggles were a part of the Otolith Tilt-Translation Reinterpretation (DSO 459).

DSO 459: Otolith Tilt-Translation Reinterpretation

Investigators: Millard F. Reschke, Ph.D.; Deborah L. Harm, Ph.D.; Donald E. Parker, Ph.D.; William H. Paloski, Ph.D.

INTRODUCTION

The research described in this final report for DSO 459 was derived from the recently hypothesized Otolith Tilt-Translation Reinterpretation (OTTR) Hypothesis, described below.

After adaptation to weightlessness, information from receptors that normally transduce stimulation due to gravity is used differently by the brain (e.g., cortical representation of movement and spatial orientation). On Earth, information from the otolith receptors is perceived (interpreted by the brain) as either linear motion or as head/body tilt with respect to gravity. Because stimulation from gravity is absent during orbital flight, interpretation of otolith input as tilt is meaningless. Therefore, the brain adapts to weightlessness by reinterpreting all otolith receptor output as linear motion, and stimulation of the otoliths is perceived as translation. Immediately following return to Earth and before the brain readapts to the normal gravity force environment, this new interpretation persists, and both linear motion (acceleration) and tilt are perceived as translation (Parker, 1985).

In this particular investigation, three specific tasks were performed by participating crewmembers:

The first task was developed to examine ocular counterrolling (OCR) during orbital flight with the intent of investigating the possibility that torsional eye movements may (1) develop as a functional orientation response in the absence of normal terrestrial otolith shearing provided by gravitational forces, and (2) support the hypothesis of central reinterpretation of otolith function in response to the stimulus rearrangement of the microgravity environment. Measurements of OCR were obtained preflight, in flight, and postflight. Estimating the amount of eye torsion (OCR) elicited by static tilt of the head in the roll plane was accomplished by placing an afterimage on the observer's retina, which could be matched to an external target.

The second task looked at postural responses with two different methods. First, postural stability was investigated by requiring crewmembers to bend at the waist in both the pitch and roll axes. Based on the OTTR Hypothesis, it was postulated that vision, proprioceptive, and vestibular signals normally provide feedback as a person attempts to bend from the waist to a particular angle of tilt. If visual signals are eliminated and if the otolith output is not interpreted as tilt immediately postflight, then the magnitude of the feedback signal during voluntary tilting should be reduced. Consequently, the astronauts should not bend too far as they attempt to perform roll or pitch movements. The second posture test estimated sway as a function of visual stabilization and platform tilt. Again, the OTTR Hypothesis would suggest that if otolith input following flight was not interpreted as tilt and vision was coupled to the person's sway (when tilting with the eyes open the visual surround tilts with the person), then postural stability would be degraded.

The third task required crewmembers to describe perceived motion as a function of voluntary head movements in flight and postflight. An attempt was made to acquire responses to head movements during the entry phase of flight and was partially accomplished by astronaut subjects whose duties permitted participation in this aspect of the investigation. It was hypothesized that roll, pitch, and yaw (because the otoliths are not co-located on the axis of motion) would result in the perception of translational self or surround motion during entry and immediately postflight. In flight, following the newly interpreted otolith signals as translation, static tilt of the head (or head and body) would be meaningless, and the response to head movements of a magnitude large enough to excite the otoliths would be perceived as translational in nature.

PROCEDURES

The procedures used in this DSO represent continuation of the procedures designed to investigate the concept of otolith reinterpretation established following the flight of STS-8 (Parker et al., 1983; Parker et al., 1984a; Parker et al., 1984b; Parker et al., 1985; Reschke et al., 1984a; Reschke et al., 1984b). Beginning with STS 41-B and including STS-28, a total of 12 astronauts had completed various portions of this investigation. Nine of the 12 astronauts participated in DSO 459 (designated as astronauts 7-12), and three were drawn from DSO 449 (designated as astronauts 4-6). Experimental methods have been varied across flights as appropriate to enhance data collection on specific procedures in need of further research and either eliminated or reduced in scope for those responses that have been adequately studied.

Astronaut Eye Torsion Measurements

After-image OCR was measured with a set of goggles that contain a reference target and a strobe to place an upside-down "T" after-image on the retina. A head strap was used for the STS-24 through STS-26 flights to hold the head and help prevent movement of the head relative to the goggles. To ensure that data observed from the early flights were not due to residual slip between the head and the goggles, a dental bite was added as a replacement for the head strap on the STS-28 flight. The interface between the main body of the goggles and the mounting surfaces was fitted with a set of suction cups and a tilt assembly. The tilt assembly allowed the goggles to be moved in 15° increments either clockwise or counterclockwise. Looking into the goggles (Figure 1) the subject saw with the left eye a digital display that indicated the amount of target rotation providing a 2000 count output for a displacement of ± 20°, allowing a resolution of 1.2 ft of rotation per count. There was, however, a small amount of hysteresis in the thumb-wheel control that the subject used to set the reference target and in the potentiometer used for the measurement of angular torsion. This resulted in an absolute accuracy of 10 ft of rotation. The inverted "T" served as both the target and reference template and was milled into a disk controlled with the thumb-wheel. Behind the disk was an electronic photo flash with the flash-ready light positioned so that the inverted "T" was visible to the subject's right eye (Figure 1).

The goggles were attached to a wall (preflight and postflight data collection) or to the forward middeck lockers (in flight). All data were collected with the crewmembers in the standing position. In flight the subjects' feet were held to the floor of the middeck with foot restraints. Eye torsion measurements were obtained with static neck tilts in the roll plane at angles of 0° and ±15°, 30°, 45°, and 60°. The order of tilt angles was randomized with the constraint that the same tilt angle would not be used consecutively.

Measurements were first made by asking the subject, while the head was aligned with the body, to set the reference target so that it was vertical by adjusting the target with the thumb-wheel until a readout of approximately 1000 was visible on the digital display. Once the reference target was in the vertical position, the subject, with assistance, tilted the goggles and head to the randomly selected angle of tilt. The subject maintained this position for 30 sec to allow for stabilization of the eye torsion; the electronic flash was enabled to establish the after-image on the retina; and then the subject's head and the goggles were returned to the upright position. Once in the upright position, the subject would shut his eyes, slightly displace the thumb-wheel either to the right or left (but never the same direction twice), then open his eyes and set the reference target with the thumb-wheel so that it matched the retinal after-image. Angle of tilt (digital count) was read from the digital display, recorded with a voice activated tape recorder (in flight), or noted in a prepared checklist (preflight and postflight). An additional two measurements were made by closing the eyes, displacing the thumb-wheel, and matching the target to the after-image for a total of three readings at each angle of tilt.

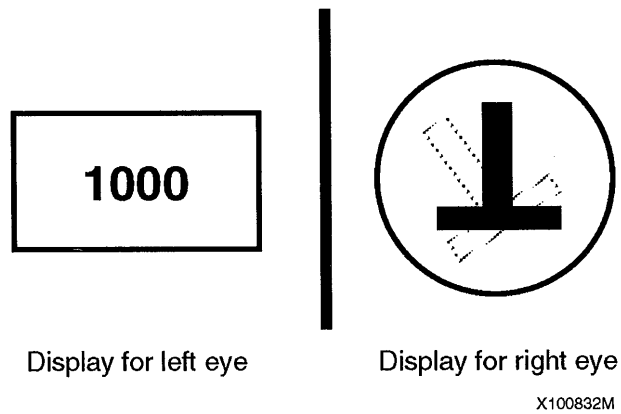

Figure 1. Goggle visual display.

On the ground the goggles were calibrated with a precision carpenter level, and prior to each data collection session the level was used to set the body of the goggles perpendicular to gravity, ensuring that the long arm of the inverted "T" when the digital display was set to 1000 was parallel to gravity. In flight the goggles were aligned with a template that had been attached to the forward locker and placed such that the head would be aligned with the body.

Measurement of Eye Torsion in the Normative Population

In addition to the flight investigation of OCR, normative responses were obtained from 12 subjects recruited from the JSC subject pool. OCR was measured in these subjects in three conditions: standing, whole body tilt, and supine. The whole body tilt condition served as a control experiment to investigate the extent of eye torsion elicited under normal terrestrial conditions without cervical input. Eye torsion was obtained in the supine position to evaluate cervical input without otolith shearing forces.

The goggles in these normative control studies was the training unit used to collect astronaut preflight and postflight data and to train the astronauts. The methods for the standing control study duplicated those used in testing the astronauts. In the supine position, subjects lay on the floor on a lightweight foam pad with the goggles fixed above them in such a way that the long arm of the inverted "T" (and the digital display set to 1000) was in line with the head, neck, and trunk. In the whole body tilt condition, a pitch and roll device (PARD) located in the JSC Neuroscience Laboratory was used to tilt the body and head together at the same angles of tilt used in the standing and supine experiments. The goggles were attached to a pallet directly in front of the subject's face and calibrated with a level. Once the subject, PARD, and goggles were in a vertical position, the subject was moved to a predetermined and randomized position of tilt under servo control at a rate less than $2°/sec^2$, remaining in the desired tilt position for 30 sec prior to establishment of the after-image on the retina. Once the after-image was in place, the subjects were immediately returned to the upright position at less than $2°/sec^2$. A minimum of three measures of eye torsion were obtained for each angle of tilt in all three control experiments.

Voluntary Tilt

The astronauts were placed adjacent to and immediately in front of two walls on which 20° off-vertical lines were located. Subjects were required to tilt from the waist with their feet together and arms folded across their chests until their torso was aligned with the reference line on the wall when the eyes were open, or to imagine the external reference when their eyes were closed. Videotape records of the subjects with targets placed on the body were obtained and later analyzed at a rate of six frames per second to determine angle between the foot and hip, the hip and shoulder, and finally between the shoulder and head. Figure 2 depicts the placement of the targets and the angles used for determination of tilt magnitude.

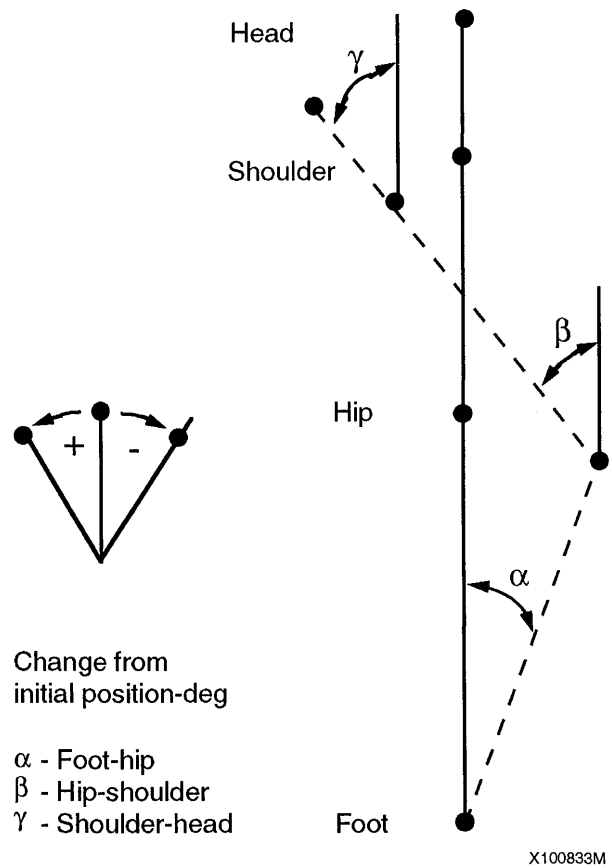

Figure 2. Body segments selected for angular measurement during active posture tests.

Postural Sway and Visual Stabilization

Tilt posture, postural sway, and the effects of visual stabilization on postflight postural ataxia were measured pre- and postflight. The test required that when the subject moved his head or body, the visual scene moved with him (visual stabilization). This was accomplished by fitting the subject with a pair of goggles equipped with a visual field display cone. The subject stood on the platform with feet together, arms folded, and ankles centered over the fulcrum of the platform which could either tilt in the pitch plane or be held stationary. The tilt of the platform was damped with foam (see Figures 3b-c). An ankle goniometer was used to measure ankle rotation in the pitch plane (rotation about the Y-axis). In conditions where the platform was free to tilt, the crewmembers' task was to keep the platform as level as possible. In conditions where the platform was fixed, the task was simply to maintain a stable upright posture. Crewmembers were tested under four visual conditions, presented in random order for 30 seconds each, once with the platform held stationary and once with the platform free to tilt. The four visual conditions were (1) goggles with a light emitting diode (LED) display pattern turned on (visual stabilization), (2) goggles with the LEDs turned off and eyes open (eyes open in darkness), (3) goggles with eyes closed, and (4) no goggles/eyes open in normal room illumination.

Figure 3a is a schematic of the posture test setup. Figure 3b is a schematic of the critical platform damping characteristics. Figure 3c is a plot of the reaction, i.e., damping characteristics of the foam, as a function of platform tilt angle. Figure 4 represents the four visual conditions that were used with this task.

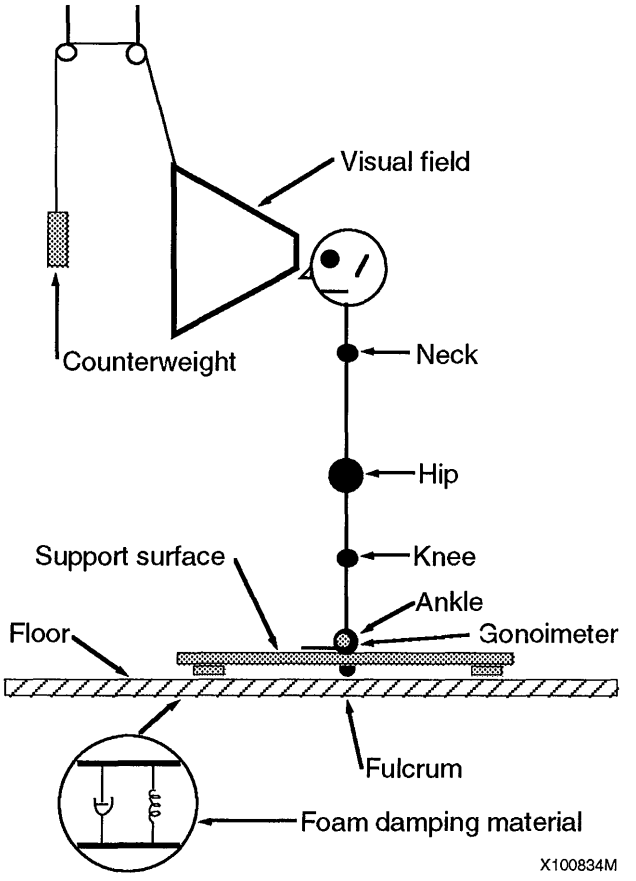

Figure 3A. Posture schematic.

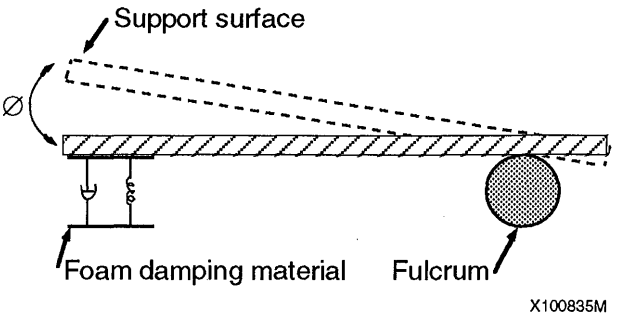

Figure 3B. Critical platform damping.

Motion Perception Reporting

Crewmembers described self or surround motion elicited by slow (.25 Hz), low amplitude (±20°) head movements in the pitch, roll, and yaw axes with their eyes open, and eyes closed in flight, during entry, and immediately after wheels stop. Preflight, crewmembers were briefed on the use of a set of vocabulary terms that provided quantitative descriptions of physical characteristics of self/surround motion. Practice in using the "Quantitative Motion Perception Reporting System" was provided by presenting crewmembers with a set of complex motion profiles in the JSC Neuroscience tilt-translation Preflight Adaptation Training (PAT) device. Self-motion and visual-surround motion perception were voice recorded in flight, during entry, and while the orbiter was stationary on the runway after landing. When possible, the audio tape was reviewed with participating crewmembers immediately following egress, and crews were interviewed in the baseline data collection facility (BDCF) on video tape. The video tapes were reviewed with the crews during additional postflight debriefs.

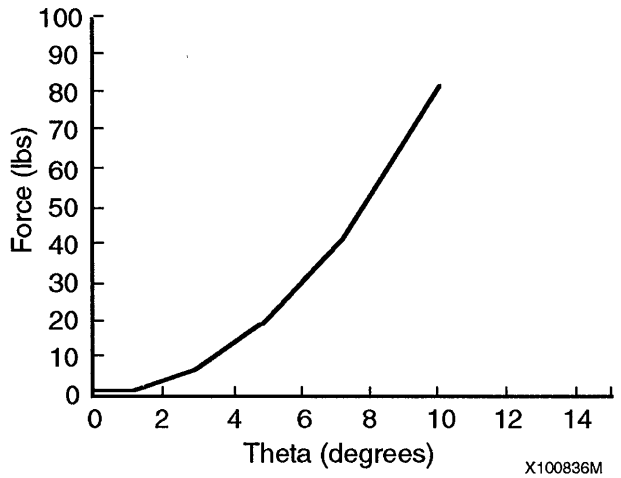

Figure 3C. Reaction of foam to platform tilt.

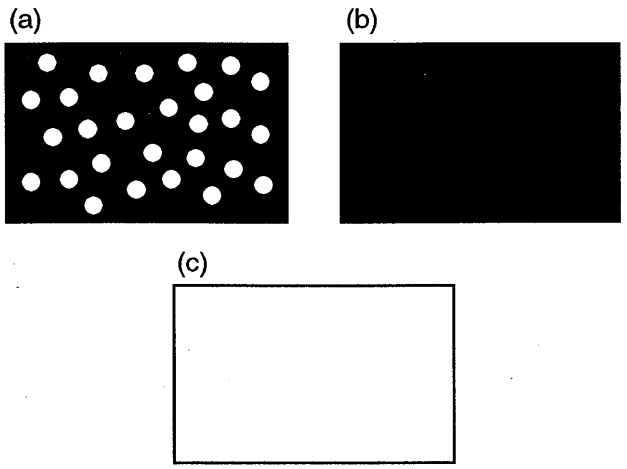

(a) Random red LED dot pattern presented in darkness.

(b) Total darkness.

(c) Head mounted visual field removed. Subject free to view surroundings or instructed to keep eyes closed.

X100837M

Figure 4. Visual display conditions.

RESULTS

After-Image OCR

Normative Eye Torsion

The data obtained during whole body tilt, presented in Figure 5 show clear counterrotation of the eye as a function of otolith shearing forces. A positive value represents a clockwise body tilt on the x-axis and a clockwise torsion of the eye on the y-axis. This figure presents the average of each of the 12 normative subjects' three trials at each of the body tilt angles. Notice that the ratio of eye torsion to whole body tilt decreases as the angle of tilt increases. An average of all points was fit with a third order polynomial which levels off at approximately ±60°. This data, though of lower magnitude compared with that obtained with more objective measures of eye torsion (i.e. photographic measures of counterroll), suggest that the after-image method of measurement is a good approximation of eye torsion (Figure 6) (Miller, 1969; Diamond et al., 1982).

Eye torsion obtained in the supine position is shown in Figure 7. Note that there is a slight offset where measurements obtained in the position where the neck and long arm of the inverted "T" are aligned with the body. This offset (points do not cross zero) probably represents the fact that, unlike the whole body or standing positions, it was not possible to precisely align the head with the trunk. Note that data were only presented for head and neck angles

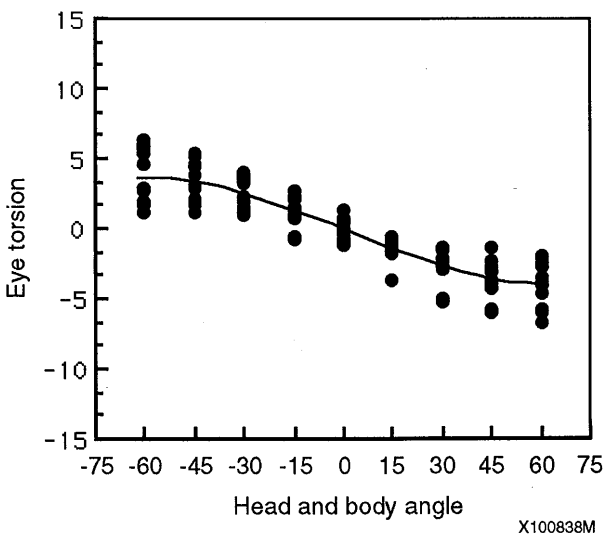

Figure 5. Whole body normative data.

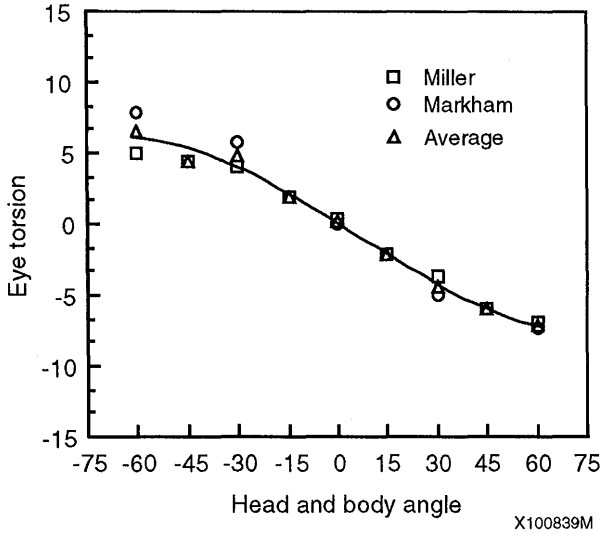

Figure 6. Photographic determination of eye torsion.

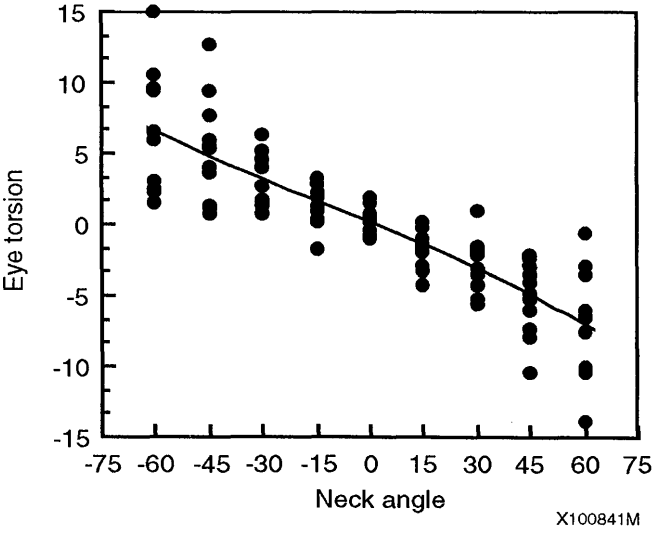

Figure 8. Standing normative data.

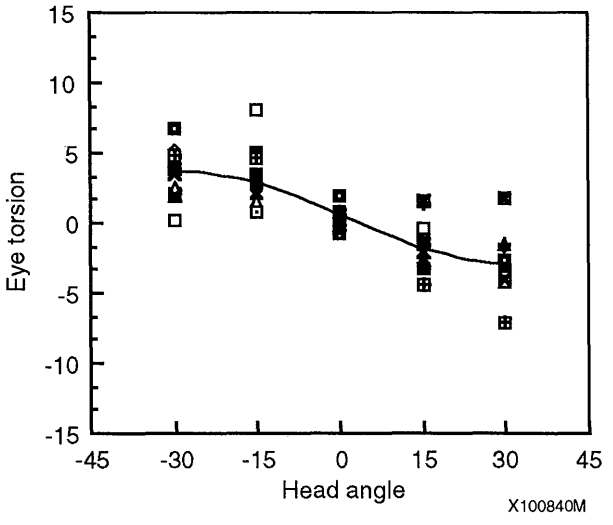

Figure 7. Normative supine plot.

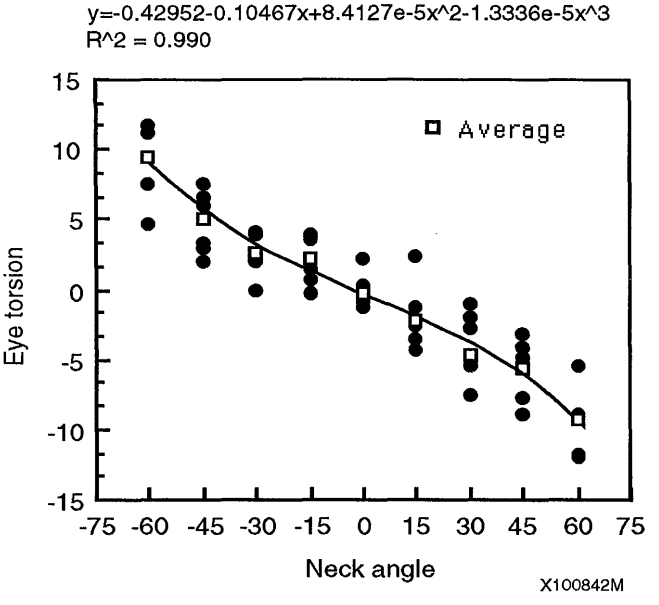

Figure 9. Preflight eye torsion.

of ±30°. Angles more extreme than ±30° resulted in a slip of the goggle relative to the head, and resulted in extreme angles of eye torsion (an additive effect between the after-image and the alignment target). In fact, there is no assurance that the eye torsion measured for neck angles less than ±30° truly represents eye torsion due to cervical input alone without goggle slip.

Standing Normative Data

The standing data observed in the normative population is presented in Figure 8. The expected ratio of decreasing eye torsion with increasing neck-to-body angle did not occur. The third order polynomial is fit to the average value for each angle of tilt. Three factors may contribute to the linear nature of this data set: (1) the goggles slipped relative to the head at the more extreme angles of head tilt, (2) variance increased as tilt angle increased, mostly due to a limited number of outlying data points, and (3) cervical input contributes in an additive fashion at the extreme angles to eye torsion normally attributed to otolith shearing.

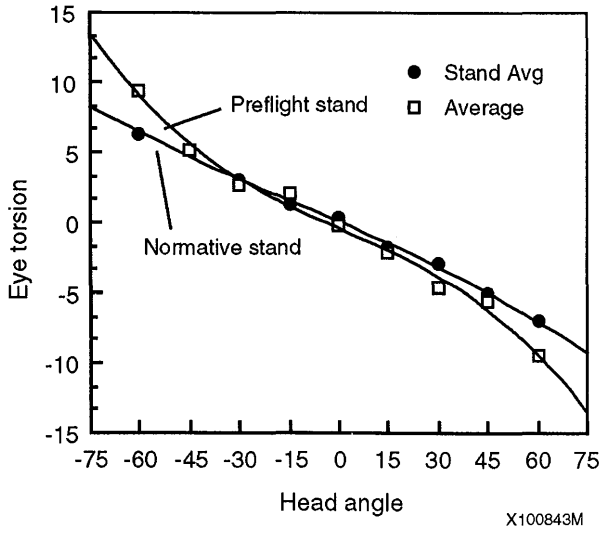

Figure 10. Preflight normative stand.

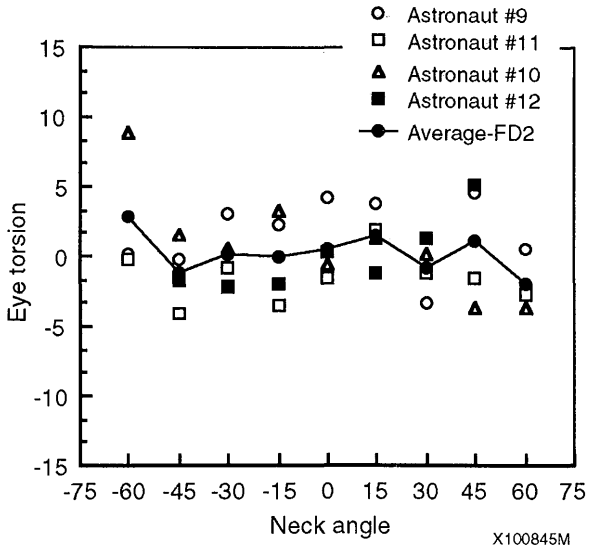

Figure 11B. FD-2 eye torsion.

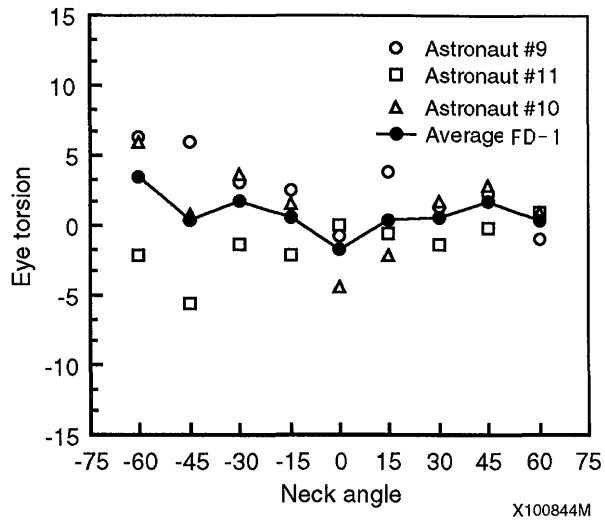

Figure 11A. FD-1 eye torsion.

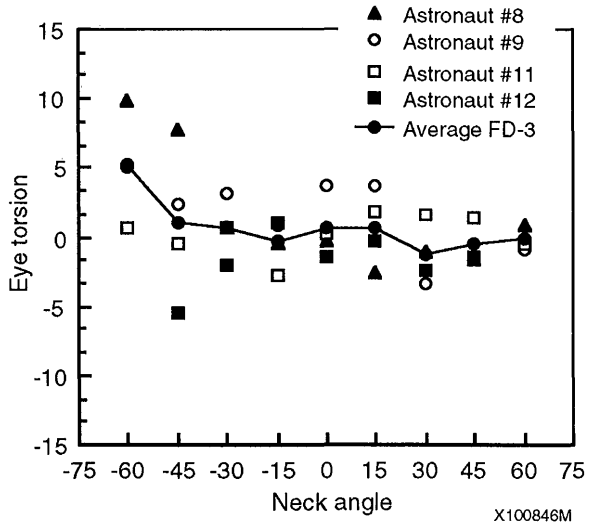

Figure 11C. FD-3 eye torsion.

Eye Torsion in the Flight Experiment

Figure 9 shows the preflight average obtained from the six participating crewmembers. Each point on the plot represents the average of three preflight measurement sessions for each of the six. Because the method of eye torsion measurement chosen for this experiment relied upon the ability of the subject to align an after-image placed on the retina with a target line, it is interesting to compare these results with data obtained from non-astronaut subjects using the more traditional photographic method of eye torsion measurement. The results from this comparison showed that the after-image method was very comparable, particularly over the range of ±45°. A third order polynomial fit to the data suggests that beyond ±45° there is an increase in the ratio of eye torsion to head tilt rather than the expected decrease in this ratio. Figure 10 compares the data (third order polynomial fit to average) from the astronaut subjects with that obtained from the normative population. Note that beginning at approximately ±30°, there is a divergence of the astronaut from the normative population. Again, the difference could be due to goggle slip, variance in the data, or cervical input.

Figures 11 a-c illustrate the eye torsion obtained in flight and plotted by day. Note that of the four astronauts participating, only three astronauts

participated on flight day 1 (FD-1). Flight days beyond FD-2 are all treated as FD-3. It is difficult to detect a pattern in this average data that would suggest the existence of eye torsion during flight that could be attributed to cervical sensory factors. Unlike data obtained on the ground, there is little to suggest that goggle slip contributes to the ratio of eye torsion to increasing angles of the neck. In addition, there is no indication that eye torsion either increases or decreases as a function of length of exposure to microgravity.

Figures 12 a-f present the data obtained in flight from the individual crewmembers. When plotted as a function of individual crewmembers, only astronauts #4 and #6 recorded data that suggest a trend of eye torsion based on increasing angles of the neck relative to the body. Figure 13 is the average across all flight days. When the average is taken for all crewmembers, it can be seen that no eye torsion exists for head tilts to ±45°. Beyond ±45° there is a slight increase in ocular counterroll, probably due to a slip between the goggles and the head. The implication is that cervical input does not contribute to eye torsion in the absence of a 1-g load.

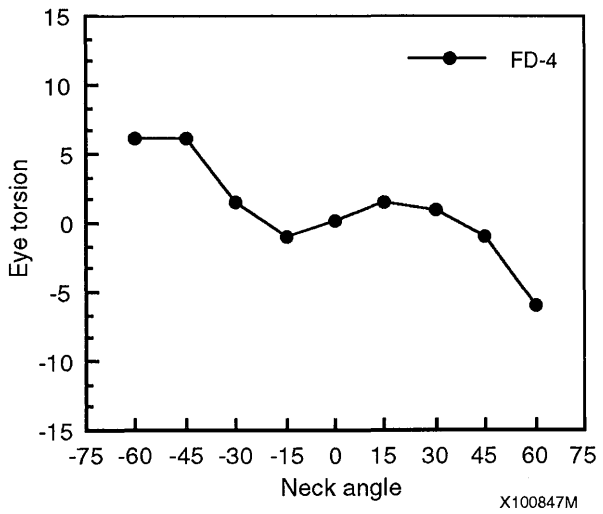

Figure 12A. Astronaut #7 in-flight data.

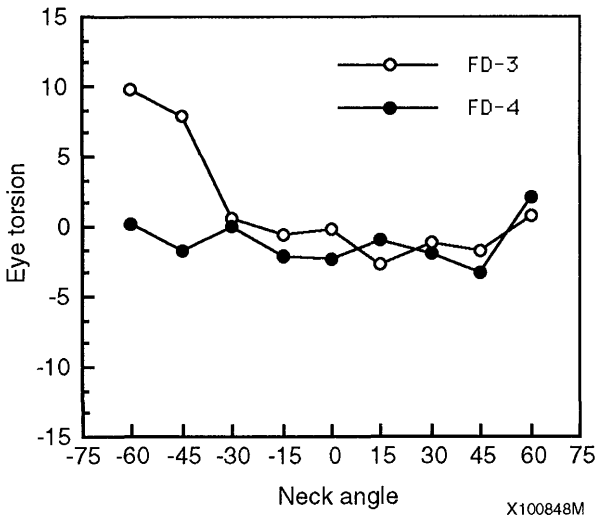

Figure 12B. Astronaut #8 in-flight data.

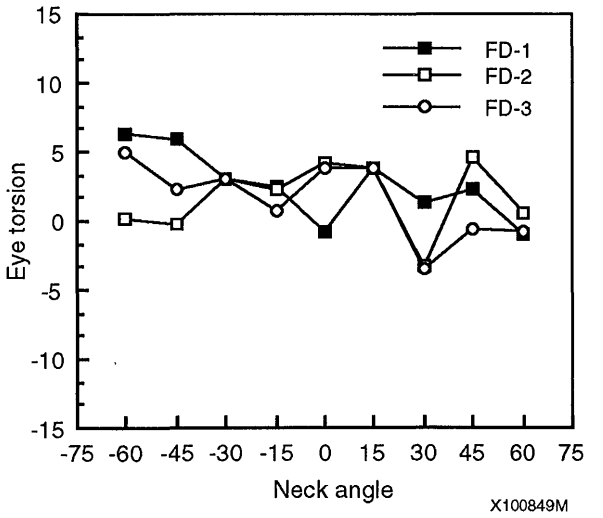

Figure 12C. Astronaut #9 in-flight data.

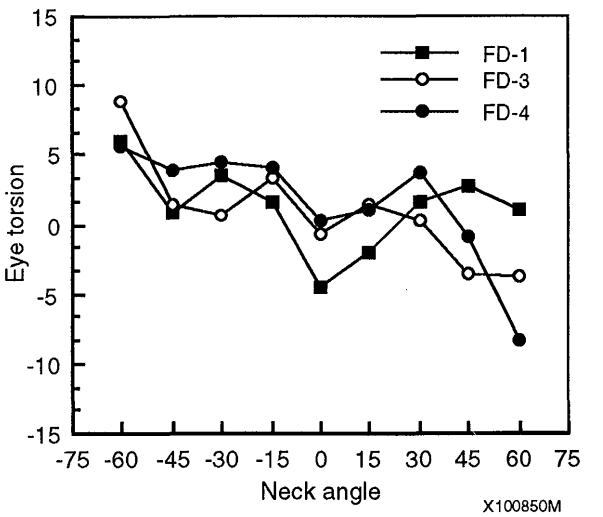

Figure 12D. Astronaut #10 in-flight data.

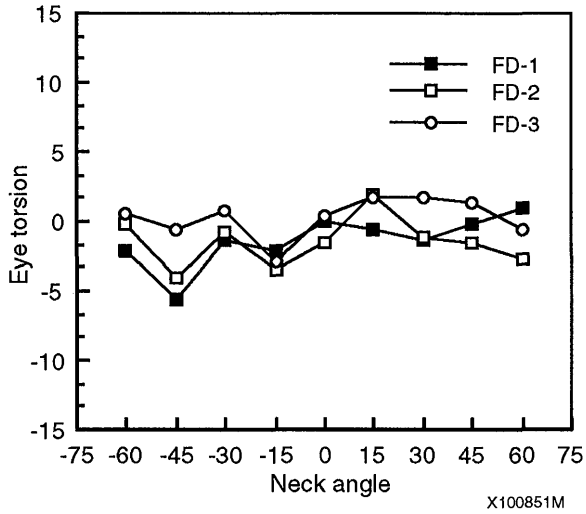

Figure 12E. Astronaut #11 in-flight data.

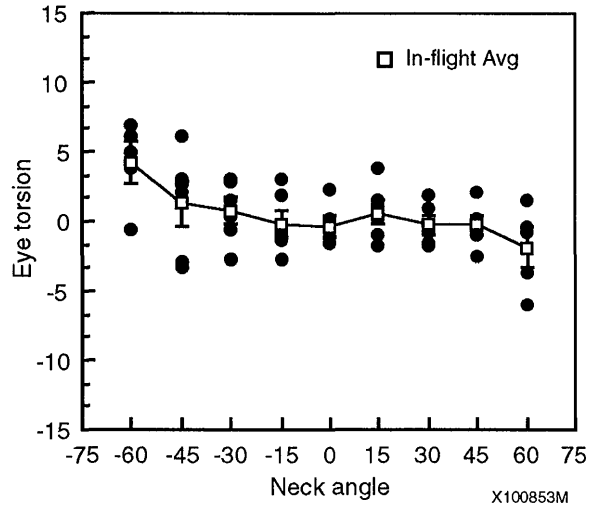

Figure 13. In-flight average.

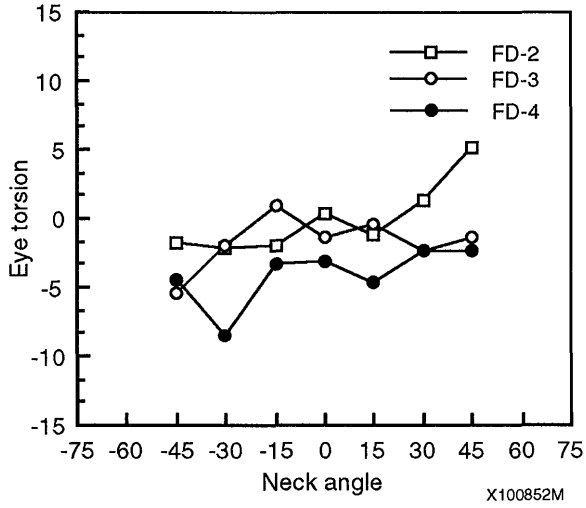

Figure 12F. Astronaut #12 in-flight data.

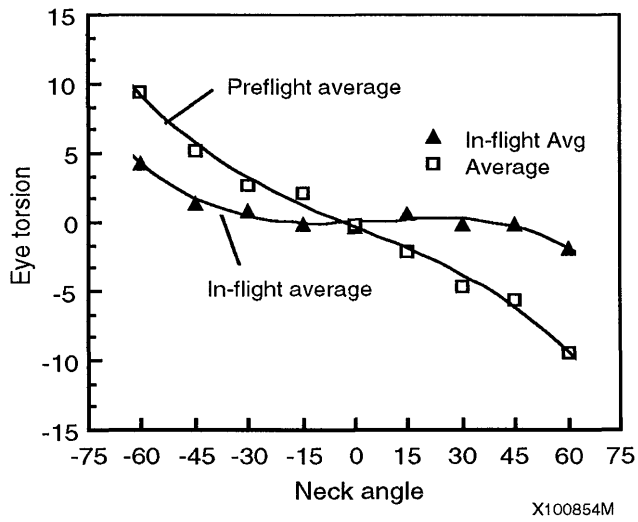

Figure 14. Preflight versus in-flight.

Figure 14 compares the average data with third order polynomial fit of the responses in flight to the preflight. If the responses are limited to ±45° in both cases, then the preflight data suggest the appropriate decrease in eye torsion to increasing angles of head tilt, and the in-flight responses show no indication of torsional eye movements during exposure to microgravity.

Figures 15 a-f show the postflight eye torsion data plotted for individual crewmembers as a function of day. Across all crewmember data, there is a trend toward reduced counterrolling immediately postflight and toward a unilateral reduction in torsion, particularly when the head is tilted clockwise and the eye responds with a counterclockwise compensatory torsion. When the data are averaged, the reduced torsion is clearly evident (Figure 16). Figures 17-19 show the average preflight data plotted against the average for R+0, R+2, and R+3 (includes all postflight data beyond R+3). There is a clear trend toward the preflight responses. By R+3 the eye torsion is almost equivalent to that recorded preflight, but recovery is not yet complete.

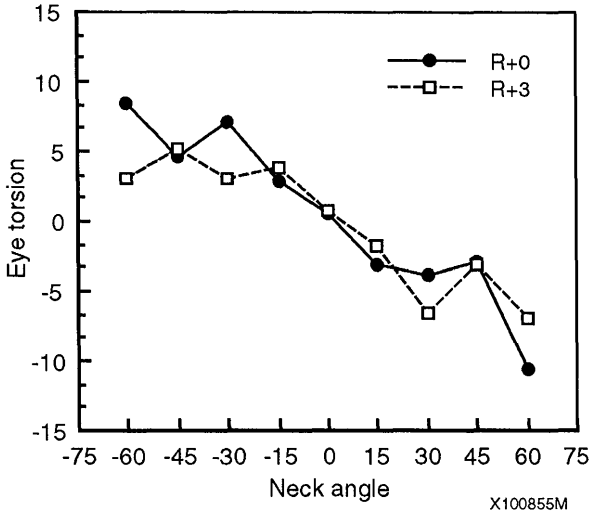

Figure 15A. Postflight torsion astronaut #7.

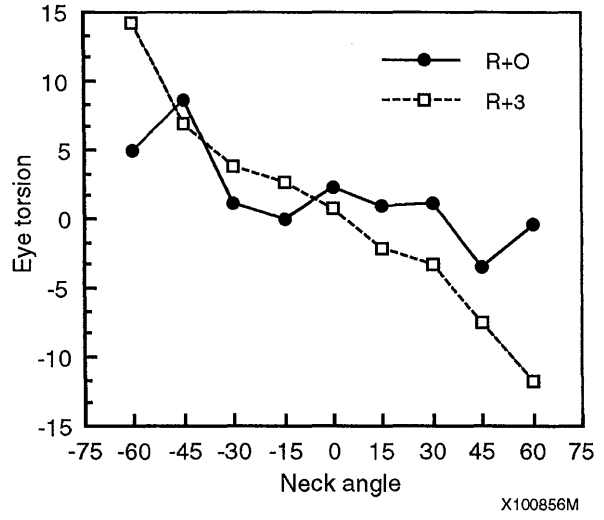

Figure 15B. Postflight torsion astronaut #8.

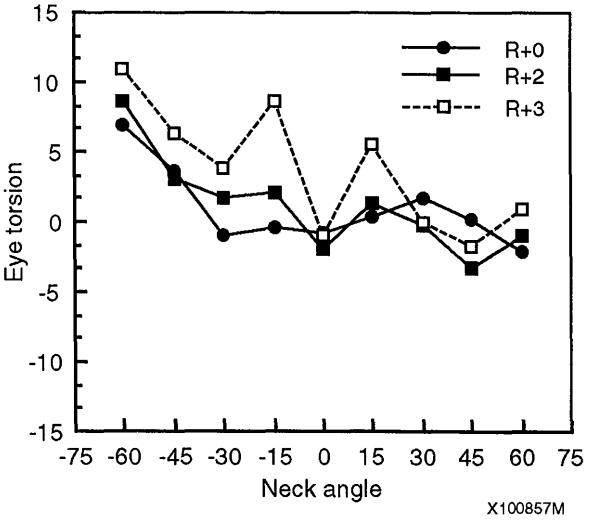

Figure 15C. Postflight torsion astronaut #9.

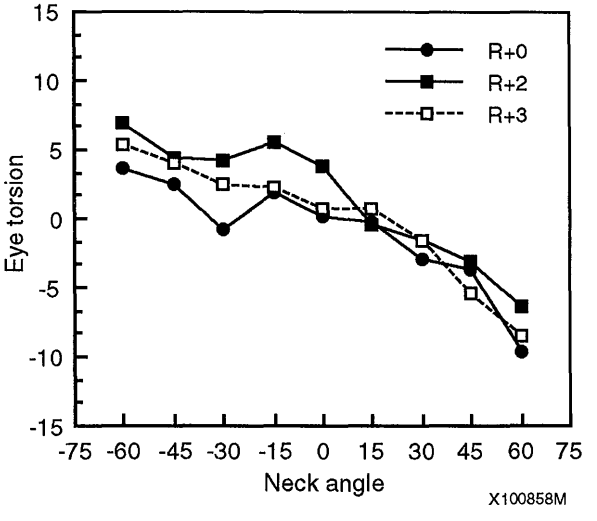

Figure 15D. Postflight torsion astronaut #10.

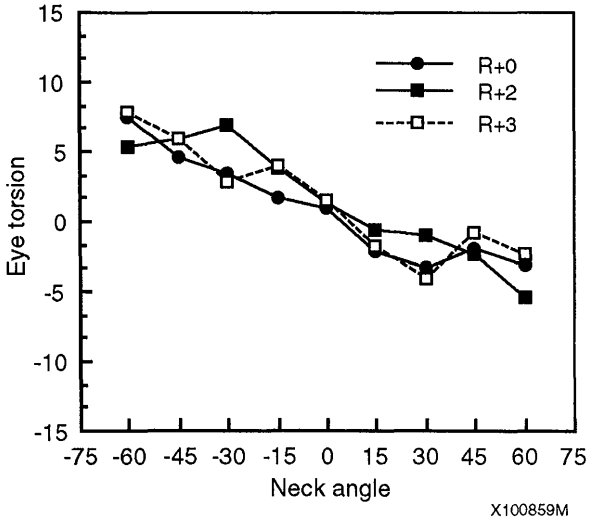

Figure 15E. Postflight torsion astronaut #11.

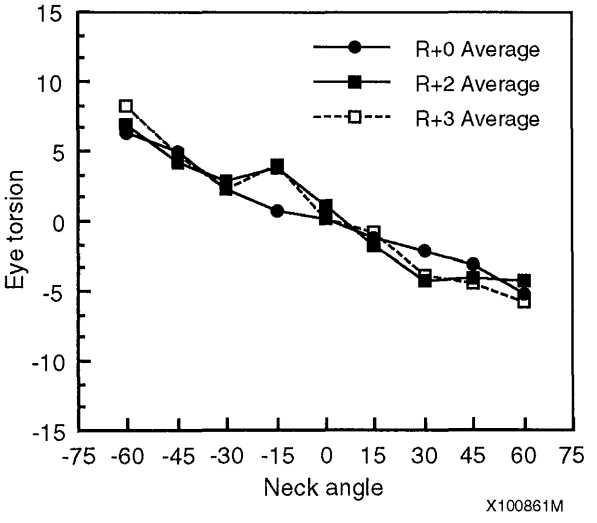

Figure 16. Postflight eye torsion average across crew-members.

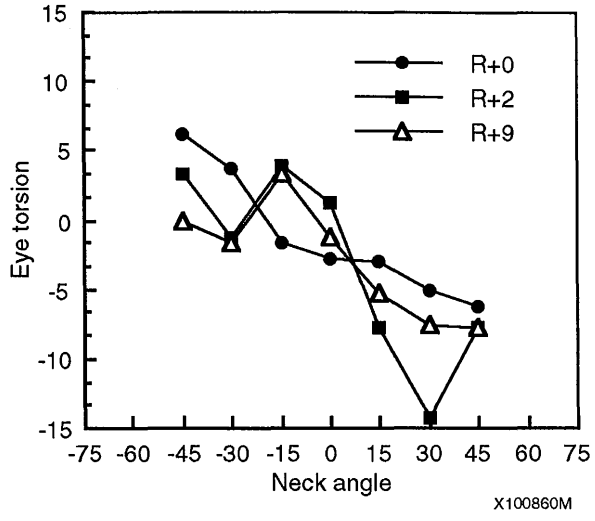

Figure 15F. Postflight torsion astronaut #12.

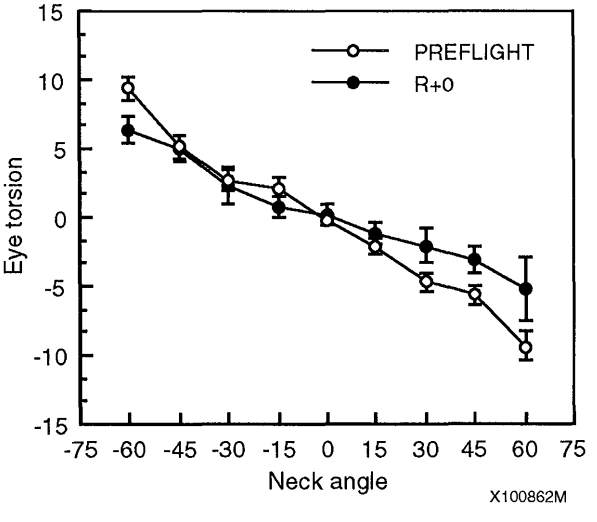

Figure 17. Preflight and R+0 average.

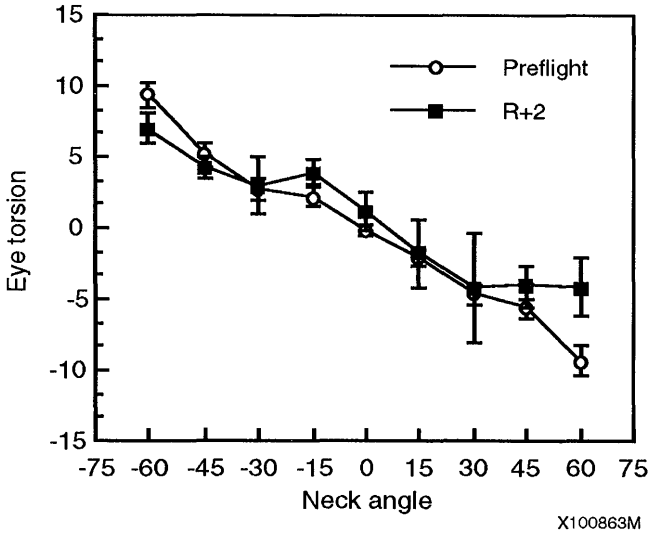

Figure 18. Preflight and R+2.

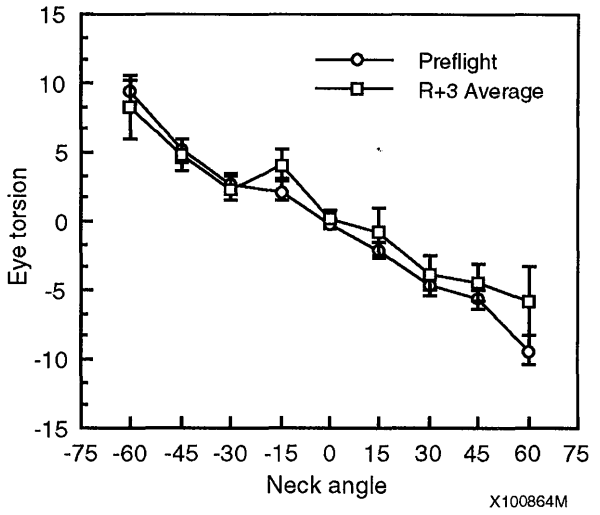

Figure 19. Preflight and R+3.

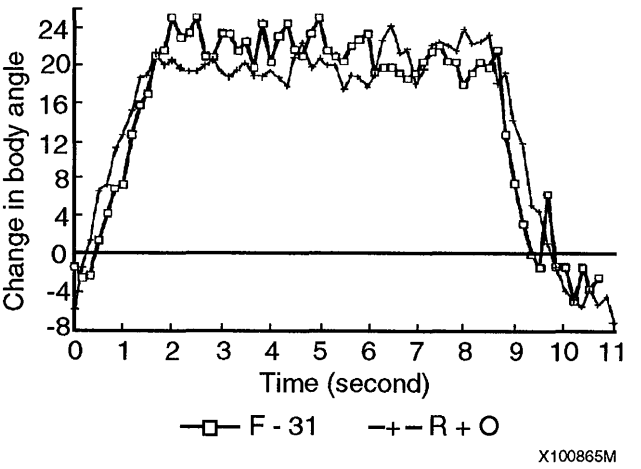

Figure 20. Tilt posture.

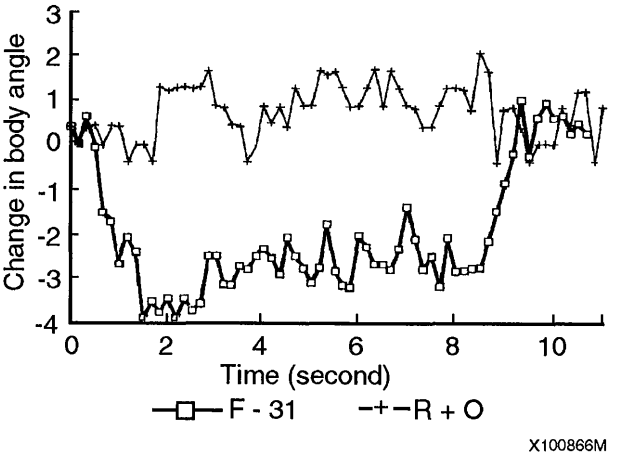

Figure 21. Tilt posture.

Voluntary Tilt

Pitch and roll voluntary body tilt immediately postflight was not different in magnitude of tilt from preflight (Figure 20). One crewmember indicated that he relied more than usual on waist joint receptor cues when performing the voluntary tilt maneuver with his eyes closed. He also stated that he probably could not have performed the task within minutes after landing. Other astronauts reported using their toes by "digging" them in to the floor as opposed to the preflight flat-footed strategy. While amplitude of tilt did not vary significantly following flight, there was a definite change in strategy between use of the hips and shoulders. The hips were thrust backward more postflight, and the angle of the head indicated an attempt to stabilize the head in space, thus ensuring that gaze was maintained (Figure 21).

Postural Sway and Visual Stabilization

Figure 22 shows one crewmember's response to the posture task where the goal was to keep the support platform balanced while wearing the visual stabilization goggles with the visual LED pattern present. This task was hypothesized to be the most difficult since there was little or no information available from the ankle joints, and the visual world was sway-referenced to the subject (providing little or no

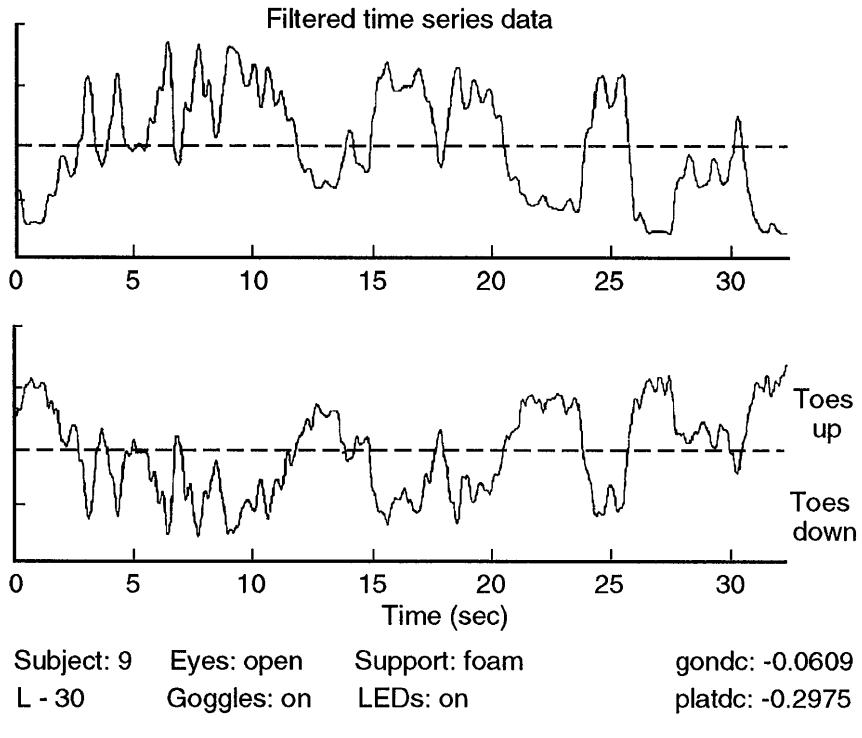

Figure 22. Body sway during posture testing.

information from the eyes as to body position in space). The top trace represents the ankle angle taken from the goniometer where upright (center) is 90°, and the lower trace represents the angle of the platform from the level position (0°). Also indicated in the lower trace is the position of the toes relative to the level position. Positive angles represent the toes up position and negative values are the toes down position. For the purposes of analysis, both the ankle and platform data were decimated by a factor of 2, then filtered using a 25-point FIR filter. The DC offset position over time is represented by a dashed line.

Figure 23 shows the data set represented in Figure 22 after the data have been rectified. The dashed lines in each trace represents the average sway value. The average values of the data were computed using the following equation:

$$\text{Average Sway Value} = \frac{\sum_{i=1}^{n} A_i \times \Delta t}{t}$$

where :
t = total time integral
Δt = change in time between samples
n = total number of samples
A = value of the i th sample of the data set

Figures 24-26 present the sway data obtained from the three crewmembers (astronauts 9, 10, and 11) under three visual conditions when the platform was fixed (i.e., equivalent to standing on the floor). The Y-axis shows the average sway for the platform and ankle, where a value of 1 represents maximum sway. The X-axis indicates the time of the test (i.e., test sessions L-30, L-10, L+0, L+2, and L+3). The sway for three visual conditions is indicated by symbols (+ = Eyes open, goggles not worn; 0 = Eyes closed, goggles on, and LED display off; x = Eyes open, goggles on, and LED display on).

The fixed platform sessions provided the subjects with information from their ankle position. And, in the fixed platform, eyes-open viewing the laboratory under normal illumination, their performance should have been near perfect in the preflight trials. Immediately following the flight it was expected that the eyes-open condition with vision sway referenced (LED pattern moved with the subjects) would prove to be the most difficult. This expectation was based on previous data that indicate reliance on vision increases after a flight and that in this condition visual input was made deliberately confusing (sensory conflict). Note that this was true for the platform performance of only astronaut subject 11, and that

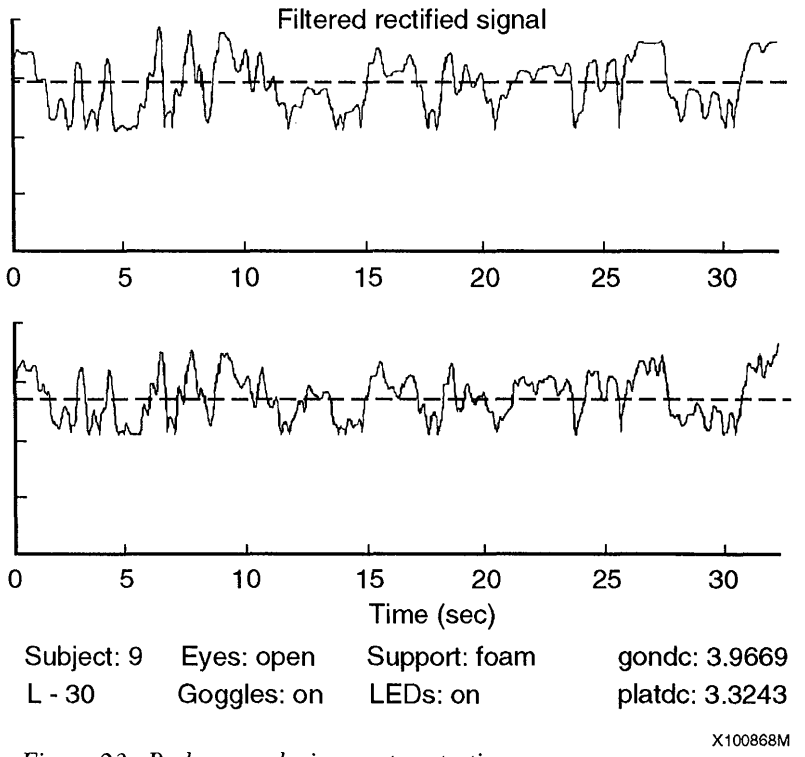

Figure 23. Body sway during posture testing.

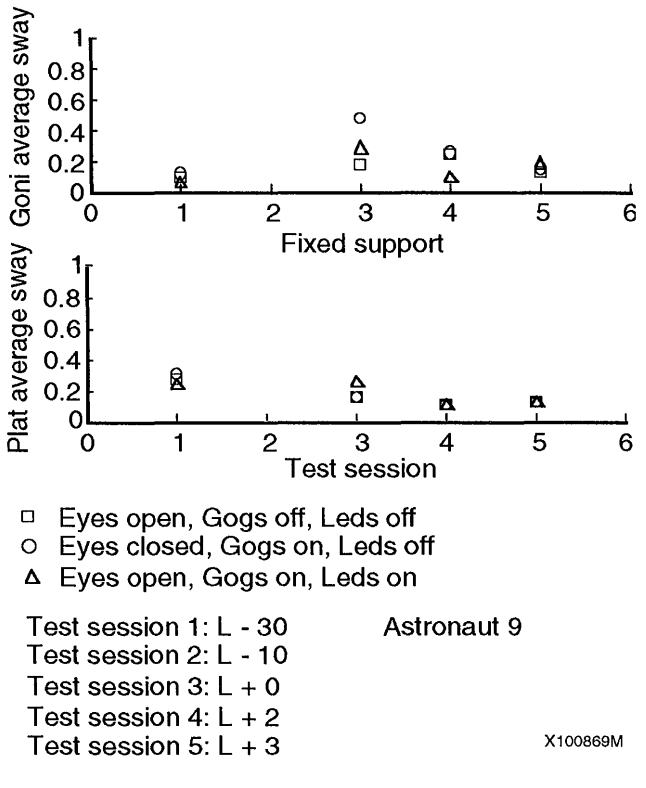

Figure 24. Astronaut #9: Sway as a function of test session with platform fixed.

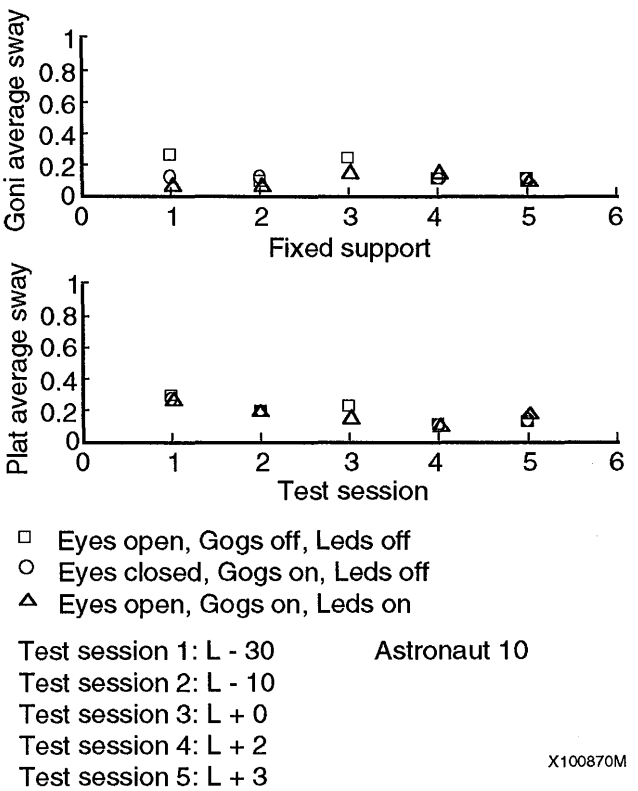

Figure 25. Astronaut #10: Sway as a function of test session with platform fixed.

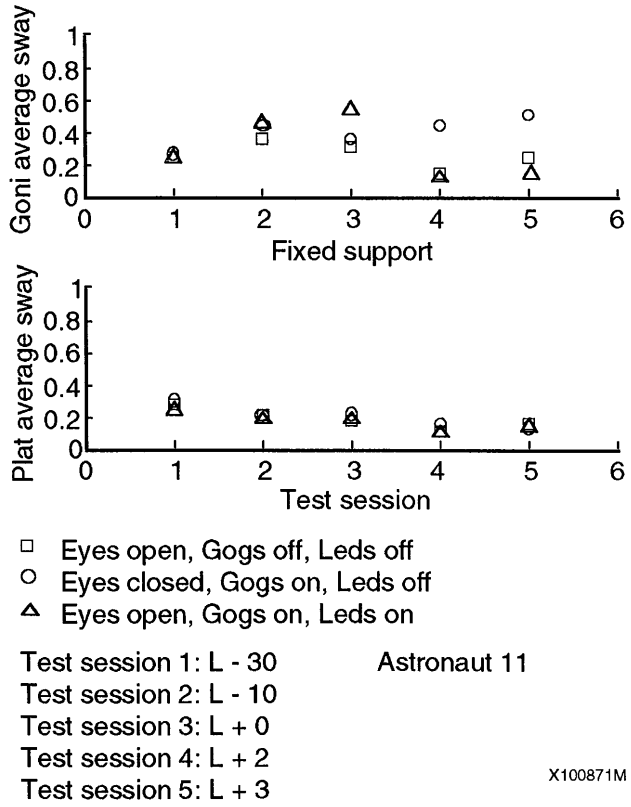

Figure 26. Astronaut #11: Sway as a function of test session with platform fixed.

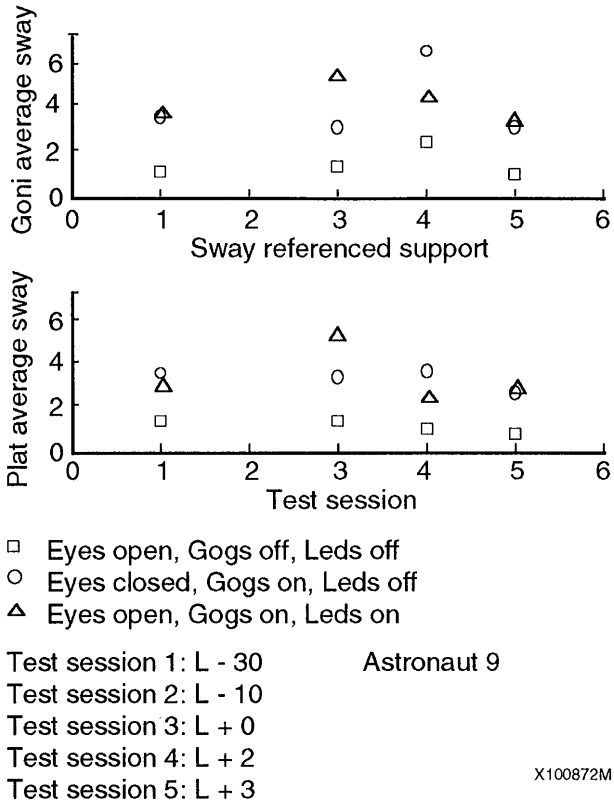

Figure 27. Astronaut #9: Sway as a function of test session with platform sway-referenced.

overall, there appeared to be no substantial difference in any of the fixed platform conditions either across subjects, test conditions, or test days.

Figures 27-29 show the data for the subjects when the platform was sway referenced (i.e., free to move, but damped with the foam). Again it was predicted that when the amount of sensory information was the most limited (both platform and vision sway referenced), performance would be the most impaired. This prediction basically held true for all subjects and was clearly the case on the day of landing for all three subjects. It was also hypothesized that in the condition where both vision and ankle position were available, crew performance would be better than it was preflight (based on the previous findings that over a limited pitch range, otolith input is much more sensitive and pitch performance is enhanced). This prediction was supported by the data for astronaut 11, whereas the performance under this condition for the remaining two subjects was essentially equal to their preflight performance.

Motion Perception Reporting

Four astronauts provided reports of self and surround motion associated with voluntary head and/or body movements during entry. One crewmember provided motion perception reports associated with voluntary sinusoidal head movements performed on orbit (early FD and late FD), during entry, and immediately after wheels stop.

The first astronaut reported strong sensations of linear surround (visual scene) motion associated with pitch motions of 30- 45° made from the waist. Yaw head movements produced a strong sensation of whole body yaw motion in the opposite direction of the head movement; i.e., the voluntary head movement and the perceived self (body) motion were 180° out of phase.

A second astronaut reported self and surround motion disturbances during entry, but the press of other activities prevented his describing these precisely.

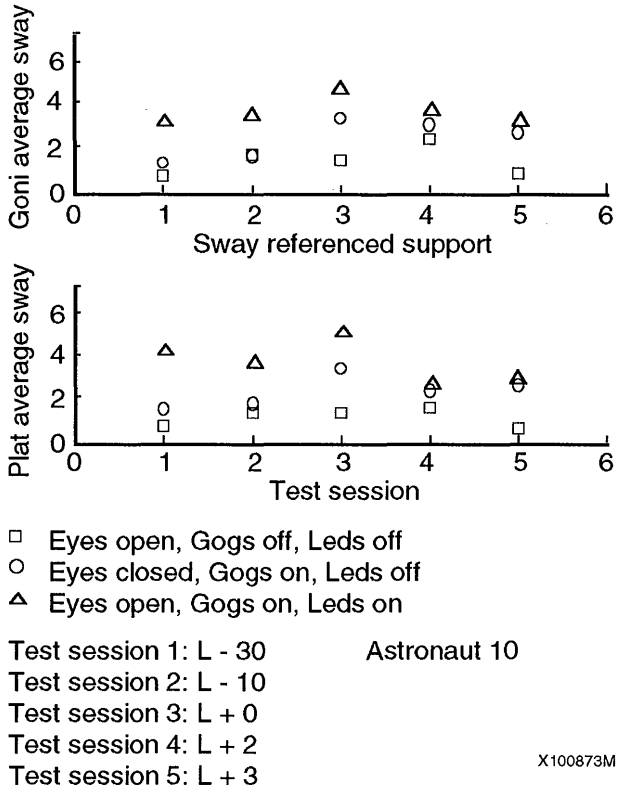

Figure 28. Astronaut #10: Sway as a function of test session with platform sway-referenced.

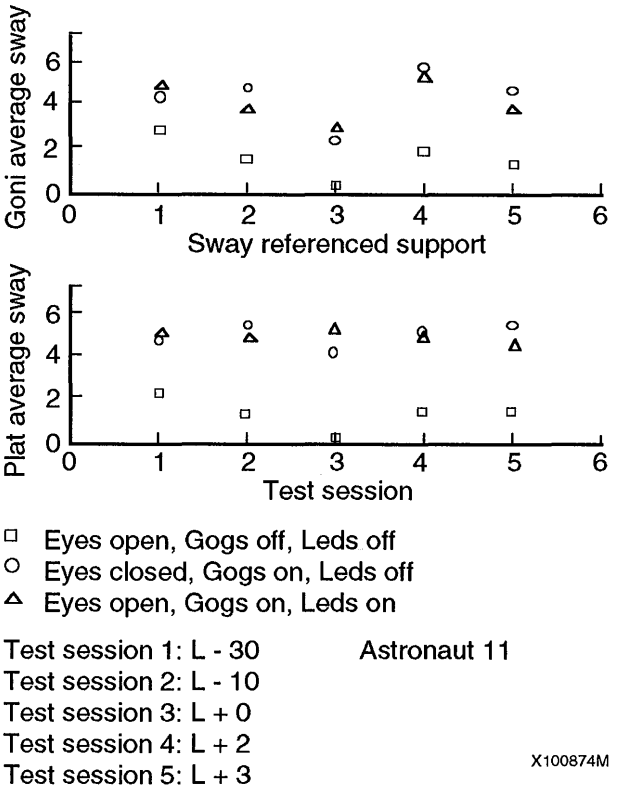

Figure 29. Astronaut #11: Sway as a function of test session with platform sway-referenced.

He also reported a new phenomenon: while floating unrestrained with his eyes closed on orbit, light tactile inputs to the top of his head produced a tumbling self-motion perception; applying pressure to the upper abdomen produced a similar tumbling sensation.

For the third astronaut, a left roll motion during entry and immediately following landing yielded self-motion roll perception in the direction of the actual roll; however, the return to upright was perceived as a continuing leftward roll motion. In addition, a backward pitch head movement immediately after landing was also perceived as backward and continued as backward during the return to upright. Roll and pitch motion perception immediately after landing were described as exaggerated when performed with the eyes closed.

The fourth astronaut provided motion perception reports on multiple occasions in flight, during entry, and immediately after wheels stop. Early in flight, only roll head movements elicited the perception of either surround or self motion, or both. Surround translation or body rotation occurred in the direction opposite the head roll. Late in flight, the same roll perceptions were reported. In addition, yaw head movements with the eyes closed elicited the perception of body rotation in yaw, equal in amplitude and opposite in direction to the head movement.

Although head movements were not performed during entry, the crewmember reported some interesting perceptions associated with the OMS-burn (1/20g). At the onset of G's, the Orbiter suddenly appeared (visually) to be in the vertical launch orientation, and the crewmember felt as though the Orbiter were travelling "uphill." At the OMS-burn cut-off and return to 0-g, the Orbiter suddenly appeared to have switched back to a horizontal orientation.

Head movements made immediately after wheels stop with eyes open elicited visual surround translation in the opposite direction of the head movement (all axes), with the greatest effects in pitch. No self-motion sensations were elicited by head movements with eyes closed.

CONCLUSIONS

After-Image OCR

Eye torsion obtained with the normative subjects during whole body tilt was consistent with that obtained by other investigators using more objective methods of recording ocular counterrolling. The observation that eye torsion was present in the supine condition was surprising given the findings by most other investigators that cervical input does not contribute to ocular counterrolling. Given that cervical input may contribute to ocular torsion, it was also surprising to observe that neck input did not appear to add to the torsion observed in the standing condition.

In flight, there was no observable torsional response. Again, this is surprising given the torsion found in the supine position. Aside from the torsional response observed in the supine controls, the astronaut data collected preflight were analogous to both the controls and data recorded by other investigators using the photographic technique of eye movement measurement. It was interesting to note that immediately postflight there was a reduction of eye torsion.

The lack of cervical contribution to eye torsion during flight and particularly reduced eye torsion observed immediately after flight supports the OTTR hypothesis. That is, all otolith signals in flight are interpreted as translation, and no other receptor substitutes for the missing tilt information. If cervical input did make a contribution to eye torsion, it would be expected that this contribution would have been carried over to those measurements made postflight. In this case the eye torsion would have been greater immediately postflight rather than reduced.

Voluntary Tilt

The failure of this investigation to obtain predicted overshoots during voluntary body tilt was surprising, particularly in view of reports that movements during walking produced sensations of exaggerated movement. However, the finding that postflight strategy changed to help stabilize the head led to the development of tests that would stabilize vision while the crewmembers were placed in an unstable position (see following section).

Postural Sway and Visual Stabilization

Several postural tasks have been used in the past to evaluate the unsteadiness that almost all crewmembers have reported following a flight. These tests have included (1) the standard rail test where a subject is asked to balance on rails of various widths, (2) tasks that have asked the participating crews to bend at the waist either in roll or pitch, (3) platforms that move parallel to the floor either in predictable or unpredictable movements; and (4) platforms that suddenly tilt with reference to the floor. None of these posture tests has provided a clear understanding of the disequilibrium displayed by the returning astronauts. The postural test design for this DSO was based upon these earlier tests (particularly the strategy adopted during voluntary tilt) and information/results from related vestibular tests to develop a new way of looking at postural instability. Specifically, the posture test that was used for the last three crewmembers tested under DSO 459 was designed to selectively and systematically remove sources of sensory input that the investigators of this study believed (based on the earlier findings) were important for the maintenance of balance.

The results showed that when a returning crewmember stands on a stable platform, there is little or no postural instability. But when the platform is an unstable base and sensory information is selectively removed, postural stability suffers. Eventually it will be desirable to equate the moving platform to actual walking and gait. In the case where both visual input and information from the ankles were unavailable, the crew showed considerable postural instability. When this information was returned but the platform was still unstable, performance was vastly improved and in one case was actually better than that observed preflight.

A more sophisticated test of postural equilibrium was designed based on the postural stability and visual stabilization platform used in this DSO and has been designated as the equilibrium tests performed as part of DSO 605, "Postural Equilibrium Control During Landing and Egress."

Motion Perception Reporting

The motion reports during and following entry are similar to those obtained during previous missions

and are generally consistent with the OTTR Hypothesis. In almost all cases the perceived motion is described as exaggerated, i.e., either or both the amplitude of displacement and the velocity of the perceived motion is greater than expected, given the amplitude and velocity of the head/body movement. These descriptions can be considered evidence of a type of input-output disturbance.

The development of a motion description vocabulary and the opportunity to provide motion demonstrations prior to flight greatly improved the data from this segment of the DSO. The investigators of this study anticipate that continued use of training in motion perception reporting will result in greater detail and precision of crew reports. Such improvements in reporting will enhance understanding of sensory adaptation to 0-g and readaptation to Earth and will provide data critical to the development of countermeasures such as the Preflight Adaptation Training (PAT).

REFERENCES

Diamond, S.G., Markham, C.H., and Furuya, N. Binocular counterrolling during sustained body tilt in normal humans and in a patient with unilateral vestibular nerve section, Ann Otol 91:198, 1982.

Miller, E.F. Evaluation of otolith organ function by means of ocular counterrolling measurements. Report #MR005.04-003.4 for Bureau of Medicine and Surgery, Naval Aerospace Medical Institute, 3/20/69.

Parker, D.E., Reschke, M.F., Arrott, A.P., Homick, J.L., and Lichtenberg, B.K. Preliminary DSO 0433 summary report for STS-8. Houston: National Aeronautics and Space Administration, 1983.

Parker, D.E., Reschke, M.F., Arrott, A.P. Patent disclosure: Proposal for prophylactic adaptation trainer (PAT). Oxford, Ohio: Dean of the Graduate School and Research, Miami University, March 11, 1984a.

Parker, D.E., Reschke, M.F., Arrott, A.P., Homick, J.L., and Lichtenberg, B.K. Preliminary DSO 0433 summary report for STS-11 (41-B). Houston: National Aeronautics and Space Administration, 1984b.

Reschke, M.F., Anderson, D.J., and Homick, J.L. Vestibulospinal reflexes as a function of microgravity. Science. 225:212-213, 1984a.

Reschke, M.F., Parker, D.E., Homick, J.L., Anderson, D.J., Arrott, A.P., and Lichtenberg, B.K. Otolith reinterpretation as a primary factor in space motion sickness. In: Results of Spacelab experiment in physiology and medicine. Neuilly Sur Seine, France: North Atlantic Treaty Organization, 1984b.

Parker, D.E., Reschke, M.F., Arrott, A.P., Homick, J.L., and Lichtenberg, B.K. Otolith tilt-translation reinterpretation following weightlessness: Implications for preflight training. Aviation, Space, and Environmental Medicine, 56:601-606, 1985.

Section Three: Biomedical Physiology

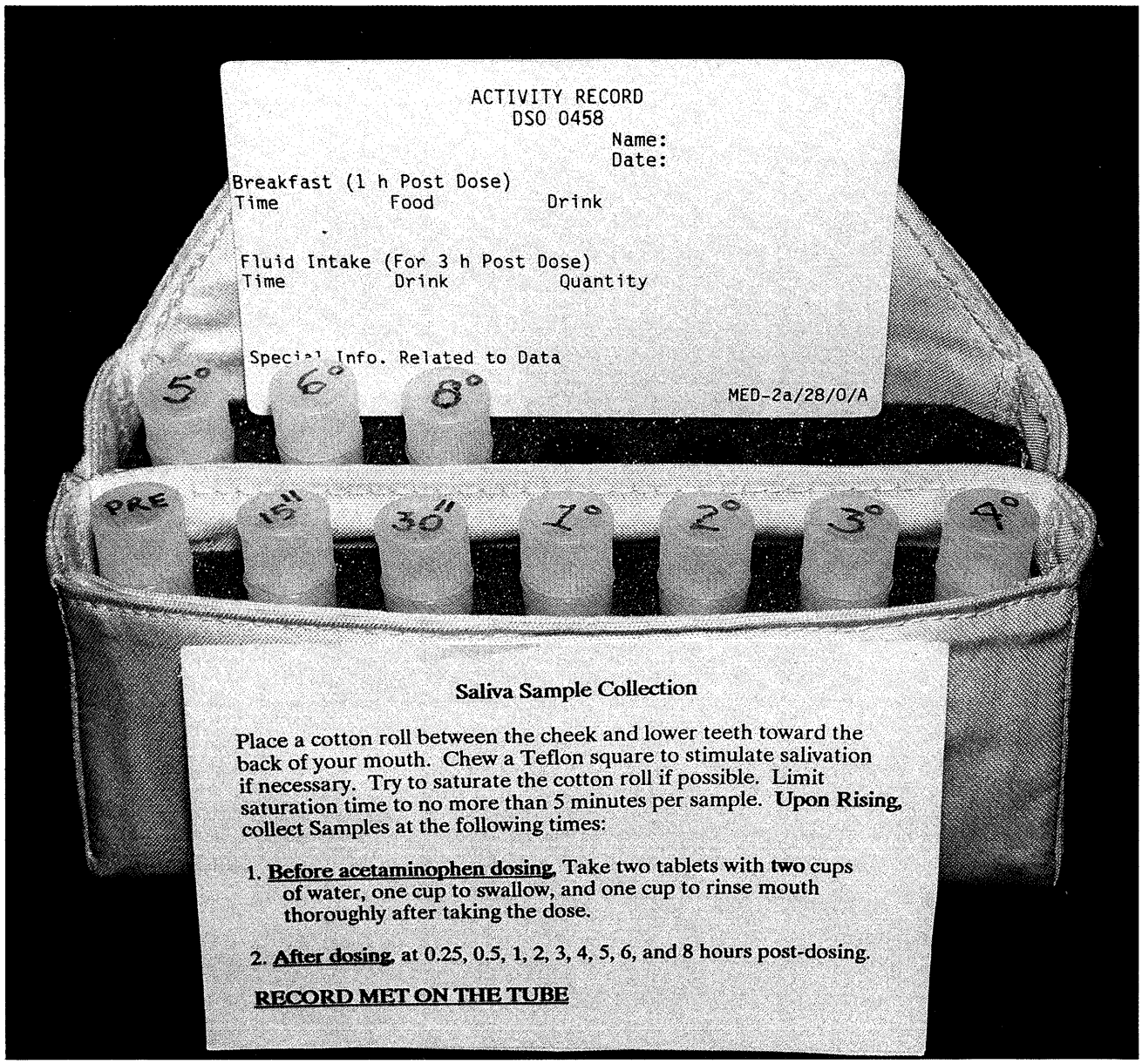

In-flight saliva collection kit. Saliva collection is simple to perform, noninvasive, and has been shown in ground-based studies to be an accurate method of tracking the concentration of certain hormones and pharmacologic agents.

DSO 450: Salivary Cortisol Levels During the Acute Phases of Space Flight

Investigator: Nitza M. Cintrón, Ph.D.

INTRODUCTION

The complexity of the physiological response to weightlessness has stimulated research into identifying biochemical and endocrine variables that might provide insight into the underlying mechanisms operative in the overall adaptation process. Available data from earlier in-flight and ground-based studies substantiate the value of performing correlative studies to determine the neuro-endocrinologic mechanisms associated with the various conditions of spaceflight-induced stress (Leach and Rambaut, 1977; Leach, 1981; Leach and Johnson, 1985). As expected, these investigations clearly indicated the central involvement of autonomic neurotransmission in the etiology of stress-related imbalances (e.g., immunosuppression, motion sickness) and pointed to the potential of correlating early changes to hormonal alterations.

Cortisol, under the direct influence of adrenocorticotrophic hormone (ACTH), is one of the key hormones associated with the control and maintenance of normal neuroendocrine processes and with the physiologic response to stress. Plasma concentrations of cortisol have been found to increase during space flight (Leach and Rambaut, 1977); however, no data are currently available on its changes immediately after the achievement of weightlessness. It is during the first hours of a mission that the most dramatic adaptive responses to weightlessness are thought to occur.

The lipophilic and neutral chemical nature of steroids has been shown to effect their rapid equilibration into saliva from plasma by passive diffusion (Riad-Fahmy et al., 1982). As a result, steroid concentrations in saliva represent those of the free fraction in the circulation and are independent of variations in salivary flow rate. Salivary cortisol levels have been demonstrated to correlate with the free steroid fraction in both plasma (Peters et al., 1982) and serum (Umeda et al., 1981). Recent improvements in steroid immunoassay and salivary extraction techniques have made feasible the routine assessment of adrenal activity by monitoring cortisol levels in saliva (Vining et al., 1983; Walker et al., 1978). Saliva collection represents a stress-free, noninvasive means of obtaining information about adrenal activity during the early in-flight period; many samples can be collected with minimal disturbance of crewmembers' activities.

The primary objectives of this investigation were to determine the feasibility of collecting saliva samples under operational Shuttle conditions for cortisol analysis and, more importantly, to examine adrenal (cortisol) activity during the acute and adaptive phases of space flight. Information about adrenal activity and about integrated neuroendocrine function has significance in formulating the total picture of the crew's health status and in predicting the possible duration of their stay in weightlessness.

PROCEDURES

The general design of the investigation involved the serial collection of saliva samples through a specified 24-hour period during pre- and in-flight phases of a mission. Four saliva samples were to be collected throughout each 24-hour period at approximately the same times (± 1 hour) during the sleep/activity cycle. To avoid an interruption of the sleep period, the first sample was collected soon after wake-up; the second sample at wake-up plus 5 hours (± 1 hour); the third sample at wake-up plus 10 hours (± 1 hour); and the fourth sample shortly before the sleep period. This protocol was performed once at approximately one month before launch and twice during flight, once early and once late in the mission. In-flight data were compared to preflight baseline data. Seven crewmembers participated in this investigation.

Saliva samples were obtained using the Salivary Collection Assembly, which consisted of a beta cloth

pouch with foam inserts to retain Sarstedt syringe tubes, each containing a dental cotton roll. The syringe barrels had a screw cap on one end and a sliding plug on the other end into which the syringe plunger screwed, so that the barrels functioned as tubes for collection of samples as well as syringes for their retrieval. Squares of Teflon film that could be chewed to stimulate salivation were also stowed in the pouch. Samples were collected by placing a roll of dental cotton between the lower teeth and cheek toward the back of the mouth. The cotton roll remained in place for 20 minutes or until it was saturated, whichever occurred first. The saliva samples were stored in the designated tubes for subsequent analysis.

Samples were frozen at -70° C as soon as possible after landing. They were thawed, and a plunger was inserted into each syringe. The contents of the cotton roll were squeezed into a 50-ml tube, which was centrifuged with the syringe in a Beckman J-6B centrifuge. The roll was squeezed again so that as much sample as possible was transferred to the 50-ml tube. Samples were analyzed for cortisol by the radioimmunoassay described by Foster and Dunn (1974).

RESULTS/DISCUSSION

Figure 1 illustrates the data obtained through this DSO; only the days for which at least three samples were collected are included here. Data from one crewmember are not included in Figure 1 because only two samples of sufficient size were obtained for each flight day.

The time of peak cortisol secretion before flight ranged from 0415 to 0900 hours for five of the crewmembers, with the peak at 2030 hours for the other (crewmember 1). Crewmember 3 had a second peak at 1305 hours.

For three of the six participating crewmembers, peak cortisol concentrations may have been delayed on varying flight days, but data were insufficient to determine the exact preflight and in-flight peaks. For two other crewmembers, salivary cortisol levels were close to preflight levels on FD2 and FD4, except that the afternoon peaks seen before flight appeared to be absent during flight. For one crewmember, the highest and lowest levels of cortisol peaked at the same times on FD6 as before flight. No relationship between the length of time in space and changes in cortisol levels was demonstrated.

The amount of data gathered did not permit statistical comparison of salivary cortisol concentrations before and during flight, but generally, space flight did not appear to affect the magnitude of cortisol levels. Data for FD6 were available from only one crewmember (crewmember 1), whose cortisol levels on FD6 were higher than his corresponding preflight levels at all time points; however, measurement times were not exactly the same. For crewmembers 4 and 6, some cortisol levels on F2 were higher than those at corresponding times of day before flight.

CONCLUSION

Salivary cortisol has been considered by some investigators to give a more accurate picture of adrenal cortisol function than serum cortisol (Vining et al., 1983). Results have shown that saliva can be collected in zero gravity in quantities sufficient to measure cortisol. The noninvasive method used in this experiment is highly advantageous for collecting samples frequently and with minimum disruption of the crewmembers' activities.

Problems encountered included insufficient saturation of the cotton rolls (possibly due to dryness of the mouth, a common side effect of antimotion sickness drugs) and inadequate labeling of some tubes. There was also some difficulty with collection of samples at the same time on every day of the experiment because of other demands on the crewmembers' time. It should be possible to solve these problems with further training and crew orientation.

The peak plasma cortisol concentration generally occurs at approximately 0700 hours (Migeon et al., 1956), but for crewmember 1 (and the crewmember omitted from Figure 1) the peak occurred much earlier, no later the 2030 hours. This might have been caused by the strenuous preflight training schedule.

There are not enough in-flight data to draw any conclusions about the early effects of flight on cortisol levels in the body or on their diurnal variation, but in at least one crewmember the diurnal rhythm appeared to be the same after approximately one week of flight as it was before flight. The cortisol peak may have shifted to a later time in three other crewmembers after 1, 2, or 3 days of flight.

In summary, collection of saliva samples for measurement of cortisol during space flight appears

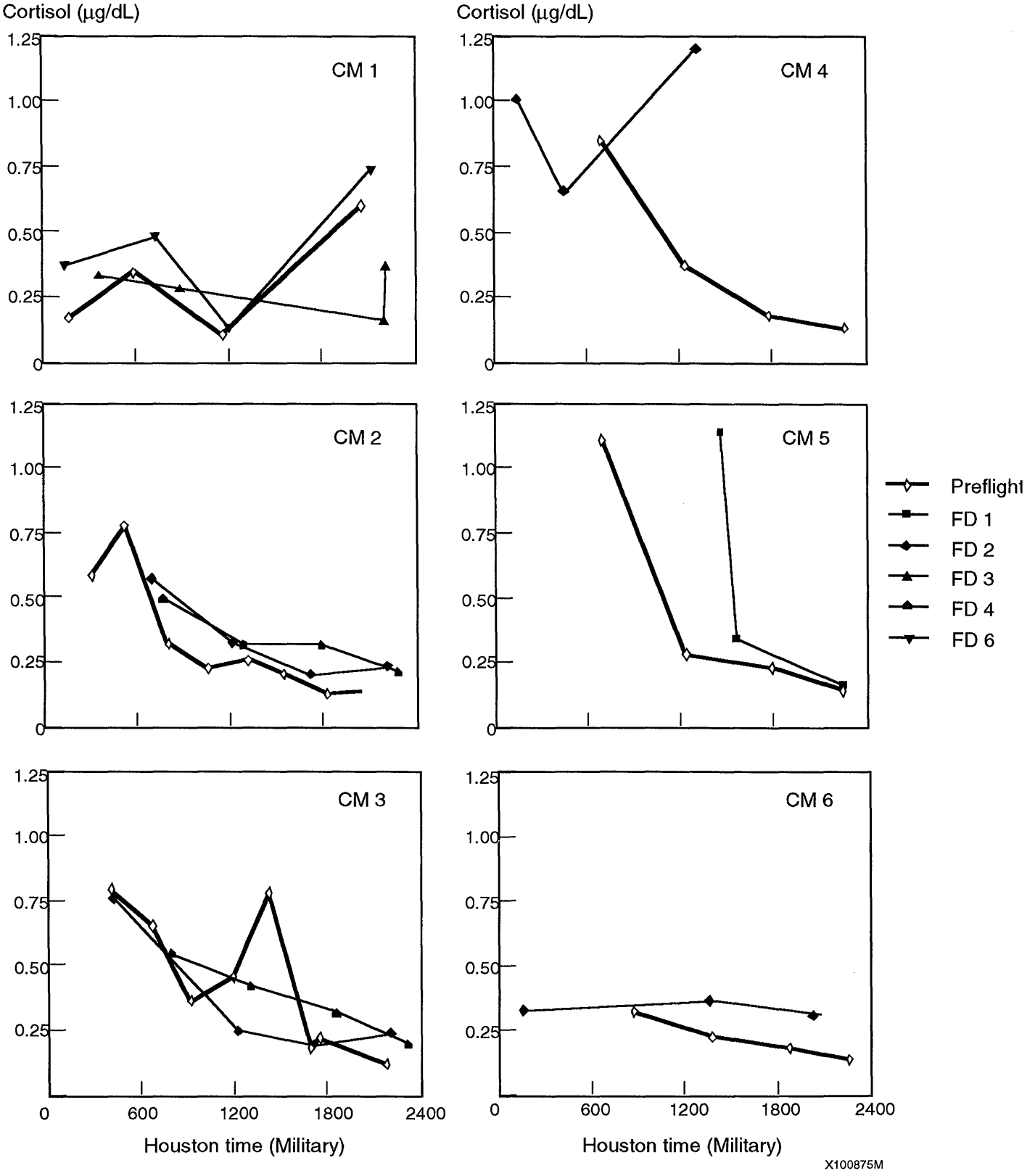

Figure 1. Salivary cortisol levels in six crewmembers (CM1-6), before flight and on flight days 1-6.

to provide a feasible approach for studying change in adrenal function during adaptation of the body to weightlessness. Because of the wide variability among subjects, appropriate assessment of changes in adrenal activity during the initial phases of space flight will require additional data. Therefore, the current, limited data must be considered strictly preliminary.

REFERENCES

Foster, L. B.; Dunn, R. T. Single-antibody technique for radioimmunoassay of cortisol in unextracted serum or plasma. Clin. Chem. 20: 365-368; 1974.

Leach, C. S. An overview of the endocrine and metabolic changes in manned space flight. Acta Astronaut. 8: 977-986; 1981.

Leach, C. S.; Johnson, P. C. Fluid and electrolyte control in simulated and actual space flight. The Physiologist. 28: S-34-S-37; 1985.

Leach, C. S.; Rambaut, P. C. Biochemical responses of the Skylab crewmen: an overview. In: Johnston, R. S.; Dietlein, L. F., eds. Biomedical Results from Skylab , NASA SP-377. Washington, D.C.: National Aeronautics and Space Administration; 1977:p. 204-216.

Migeon, C. J.; Tyler, F. H.; Mahoney, J. P.; Florentin, A. A.; Castle, H.; Bliss, E. L.; Samuels, L. T. The diurnal variation of plasma levels and urinary excretion of 17-hydroxycorticosteroids in normal subjects, night workers, and blind subjects. J. Clin. Endocrinol. 16: 622-633; 1956.

Peters, J. R.; Walker, R. F.; Riad-Fahmy, D.; Hall, R. Salivary cortisol assays for assessing pituitary-adrenal reserve. Clin. Endocrinol. 17: 583-592; 1982.

Riad-Fahmy, D.; Read, G. F.; Walker, R.F.; Griffiths, K. Steroids in saliva for assessing endocrine function. Endocrine Rev. 3: 367-395; 1982.

Umeda, T.; Hiramatsu, R.; Iwaoka, T.; Shimada, R.; Miura, F.; Sato, T. Use of saliva for monitoring unbound free cortisol levels in serum. Clin. Chim. Acta. 110: 245-253; 1981.

Vining, R. F.; McGinley, R. A.; Maksvytis, J. J.; Ho, K. Y. Salivary cortisol: a better measure of adrenal cortical function than serum cortisol. Ann. Clin. Biochem. 20:329-335; 1983.

Walker, R. F.; Riad-Fahmy, D.; Read, G. F. Adrenal status assessed by direct radioimmunoassay of cortisol in whole saliva or parotid saliva. Clin. Chem. 24: 1460-1463; 1978.

DSO 458: In-flight Pharmacokinetics of Acetaminophen in Saliva

Investigators: Nitza M. Cintrón, Ph.D.; Lakshmi Putcha, Ph.D.; and Cecelia Parise, B. Pharm.

INTRODUCTION

Space flight induces a wide range of physiological and biochemical changes in crewmembers (Nicogossian, 1982), including disruption of gastrointestinal (GI) function and physiology, fluid and electrolyte imbalances, alterations in circulatory dynamics and organ blood flow, and hormonal and metabolic perturbations. Any of these changes can influence the pharmacokinetic behavior and pharmacodynamic consequences of medications administered during space flight. Characterization of the pharmacokinetic and/or pharmacodynamic behavior of operationally critical medications is crucial in order to ensure effective in-flight pharmacologic treatment.

The possibility that space flight alters bioavailability was raised early in the Space Shuttle Program, when drugs prescribed to alleviate space motion sickness (SMS) had little therapeutic effect. Implications of altered drug bioavailability extend beyond the treatment of motion sickness as a number of pathophysiological disorders induced by space flight will require pharmacological intervention. Therefore, the primary purpose of this investigation was to determine whether drugs actually reach the site of action at concentrations sufficient to elicit a therapeutic response.

PROCEDURES

A noninvasive saliva sampling technique was used to evaluate the absorption and distribution of acetaminophen. The pharmacokinetic and pharmacodynamic behavior of this common pain reliever has been well characterized (Rawlins et al., 1977; Adithan and Thangam, 1982). In a preliminary ground-based study, saliva and blood samples were collected simultaneously from control subjects in order to establish the acetaminophen saliva-to-plasma ratio. This value was found to be close to one, indicating that measuring salivary concentrations of acetaminophen can be useful for determining its pharmacokinetic behavior. Based on this information, acetaminophen was chosen to monitor potential changes in drug pharmacokinetics during space flight, using the salivary analysis technique described below.

The drug was administered as two 325-mg tablets before and during flight. Crewmembers collected saliva samples before taking the tablets and at 15 minutes, 30 minutes, 1, 2, 3, 4, 5, 6, and 8 hours afterwards. Thirteen crewmembers repeated this protocol twice before flight. Eight crewmembers performed the protocol twice and the other five once during flight. Samples were collected using a saliva collection kit designed and developed at Johnson Space Center.

A high performance liquid chromatographic method (O'Connell and Zurzola, 1982) was used to determine acetaminophen concentrations. Samples were precipitated with 1 ml each of 0.3 N barium hydroxide and 5% zinc sulfate. Drug concentrations in the supernatant were determined by an ultraviolet detector using paraacetaminophenol as an internal standard. Initial parameter estimates were obtained by analyzing the data using RSTRIP, an exponential curve stripping program; final parameters were estimated using nonlinear regression analysis.

RESULTS/DISCUSSION

Results from ground-based feasibility studies confirmed that therapeutic concentrations of acetaminophen can be detected in saliva after oral administration. Furthermore, its saliva/plasma ratio was consistent, remaining close to 1 over a wide range of plasma concentrations during the pre- and postabsorptive phases ($r = 0.93$). Pharmacokinetic parameters and estimates of bioavailability calculated from saliva concentrations were consistent with those calculated from plasma concentrations (Putcha et al., 1986), indicating that saliva concentration profiles can be used to evaluate the pharmacokinetics and

bioavailability of acetaminophen. Acetaminophen concentration profiles during space flight were significantly different from that of their ground-based controls, with more pronounced changes in the absorption phase than in the elimination phase, possibly suggesting a progressive decrease in absorption rate during flight.

Representative saliva concentrations over time after oral administration of acetaminophen before and during flight are depicted in Figure 1. Time to reach maximum concentration (T_{max}) during flight is increased, indicating that absorption time is prolonged. One crewmember's maximum salivary concentration of the drug (C_{max}) was lower on FD 1 than on FD 3, indicating a change in the rate of absorption (Figure 1A). In another crewmember, T_{max} was longer on FD 2 than on FD 0 (Figure 1B). The third crewmember exhibited a significant increase in T_{max} with a concomitant reduction in C_{max} (Figure 1C). However, in all cases C_{max}, the maximum concentrations of the drug in saliva, was lower on FD 0 than it was before flight.

Saliva concentrations over time were highly variable in the same subject on different flight days. Figure 2 illustrates the means and standard errors for C_{max} and T_{max} as a function of flight day. These data were obtained from 13 subjects on seven different flights. The large degree of variability during flight makes statistical evaluation of these changes difficult; however, C_{max} had a tendency to decrease on FD 0 and increase on FD 2 and FD 3 (Figure 2A). T_{max}, in contrast, had a tendency to increase on these days. There appears to be a bimodal distribution of the means for C_{max} and T_{max} on FD 2 (Figure 2).

Since intersubject variability before flight was minimal, the effects of space flight on pharmacokinetics is likely to vary among individuals, probably because of differential physiologic adjustments to microgravity. It is unclear why C_{max} and T_{max} exhibited bimodal distribution of the means during FD 2. These results may be associated with SMS and/or GI motility on that particular day; this correlation needs to be examined further. However, the increase in lag time and absorption half-life, coupled with a decrease in C_{max}, suggests that gastric emptying rate decreases during space flight because acetaminophen absorption rate is directly proportional to gastric emptying rate (Clements et al., 1978). The progression of these changes during longer flights should be characterized to determine the extent of changes in GI function,

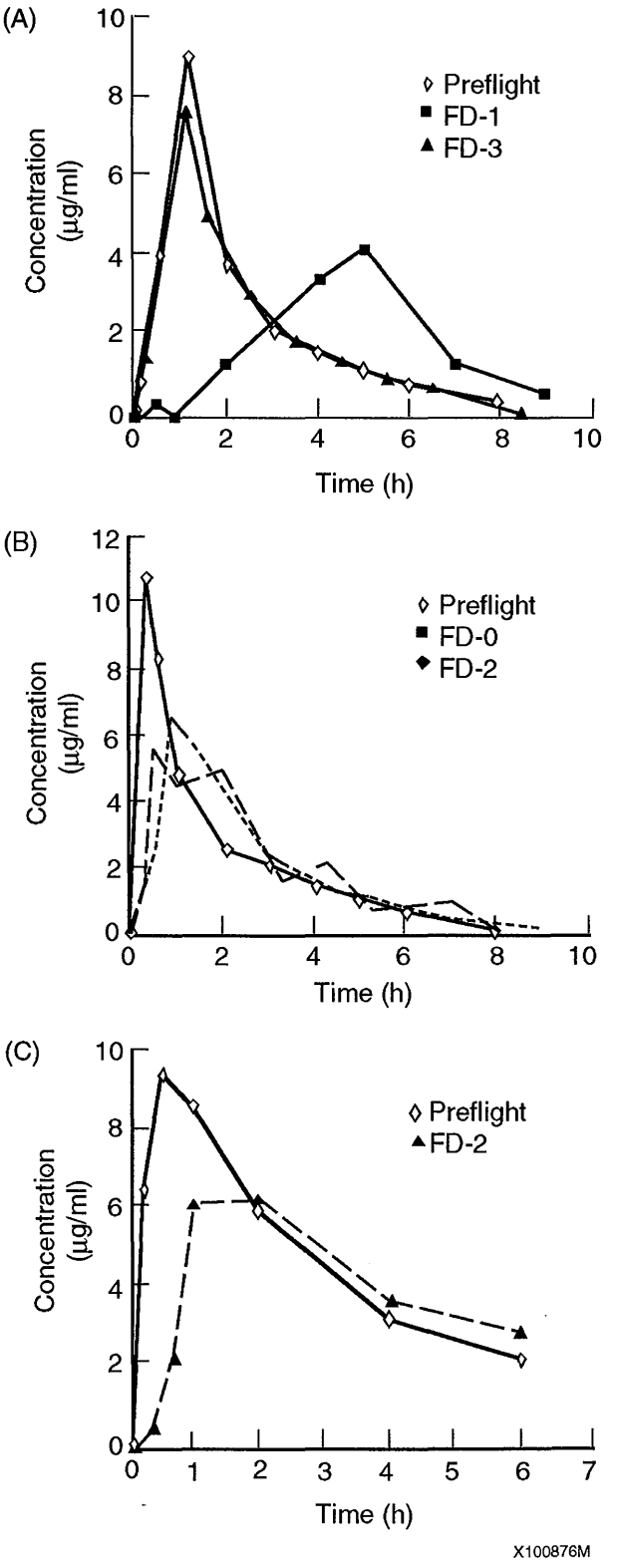

Figure 1. Saliva concentration-time profiles of acetaminophen after oral administration of a 650 mg dose to crewmembers.

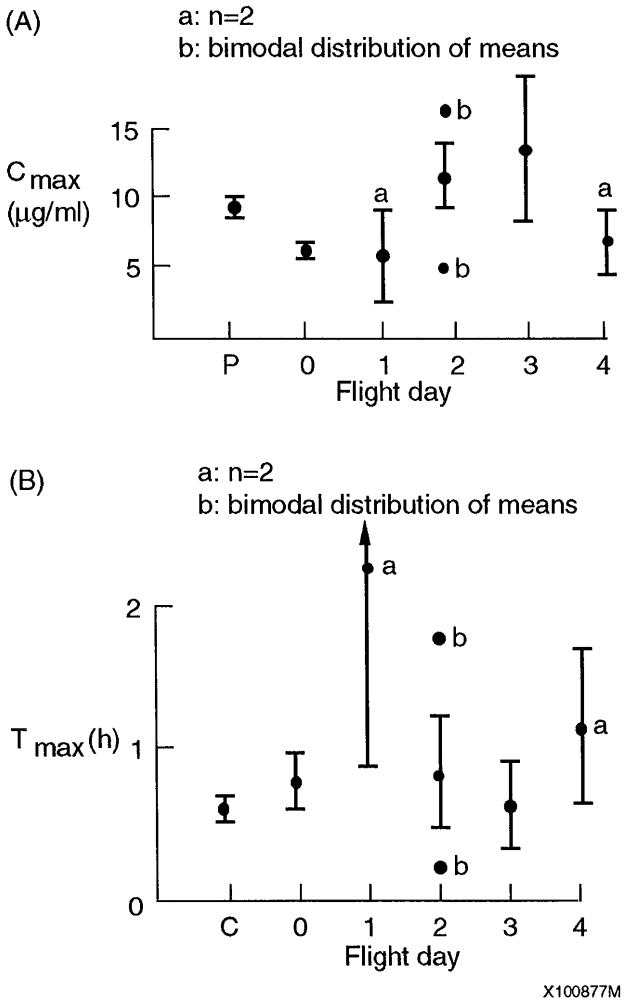

Figure 2. Average maximum concentration in saliva (C_{max}) and time to reach maximum concentration (T_{max}) of acetaminophen after oral administraiton of a 650 mg dose to crewmembers.

which affects the absorption and bio-availability of nutrients as well as orally administered medications.

CONCLUSIONS

These preliminary results, although limited, collectively support predictions that drug dynamics change during flight and suggest that these changes depend upon mission length. The limited in-flight data accumulated thus far are insufficient to characterize the degree and magnitude of pharmacokinetic changes and the mechanisms underlying them. Some variables that influence disposition and kinetics of drugs can be easily identified (e.g., mission day); others are not. GI function, degree of motion sickness, ingestion of other medications, and overall physiologic responses must all be examined in greater detail. Decreases in drug concentration and rate of absorption may result in ineffective therapeutic responses or unexpected side effects. A compre-hensive evaluation of in-flight pharmacokinetics under controlled experimental conditions is planned for future Spacelab missions. Information thus obtained can be applied not only to predicting the therapeutic consequences of operationally critical drugs administered in flight, but also to identifying and describing alterations in key processes within the body that are relevant to overall metabolic homeostasis in humans.

During recent years, space medicine research in the United States has focused on the 4- to 7-day Space Shuttle missions. As missions are lengthened, the effects of spaceflight-induced physiologic changes and the resulting pharmacokinetic and pharmacodynamic deviations will be magnified and must be countered to maintain optimum health and performance during flight and prompt readaptation to gravity upon return.

REFERENCES

Adithan, C.; Thangam, J. Comparative study of saliva and serum paracetamol levels using a simple spectrophotometric method. Br. J. Clin. Pharmac. 14:107-9, 1982.

Clements, J. A.; Heading, R. C.; Nimmo, W. S.; Prescott, L. F. Kinetics of acetaminophen absorption and gastric emptying in man. Clin. Pharmacol. Ther., 24:420-431, 1978.

Nicogossian, A.E.; Huntoon, C. L.; Pool, S. L., editors. Space Physiology and Medicine, 2nd edition. Philadelphia: Lea and Febiger; 1989.

O'Connell, S. E.; Zurzola, F. J. A rapid quantitative determination of acetaminophen in plasma. J. Pharm. Sci. 71:1291-94, 1982.

Putcha, L.; Cintron, N. M.; Vanderploeg, J .M.; Chen, Y.; Dardano, J. Comparative concentration profiles of acetaminophen in plasma and saliva of normal subjects. Clin. Pharm. Ther. 39 (2), 1986.

Rawlins, M. D.; Henderson, D. B.; Hijab, A. R. Pharmacokinetics of paracetamol (acetaminophen) after intravenous and oral administration, Europ J. Clin. Pharmacol. 11:283-6, 1977.

Section Four: Radiation Monitoring

Phantom Head Assembly. This simulation of a human head consists of a human skull imbedded in plastic material that is radio-equivalent to soft tissue. Radiation-sensing devices placed inside the head were analyzed to measure radiation dose distribution within the head.

DSO 469A: Low Earth Orbit Radiation Dose Distribution in a Phantom Head

Investigators: A. Konradi, Ph.D.; W. Atwell; G. D. Badhwar, Ph.D.; B. L. Cash; K. A. Hardy

ABSTRACT

In order to compare analytical methods with data obtained during exposure to space radiation, a phantom head instrumented with a large number of radiation detectors was flown on the Shuttle on three occasions: 8 August 1989 (STS-28), 28 February 1990 (STS-36), and 24 April 1990 (STS-31). The objective of this experiment was to obtain a measurement of the variability in the dose distribution within a phantom head volume.

The orbits of these missions were complementary: STS-28 and STS-36 had high inclination and low altitude, while STS-31 had a low inclination and high altitude. In the case of STS-28 and STS-36 the main contribution to the radiation dose comes from galactic cosmic rays (GCR) with a minor to negligible part supplied by the inner belt through the South Atlantic Anomaly (SAA) and for STS-28 an even smaller one from a proton enhancement during a solar flare associated proton event. For STS-31 the inner belt protons dominate, and the GCR contribution is almost negligible. The internal dose distribution is consistent with the mass distribution of the orbiter and the self-shielding and physical location of the phantom head.

INTRODUCTION

A lifetime study of the effects of total body proton irradiation in rhesus monkeys was initiated in 1964 and conducted in cooperation between U. S. Air Force School of Aerospace Medicine (USAFSAM) and the National Aeronautics and Space Administration (NASA). In this experiment rhesus monkeys were irradiated with total body surface doses from 25 to 800 rad of 55 MeV protons. A significant fraction of the 72 irradiated animals subsequently developed glioblastoma multiforme (Wood et al., 1986). The dimensions of the monkey head are such that if it is irradiated uniformly by a broad beam of 55 MeV protons, one would expect Bragg peak hot spots to form inside the brain where the deposited dose would exceed the surface dose. A detailed analysis of the theoretical dose distribution was later performed by Leavitt (1991). It was shown that under experimental conditions prevailing at the time of the irradiation, a dose enhancement in various places inside the brain would indeed be expected.

Because the human head is larger than the monkey head and because inner belt protons measured inside the Shuttle arrive from a variety of directions and their energy spectrum has a peak in the 80-100 MeV range (Richmond et al., 1987a), the question arose whether it were possible during a typical STS mission for a relative increase in dose absorption to occur somewhere inside the human head. In reality both the mass distribution of the Shuttle and the proton flux incident on it during a mission are highly anisotropic, and thus most of the flux arrives from a preferred direction and may have an instantaneous energy spectrum that depends on the direction and differs from the average. Consequently, with the phantom head held rigidly in a fixed position, one would not necessarily find the dose enhancement at the center of the head. However, some unambiguous pattern in the dose distribution would be of great interest.

PROCEDURES

In this experiment the human head was simulated by a phantom head assembly (Rando Phantom - Alderson Research Laboratories, Stamford, Conn.). This phantom consists of a human skull imbedded in a plastic material that is radio-equivalent to soft tissue. As shown in Figure 1, the phantom head is sliced horizontally into nine 2.54 cm thick sections. Starting with the second section from the top, each section contains symmetrically drilled holes distributed in a 3-cm^2 grid. During the flights the 120 holes in the eight sections were filled with thermoluminescent detectors (TLD). In addition, 6.45 cm^2 pieces of CR-39 nuclear track detectors, which served to measure

Accepted for publ. by *Nucl. Tracks Radiat. Meas.*

particles with $LET_{\infty} \bullet H_2O \geq 5$ keV/μm, were sandwiched between each odd and even numbered sections, and smaller pieces of these detectors were placed into a single hole in each section (Benton et al., 1990). The sections were numbered 0, 1, 2, ..., 8 and the TLDs measured the dose at a depth of 3.81, 6.35, 8.89, ... , 21.59 cm from the top of the head. Section 0 had no TLDs. On all flights the head was located with its right cheek adjacent to the starboard wall of the crew cabin with about 1 g/cm^2 of Al between it and the external radiation. As a result of this positioning the irregular Shuttle mass distribution was located mostly on the other side. The experiment was deployed during Shuttle missions STS-28, STS-36, and STS-31.

Mission STS-28 lasted from 12:37 GMT, 8 August to 14:38 GMT, 13 August 1989 for a total of 122 hours. Orbital inclination was 57°, and altitude was 296 km. Because of the relatively low altitude and the high orbital inclination, this mission received a relatively low exposure from the South Atlantic Anomaly (SAA) but a high one from galactic cosmic rays (GCR). In addition, the flight took place during the solar maximum. On 12 August 1989 at 13:57 UT, a class X-2.6/2B solar flare occurred on the west limb of the sun which precipitated a solar proton event at the Earth. The temporary radiation enhancement caused by this event was seen on the Shuttle on 13 August 1989 at 8:17 UT by the Air Force Radiation Measuring Instrument (RME), a tissue-equivalent proportional counter.

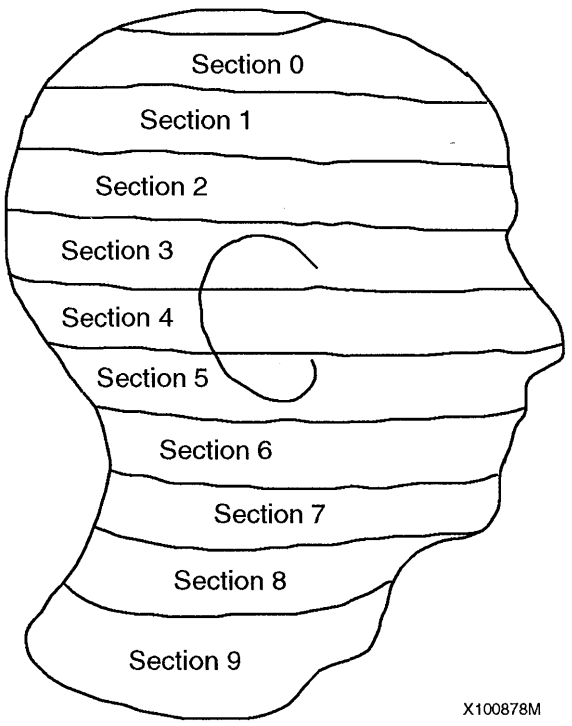

Figure 1. Lateral view of the phantom head. Sections 1-8 contain the TLDs.

Mission STS-36 lasted from 6:50 GMT, 28 February to 17:08 GMT, 4 March 1990, a total of 106 hours and 18 minutes. Orbital inclination was 62°, and altitude was 250 km. To date it was the lowest altitude Shuttle flight on record. Solar conditions were quiet, and no solar events occurred. Because of this, we expect that the GCR dose would far outweigh any contribution from the SAA.

Mission STS-31 lasted from 12:35 GMT, 24 April to 13:49 GMT, 29 April 1990, a total of 121 hours and 14 minutes. The orbital inclination was 28.5° while the altitude was 620 km. As a result of the high altitude and low orbital inclination, the radiation dose obtained in the SAA exceeded the dose due to the GCR by a factor of about 44. No solar particle events were observed during that period.

Analysis

After each landing the phantom head was returned to the laboratory, disassembled, and the TLDs were processed. Each of the holes in the phantom contained 5 TLD crystals which were read out and averaged, the standard deviations calculated, and the background subtracted (Richmond et al., 1987b). The background was obtained by sending a set of control dosimeters by plane to Kennedy Space Center and then returning them to Johnson Space Center. The dose measured in those detectors was then subtracted from the dose measured in the phantom. The resultant radiation doses for Sections 1 to 8 were recorded and presented as contour plots. Because of the large volume of data involved, we shall display only the contour plots from Section 3 which represents a typical slice through the phantom head.

STS-28: Figure 2 shows isodose contours for Section 3.

These contours are plotted at intervals of 1.7 mrad, which correspond to the typical experimental uncertainty in the readout. The average dose deposited in the phantom is about 53 mrad. While there seem to be individual islands of dose enhancement as well as of dose reduction, these non-

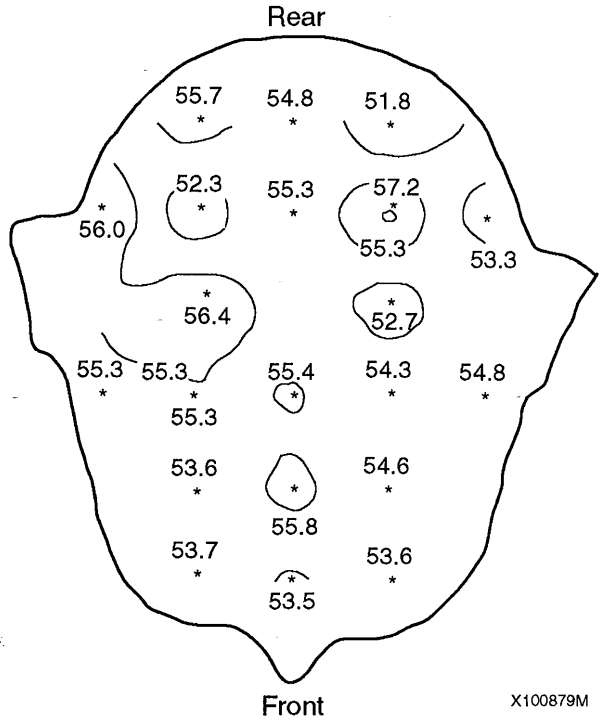

Figure 2. Isointensity contours of the radiation dose distribution in Section 3 recorded during STS-28.

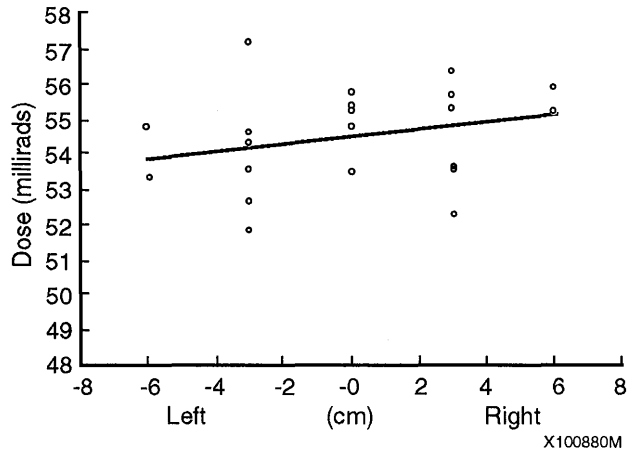

Figure 3. Dose measured during STS-28 in Section 3 at 8.89 cm below the top. The dose is plotted as a function of position from the symmetry plane. The front-to-back position is ignored.

uniformities are almost totally within statistical fluctuations. A clear-cut pattern is hard to discern. However, when the dose is plotted in each section as a function of the distance from the symmetry plane of the head, regardless of the position of the TLDs along the front-to-back axis, as shown in Figure 3, it becomes clear that the right side of the phantom head, which was adjacent to the starboard crew cabin wall, received an approximately 8% higher dose than the left side.

Since our dose measurements are cumulative over the mission, it is not possible to determine the contributions of individual sources directly. An indirect assessment based on time-resolved measurements obtained by the Air Force RME, the crew passive dosimeters, and calculations using radiation belt models for solar maximum and minimum, show that the average dose measured inside the phantom can be broken down as follows:

Total dose:	53.0 mrad
Galactic cosmic ray dose:	47.5 mrad
SAA dose:	4.8 mrad
Solar proton dose:	0.7 mrad

Since the GCR proton energy spectrum is very hard compared to 100 MeV protons, one would expect a fairly uniform dose distribution. The SAA and the solar proton spectra, however, are rather soft, and most of the flux enters the phantom head from the direction of the adjacent cabin wall, which should result in the dose fall-off with distance from that direction. This effect is seen superimposed on a larger, rather uniform, GCR background.

STS-36: STS-36 flew some 46 km lower than STS-28. Because of the very steep radiation gradient as a function of altitude, the inner belt radiation contributed a negligible amount to the total measured radiation dose, virtually all of which came from the GCR and GCR-induced secondaries. This also shows up clearly in the time-resolved RME measurements. Indeed, the dose measured with TLDs at six locations distributed about the middeck and the flight deck show an average dose of 34.3 mrad with a standard deviation of only 2.5%. This translates to 7.74 mrad/day. The calculations, however, indicate an expected dose of 21.3 mrad at the same locations. A very similar discrepancy was observed between model calculations and data obtained from a tissue-equivalent proportional counter (TEPC) flown on

that mission (Badhwar et al., 1991). The discrepancy may be attributable to the inadequacy of the model's ability to account properly for the phase of the solar cycle.

A review of the dose distribution within the phantom also indicates a remarkable uniformity with no pattern other than statistical fluctuations of about 3% about a mean of 34.9 mrad. This again confirms the hardness of the GCR spectrum because at the center of the phantom the depth is about 7.6 g/cm^2 tissue equivalent.

STS-31: A typical contour plot of measured dose for Section 3 is shown in Figure 4. It should be noted that during this flight the dose received was the highest of any Shuttle flight, and near the phantom head was measured by an unshielded TLD to be equal to 1.8 rad. The contribution from the GCR should be about 5.5 mrad/day or about 2.5% of the total dose. As can be clearly seen, the side of the head close to the bulkhead shows a higher dose than the side facing the interior of the orbiter.

The investigators have also calculated the dose distribution within the phantom. In general this is a complex task; however, during this mission the head was deployed in such a way that computationally the mass distributions of both the phantom and the orbiter could be added in a rather manageable way and the projected dose computed. The expected dose, calculated using the AP-8 trapped proton model for the solar maximum and the mission orbit, is shown in Figure 5.

Note that there is a clearly defined lateral asymmetry in the dose distribution. The overall calculated dose is about 20% lower than measured. Considering the age of the models and the factor-of-two advertised accuracy, the agreement is excellent. Also, the flux used in the calculations was omnidirectional, and the computational model of the phantom deviated somewhat from the actual object. To view the distribution in some detail the investigators have plotted in Figure 6 the dose distribution of a lateral cut through section 3 at the fourth level from the top as shown in Figures 4 and 5. Even though the phantom head was held in a rigid position throughout the flight and thus was exposed to a very non-symmetric particle flux, a dose enhancement can be emulated at the center of the head. This can be achieved by reflecting the dose about the plane of symmetry of the

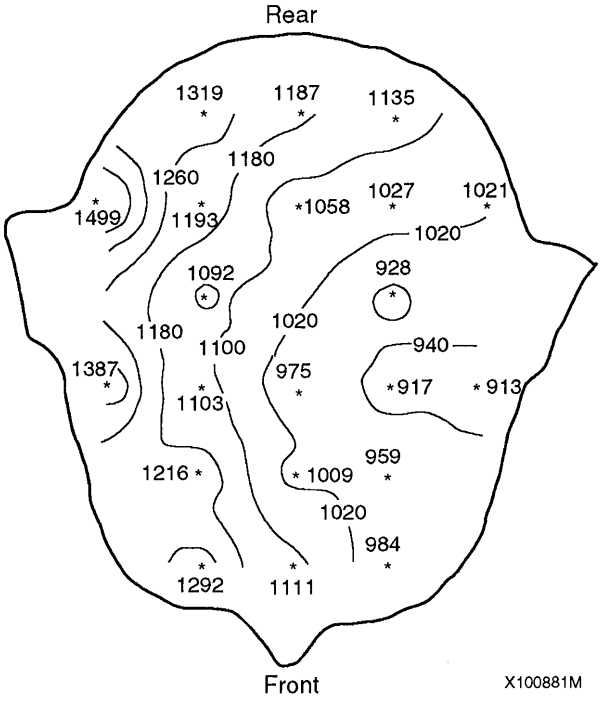

Figure 4. Isointensity contours of the radiation dose distribution in Section 3 recorded during STS-31.

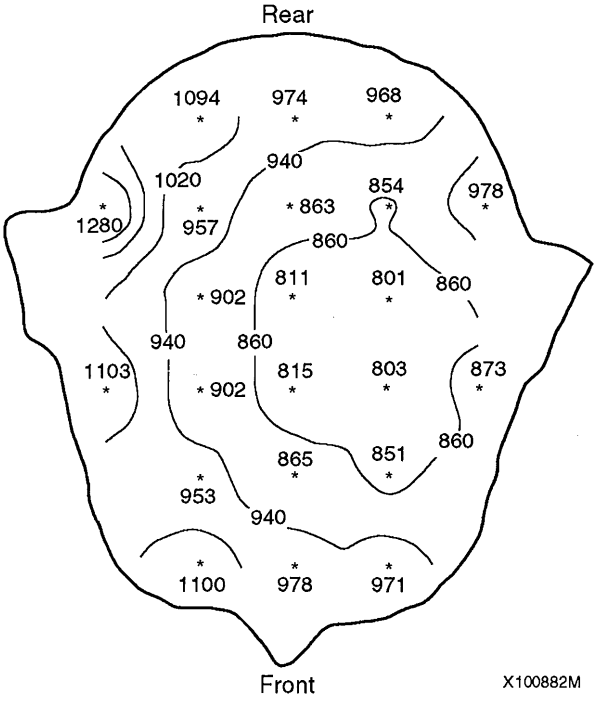

Figure 5. Isointensity contours of the radiation dose distribution in Section 3 recorded during STS-31.

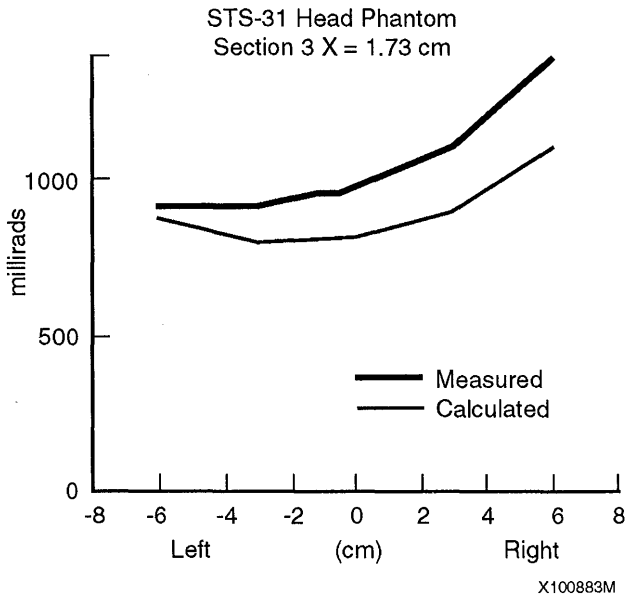

Figure 6. Calculated and measured STS-31 dose distributions in Section 3, fourth row of TLDs counting from the rear.

head and adding it to the original dose. Such a treatment would be equivalent to moving the head from the starboard bulkhead to the port bulkhead halfway through the flight. This approach should give a good indication of whether a dose increase is present near the center of the head.

Alternately, it can be deduced from Figure 6 without replotting that if the second derivative of the dose with respect to the lateral position is negative (the dose curve is concave), then under a uniform, omnidirectional irradiation, a dose minimum should be present at the center of the head. Clearly, the dose curve is concave, and no enhancement is found. In addition to the cut through Section 3 shown in Figure 6, we have reviewed cuts through all the other sections. All exhibit the same characteristics. None of them imply a dose buildup in the center of the head. In a recent study, Leavitt (1990) calculated the depth dose distribution within a human head from solar flare protons. The proton events used were those of 10 July 1959, 23 February 1956, and 16 February 1984. He found that "in all calculation configurations the maximum predicted dose will be on the exterior surface of the head phantom" (Leavitt, 1990). While for STS-31 we are dealing with fluxes of trapped protons, the energies of particles produced during solar proton events are in general quite similar, and the conclusions drawn by Leavitt also apply to our measurements.

RESULTS/DISCUSSION

Overall, the doses measured inside the phantom head compared well with those obtained from the crew passive dosimeters. A tissue equivalent human phantom head was flown on three Shuttle missions that included the lowest and the highest altitude orbits achieved to date. This fortuitous circumstance allowed investigation of the dose distribution under two extreme conditions: (a) when the flux was dominated by galactic cosmic rays and (b) when it was dominated by inner belt protons in the SAA. These two radiation sources, which differ both in atomic composition and energies of the incident particles, have a profound effect on the dose distribution within the phantom.

The dose distribution produced by GCRs and associated spallation products and measured by TLDs within the phantom is very uniform throughout the head volume. It also shows only about a +3% difference from place to place within the orbiter. This can be explained by the high energies and penetrating power of the GCR and by the creation of spallation products and secondaries during nuclear interactions with matter. Indeed, this measurement coupled with corrections for the body shielding due to the Earth and the geomagnetic cutoff, can in principle, be used as a benchmark for assessing the total dose expected in interplanetary flight during the current phase of the solar cycle. However, it is important to point out that while the measurements are consistent between the detectors carried on board the spacecraft, there is a very significant difference between the GCR doses measured on STS-28 and STS-36 that cannot be explained by the differences between their orbits. The explanation of this difference between doses must be sought in the temporal variation of the flux incident on the detectors. Clearly, further work needs to be done to explain the differences.

The dose distribution obtained from the SAA, on the other hand, shows a significant anisotropy due, no doubt, to the location of the phantom adjacent to the bulkhead. Using appropriate analysis of the data it was possible to determine that for inner belt protons no "hot spots" due to the Bragg peak are being produced in the phantom brain. Consequently, the analogy with the dose increase in the brain of rhesus monkeys subjected to 55 MeV proton fluxes is not valid.

REFERENCES

Badhwar, D. G.; Braby, L. A.; Konradi, A. Real-time measurements of dose and quality factors on board the Space Shuttle. Nucl. Tracks Radiat. Meas.; 1991 (In press).

Benton, E. V.; Frank, A. L.; Yang, D.; Benton, E. R. Preliminary measurements of LET spectra in the head of a phantom flown on STS-28. Progress Report, NASA Grant NAG9-235. Available from: University of San Francisco, San Francisco, CA. 1990.

Leavitt, D. D. Analysis of primate head irradiation with 55-MeV protons. Accepted for publication in Radiation Research; 1991.

Leavitt, D. D. Proton depth dose distribution: 3-D calculation of dose distributions from solar flare irradiation. USAF School of Aerospace Medicine Tech. Report TR 90-17; 1990. Available from: Brooks AFB, San Antonio, TX.

Richmond, R. G.; Badhwar, G. D.; Cash, B. L.; Atwell, W. Measurement of differential proton spectra on board the Space Shuttle using a thermoluminescent dosimetry system. Nuclear Instruments and Methods in Physics Research A256: 393-397; 1987.

Richmond, R. G.; Cash, B. L.; Jones, K. L.; Mizner, A. A. Operational dosimetry for the Space Shuttle. A short summary of techniques and results. Proceedings of the Topical Conference on Theory and Practices in Radiation Protection and Shielding. 1987, April 22-24, American Nuclear Society, Knoxville, TN.

Wood, D. H.; Yochmowitz, M. G.; Hardy, K. A.; Salmon, Y. L. Occurrence of brain tumors in rhesus monkeys exposed to 55-MeV protons. Adv. Space Res. 6: 213-216; 1986.

DSO 469B: Active Dosimetric Measurements on Shuttle Flights/Interim Report

Investigators: Gautam D. Badhwar, Ph.D.; Andrei Konradi, Ph.D.; Alva Hardy, Ph.D.; and Leslie A. Braby, Ph.D.

ABSTRACT

A tissue-equivalent proportional counter spectrometer capable of measuring the absorbed dose and dose distribution as a function of linear energy transfer and time, for all penetrating radiation in space, is described. This instrument weighs about 0.7 kg and was flown on the STS-31 (28.5° x 620 km) flight of the Shuttle, April 24-29, 1990. The measured total dose is in excellent agreement with the calculations based on the AP8MAX model of the trapped radiation belt protons. The observed linear energy transfer (LET) frequency distribution is also in excellent agreement with calculations based on this model. Active instruments can provide more detailed dosimetry for crew risk assessment than the thermoluminscent detectors or a plastic track detector system.

INTRODUCTION

The radiation environment in space is unique. In low Earth, typical Shuttle orbits the incident radiation is dominated by high energy, trapped protons. These protons have an energy spectrum extending from a few MeV to about 500 MeV, with peak around 100 MeV (Richmond et al., 1987). The second source of radiation is the galactic cosmic radiation (GCR) consisting of ions of all elements and energy spectrum extending from a few MeV/nucleon to thousands of GeV/nucleon. These high energy particles produce nuclear fragmentation with high LET secondaries that can add significantly to the dose equivalent.

The physical basis of the relative biological effectiveness of different types of radiation is now generally believed to be attributable to the difference in the spatial distribution of ionization along the track of the charged particles (Katz et al., 1972). Thus it is possible to measure physical quantities that are related to biological damage and estimate the biological relevant quantity (RBE). The principle of microdosimetry is based on measuring the energy deposition in micrometer diameter volumes of tissue (Rossi et al., 1977). This stochastic quantity depends on the charged particle stopping power, path length through the site, energy loss straggling, and energy transport by delta rays. The distribution of the energy deposition can be used for defining the radiation quality factor (ICRP-26, 1977). In terms of energy loss by charged particles, tissue volumes of one-third to several micrometers in diameter can be replicated using gas at low pressure. Microdosimetry instruments thus provide an efficient method for determining the dose and dose-equivalent in a complex radiation environment. This paper describes results from such an instrument.

Instrumentation

The prototype instrument is a completely automatic microdosimetry system that records the lineal energy, y, spectra for evaluating the dose and dose-equivalent. It is a system designed for minimum size and power consumption. The basic system consists of one detector which is operated at a gas gain of approximately 200 and is used to detect events of between 0.26 and 300 keV/μm. Detector systems using conventional techniques are unsatisfactory because the tissue-equivalent plastic gradually evolves vapors which cause a reduction in detector gain and resolution. In addition, vibration loads and gravitational acceleration lead to additional constraints for a space-based system. With advancements in improved materials processing techniques (EG&G, Santa Barbara Division, CA) and improved detector design, detectors can be built that can be filled and sealed and produce gain stability for over a year. The current instrument uses such a detector.

To reduce stray capacitance and, therefore, preamplifier noise, a charge-sensitive preamplifier is fitted into the mounting base of the detector. The overall system noise is about 120 electrons rms with the voltage applied to the detectors. The pulse height from the detector is processed through a 128-channel ADC. This is actually a pulse height-to-pulse width

Accepted for publ. by *Nucl. Tracks Radiat. Meas.*

convertor that is used to gate on a 4 MHz clock. The number of output clock pulses from the ADC is proportional to the height of the input pulse. The conversion time per pulse is about 13 microseconds, which is about the resolving time of the detector-amplifier circuits. The accuracy of the conversion may be increased by increasing the conversion time or the clock frequency. The linearity of this design is very good. The total LET range is divided into 15 approximately semi-logarithmically spaced intervals. Each of these channels records the number of events in the appropriate LET range based on the ADC channel values and calibration. Precision storage is utilized giving a count capacity of 48K counts. The data are accumulated for a preset time interval that is EPROM controlled and can be varied from 55 msec to 10 minutes. For this particular flight the data were recorded at 1-minute intervals. Thus the data consist of a time stamp and of the number of events in each of 15 LET channels. One of the channels is reserved for accumulating the total energy of all particles that have an LET value between 0.26-10 keV/μm. Gain stability tests were performed on an earlier version of this instrument (Braby, 1983) and showed long-term drift of less than 1% per month, and short-term (less than 24 hours) variations of ± 2%. The performance of the instrument has also been studied using Fe^{56} ions at the BEVALAC. The iron beam was scattered using 6 μm of lead to provide uniformity over the detector. The measured stopping power of 234 keV/μm is in good agreement with the calculated stopping power of 220 keV/μm considering the lack of beam uniformity.

The flight instrument was calibrated using a Cf^{252} neutron source just before and after the flight and showed no gain change. This LET spectrum exhibits a "proton edge" which is used for calibration. The point of inflection on the proton edge corresponds to a value of 98 keV/μm. Braby (1985) has discussed in detail the results of testing the prototype instrument using accelerator-produced neutrons and neutron and gamma ray from radioactive sources. The results of these calibrations show that the system accuracy is ±6% for the calculation of an average quality factor and ±15% for the calculation of the dose equivalent.

The tissue-equivalent proportional counter was flown on STS-31 that carried the Hubble Space Telescope (HST) into 28.5° x 620 km orbit on April 4, 1990. The TEPC instrument was turned on approximately 300 minutes into the flight and collected data for a period of 5657 minutes (3.93 days). Figure 1 gives the details of the flight trajectory and the orientation of the Shuttle as a function of time. Approximately 1200 minutes into the flight the HST was taken out of the Shuttle cargo bay and deployed.

PROCEDURES

The data from the on-board memory was downloaded to a PC and processed. Figure 2 is the probability density of the chord length distribution for assumed isotropic flux of particles on the proportional counter. Although it has a long tail, the distribution is very highly peaked at a value of 2, and, for all practical purposes, the detector system can be assumed to have a fixed chord length. Thus the lineal energy, y, and linear energy transfer (LET) can be used essentially interchangeably. Table 1 gives the LET range of each channel and the most probable calibration of each channel. Using these calibration values, the dose, dose equivalent, and quality factor can be calculated at 1-minute intervals. The absorbed dose can be found by summing the individual energy depositions, E, from the events recorded by the TEPC, since for each event the pulse height is proportional to the energy deposition in a known mass, m, of tissue-equivalent gas.

$$D = \left(\frac{c}{m}\right) \sum_{i=2} F_i N_i - \left(\frac{F_2}{80}\right) \sum_{i=3} F_i N_i \qquad \text{(Eq. 1)}$$

where D is dose rate (mrad/minute), F_i is the mean value of lineal energy channel i, with N number of particles in this channel. The second term in the expression is due to the overflow in channel one.

If the quality factor is defined in terms of lineal energy, and since the TEPC measures the dose distribution in terms of average lineal energy, the dose equivalent can be calculated directly and is given by

$$H = \left(\frac{c}{m}\right) \sum_{i=2} F_i Q(F_i) N_i - \left(\frac{F_2}{80}\right) \sum_{i=3} F_i Q(F_i) N_i \qquad \text{(Eq. 2)}$$

The ICRU Report 40 (1986), however, defines the quality factor in terms of lineal energy, y, which is defined as the energy deposited in a volume of interest divided by the mean chord length in that volume.

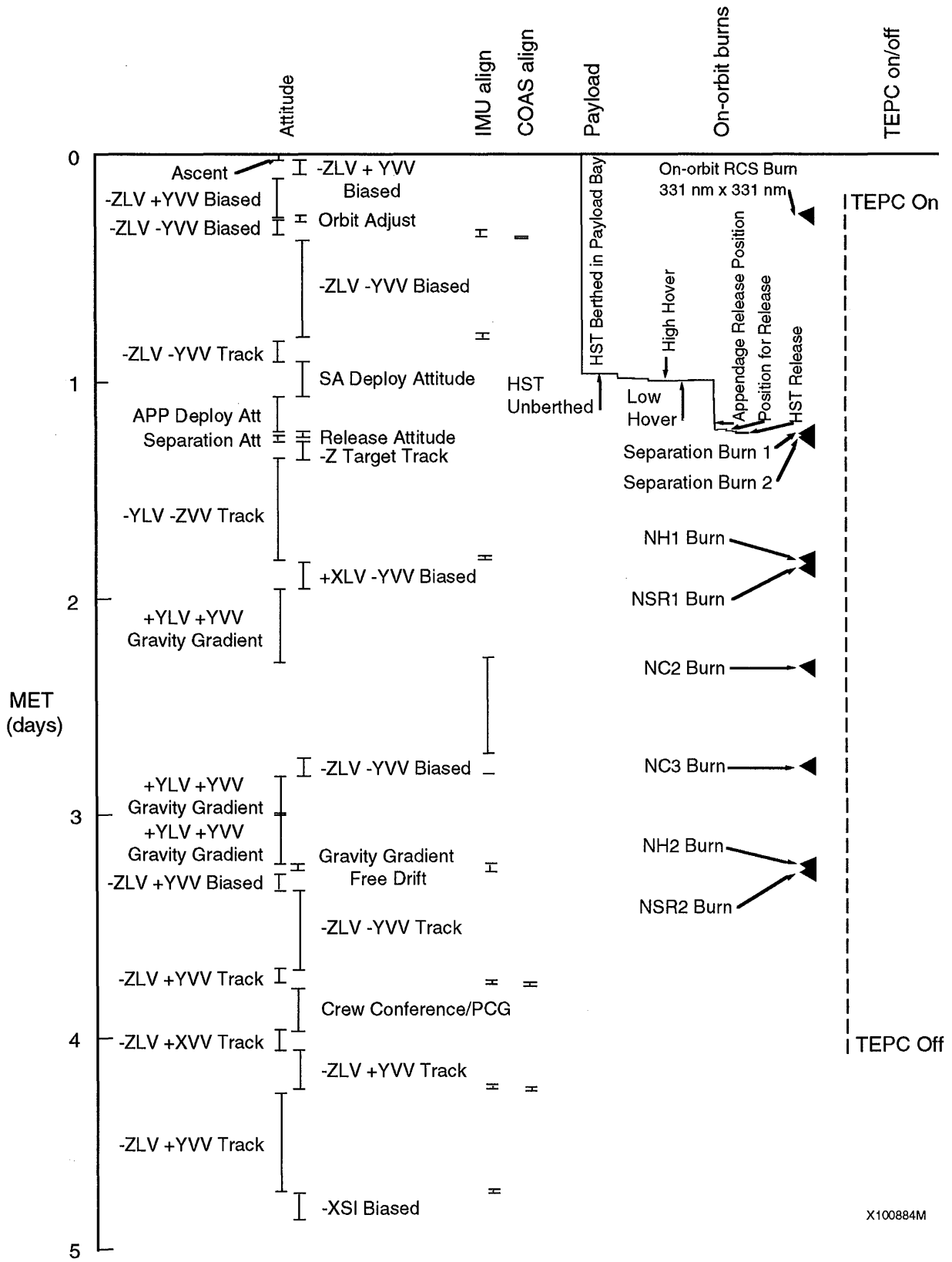

Figure 1. A plot of attitude of the Shuttle as a function of mission elapsed time (MET). Note the deployment of the Hubble Space Telescope at around 1200 minutes into the flight. This does not lead to an isotropic flux on the detector.

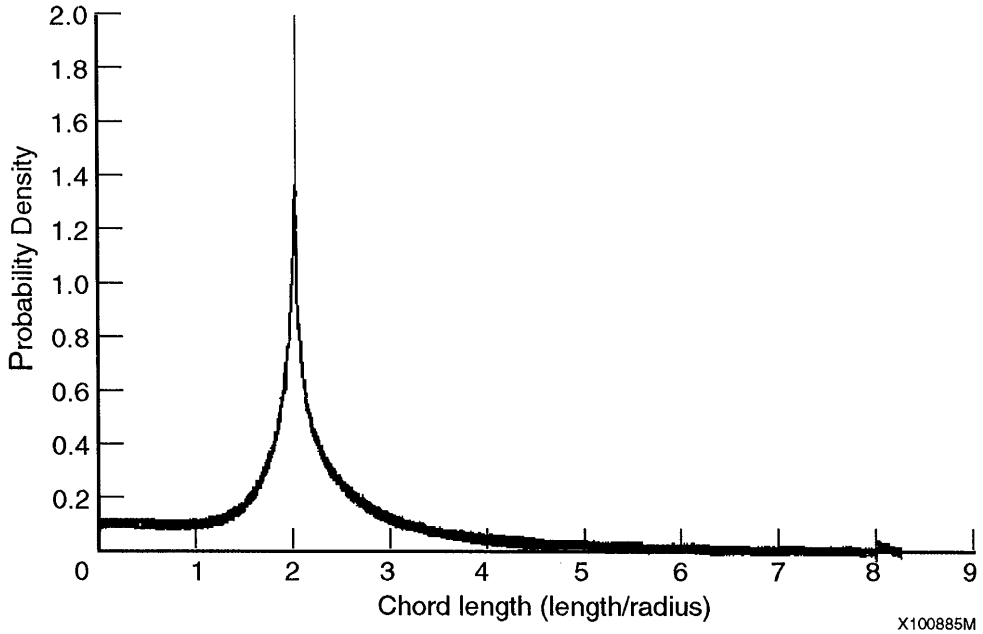

Figure 2. Probability density distribution of the chord length distribution for counter of length four times the diameter for an isotropic flux distribution.

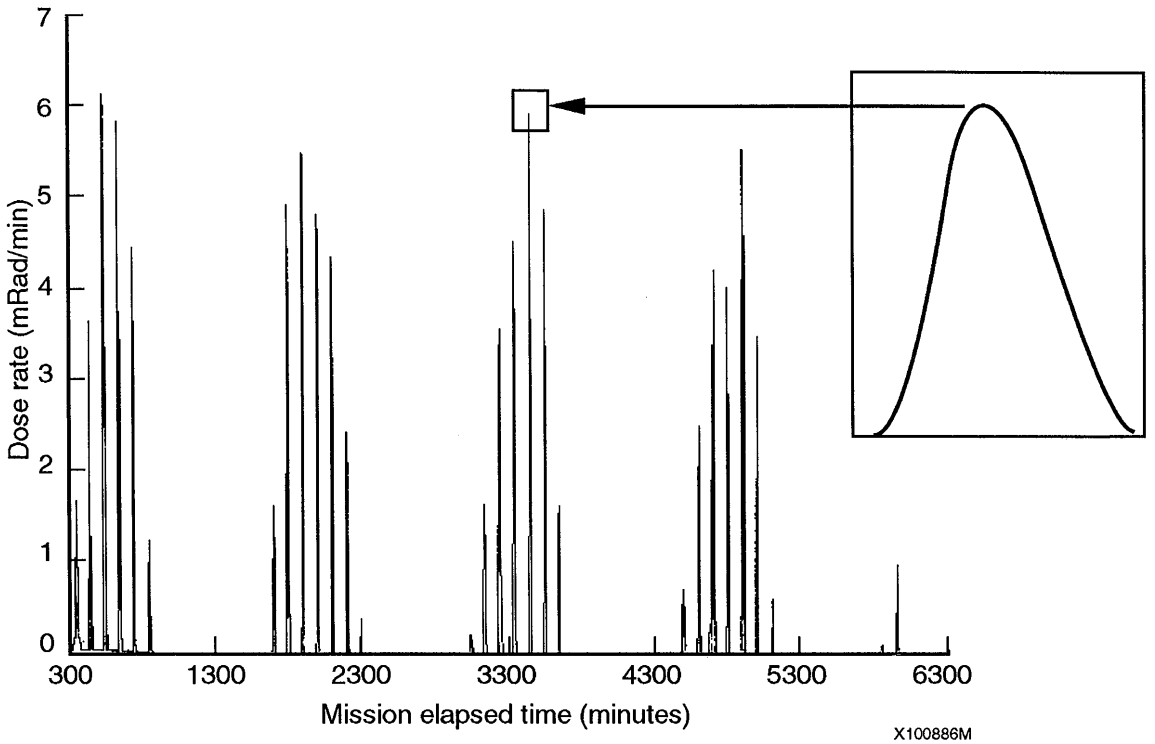

Figure 3. A plot of the dose rate (rad/minute) versus the mission elapse time (MET) in minutes. The inset shows just one pass through the South Atlantic Anomaly.

TABLE 1. RANGE AND CALIBRATION OF CHANNEL NUMBER TO LET

Channel No.	Lower LET Value	Mid LET Value	High LET Value
2	80.0	80.0	80.0
3	11.25	14.06	16.87
4	16.87	19.69	22.50
5	22.50	25.31	28.12
6	28.12	33.75	39.37
7	39.37	45.00	50.62
8	50.62	56.25	61.87
9	61.87	70.31	78.74
10	78.74	87.19	96.18
11	96.18	104.06	112.49
12	112.49	123.75	134.98
13	134.98	146.25	157.48
14	157.48	171.56	185.60
15	185.60	199.68	213.72
16	213.72	257.06	298.09

The number one defines the effective quality factor, Q, as the dose-weighted quality factor:

$$H = \overline{Q}\, D$$

then

$$\overline{Q} = \frac{1}{D} \int D(y)\, Q(y)\, dy \qquad \text{(Eq. 3)}$$

The energy deposited in the TEPC is the product of the LET multiplied by the path length of the charged particle traversing the gas cavity. The energy deposition pattern distributions are measured by the TEPC, and the path length distribution can be calculated from the knowledge of the geometry of the detector and the angular distribution of the radiation. Using an algorithm similar to those developed by Rossi (1985), the LET distribution can be unfolded. A simpler method, however, was suggested by Kellerer (1969) who predicted a linear relationship between the first moment of the dose distribution measured by TEPC and the first moment of the dose distribution as a function of LET. With the fast Fourier inversion techniques the dose-equivalent can be directly calculated. However, in this particular detector system, the chord length distribution is essentially a Dirac g-function, and the method of Equation 2 will give the same results as this more involved method.

RESULTS

Figure 3 shows the dose rate as a function of the mission elapsed time (MET). The sharp spikes are the passes through the South Atlantic Anomaly (SAA). A particular pass, which typically takes about 20 minutes, is shown in the inset. Figure 4 is a plot of the dose rate as a function of the latitude and longitude projected on a grid of the world map. The color coding reflects the magnitude of the dose as the Shuttle enters and exits the SAA. The sharp cutoff of the bell-shaped curve is a direct consequence of the inclination of the Shuttle orbit (28.5°). A projection of this plot is shown in Figure 5, and it is quite clear that the SA anomaly is mapped well. The yellow area reflects the GCR dose rates and, as expected, is quite small. An integration time of 10 to 60 minutes will be required to show this component on this kind of plot. It is thus clear that active instruments of this kind can provide dose contours of the SAA passes and, given sufficient time resolution, can locate the anomaly accurately.

As the anomaly drifts westward at the rate of about 0.27°/year and the current models are based on data about 20 years old, this information can be quite important in improving the accuracy of the existing models. Integrating this data over the flight time gives a total dose of 0.96 rad at the location of the instrument. Using (i) the solar maximum model for the trapped radiation, AP8MAX (Vette and Sawyer, 1979), (ii) the GCR spectra calculated using the CREME

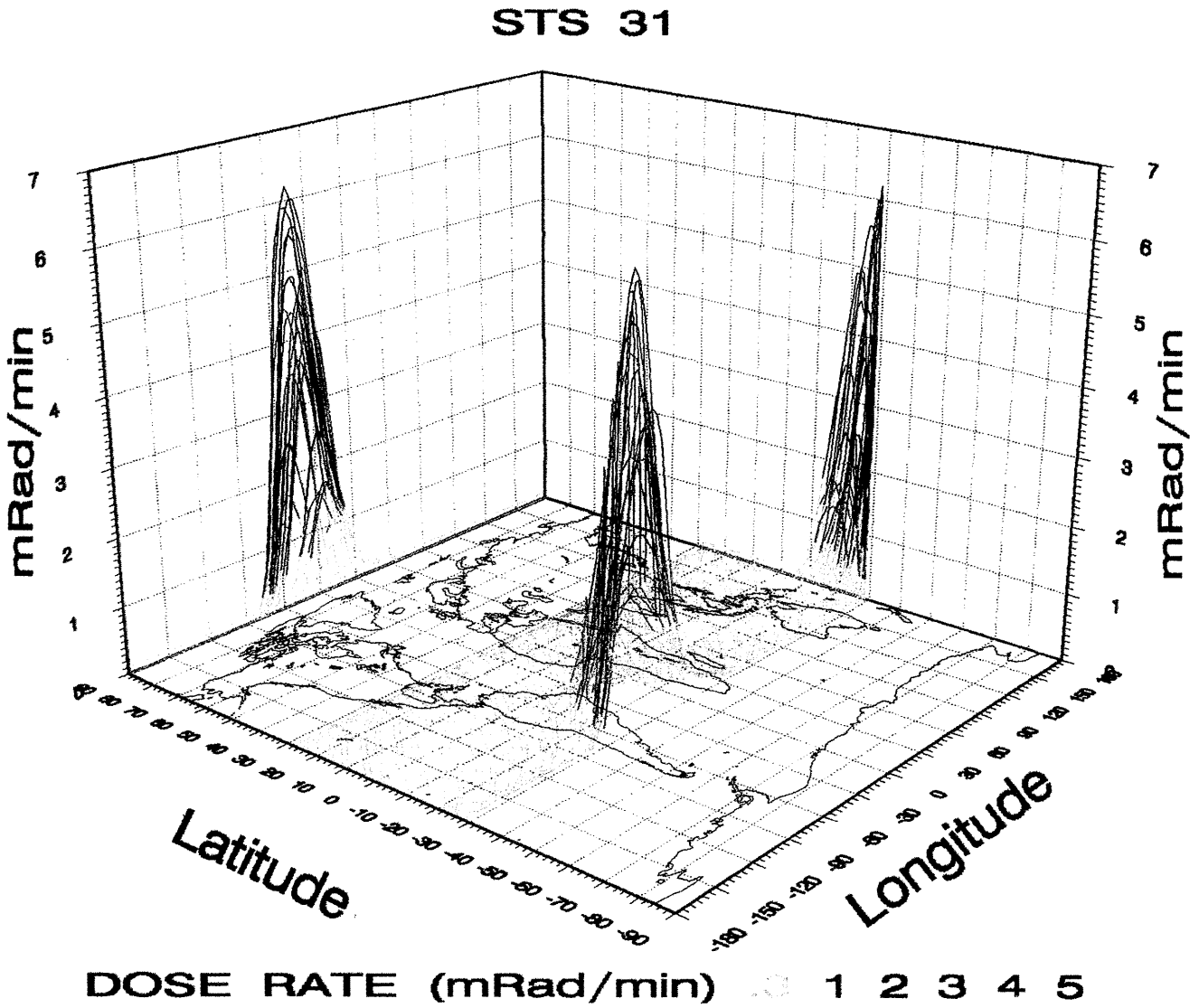

Figure 4. A three-dimensional plot of the dose rate versus geographic latitude and longitude superimposed on the world map. The color coding is due to different levels of the dose rate.

model (Adams et al., 1986), and (iii) the contribution of secondary protons using the BRYNTRN code (Wilson et al., 1988), the expected dose at the detector is calculated to be 0.93 rad. In calculating this dose, the Shuttle mass distribution was taken into account using 968 section radial outwards from the location of the TEPC and includes the shielding around the proportional counter tube itself. This calculation also assumes that all of the radiation, including the trapped protons, is omni-directional and includes no contribution from either the electrons or the secondary neutrons. Considering the uncertainty in calibration and in the AP8MAX model, the agreement between the observed and calculated dose is remarkably close. This, however, does not imply that AP8MAX itself is that accurate because it is quite clear from Figure 1 that in the approximately 4 days that the instrument was on, both the mass distribution (due to the deployment of the Hubble Telescope) and orientation of the Shuttle itself changed significantly so as not to provide a truly omni-directional flux. Thus, pitch angle effects would have to be considered. This is a difficult task and will be addressed in a forthcoming report. The agreement between the calculations and observation doses, however, suggest that the calibration using the Cf^{252} can be applied to the mixed radiation field environment of the Shuttle, and real-time detailed dosimetry in space is practical. A bare TLD detector was flown approximately 3 feet from the location of the TEPC. If the observed TLD is

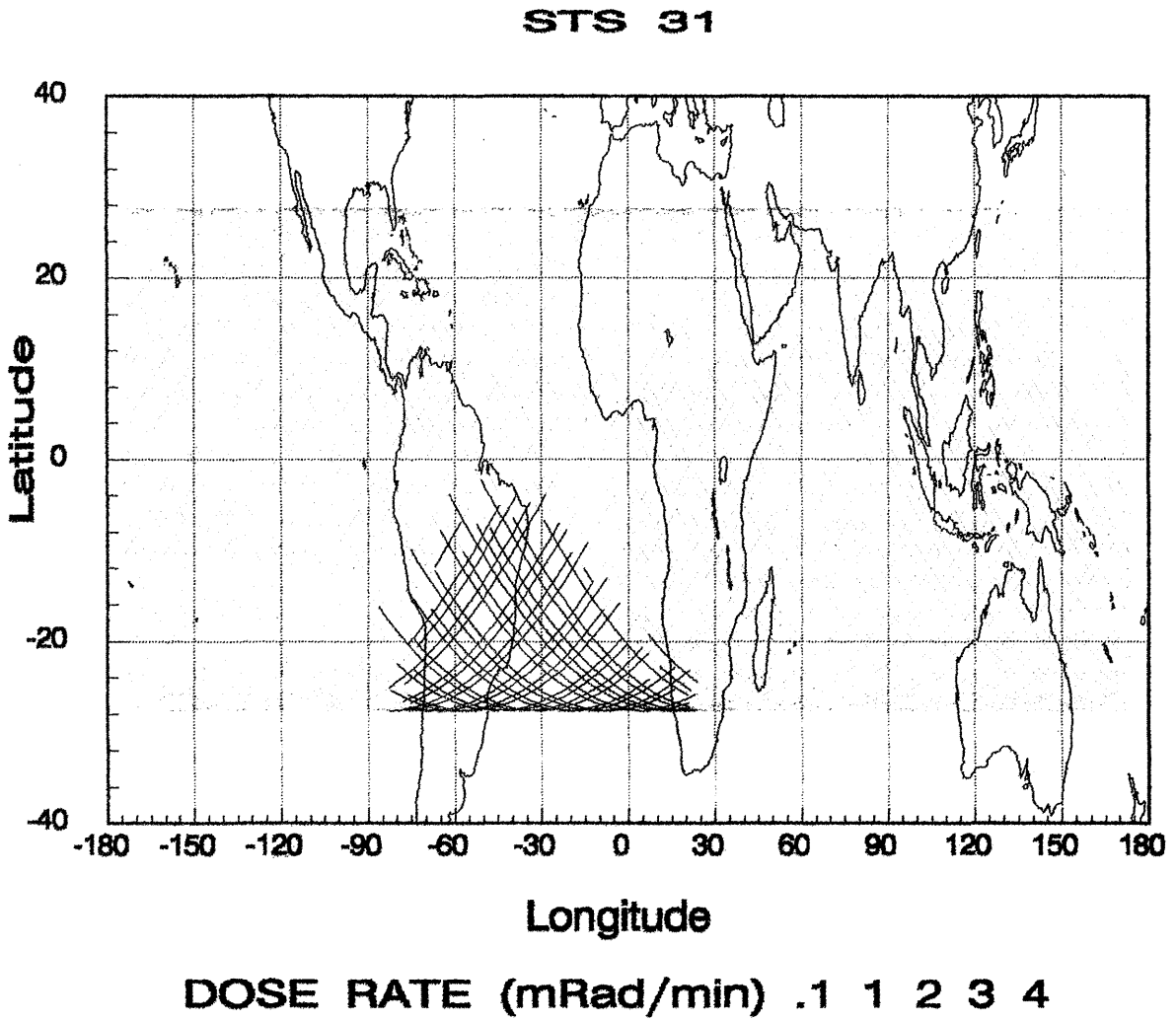

Figure 5. A two-dimensional projection of the plot in Figure 4 as viewed from the top.

corrected for the additional material around the proportional counter tube, the TLD would have measured approximately 1.12 rad. That is, if the TLD detector had been at the location of the proportional counter tube, it would have read 1.12 rad. This is in agreement with the TEPC measured value of 0.96 ± 0.14 rad and thus independently confirms the performance of the instrument.

The average dose-equivalent calculation can be done using Equation 2. As already noted, channel 1 records the total number of particles with 0.26 < LET < 10 keV/μm whereas channel 2 records the total energy deposited by these particles. Thus one only has the average energy deposited for this broad LET band. The distribution of the average value of LET in this channel is, as expected, very narrow and centers on 2.59 keV/μm. The value of the quality factor, Q, for this channel is then calculated for this average value at 1-minute intervals. For the remaining channels, the value of Q is calculated at the mean calibration value. Using this method of calculation leads to dose-equivalent for whole flight of 2.33 Rem or average Q of 2.41. This value of Q is much higher than is usually associated with trapped proton (Q = 1.4). This is a direct result of the broad first band which includes a very large fraction of all protons seen in this flight. If j(l) is the differential LET spectrum, then

$$\overline{Q} = \frac{\int Q(\ell)\, j(\ell)\, d\ell}{\int j(\ell)\, d\ell} \neq Q\left\{\frac{\int 1\, j(\ell)\, d\ell}{\int j(\ell)\, d\ell}\right\} \qquad \text{(Eq. 4)}$$

Thus, the values of dose-equivalent from this instrument are expected to be higher than the "real" values. As will be shown, the observed differential LET spectrum is in good agreement with the calculated spectrum and can be used to derive the dose-equivalent. However, the real solution lies in either narrowing the first channel to cover no more than 2.5 keV/μm, or better still, to provide additional channels to cover this LET range.

Figure 6 is a plot of the observed spectrum and its comparison to the calculated LET spectrum for the entire flight. The calculated spectrum uses the same method of calculation as discussed earlier for the dose calculation. The observed data is plotted as a stair-step, each step representing the width of the LET interval. As can be seen, the agreement is good, except near the Bragg peak of protons where the calculated values are higher than the observations. This is due to the straight-head approximation that is made in the BRYNTN calculation code. The model assumes that the direction of the outgoing and incoming proton is the same. This is a good approximation for high energy protons, but breaks down completely near the Bragg peak energy of protons. This neglect of scattering effects leads to higher differential values. It should also be noted that in the lowest LET interval, the agreement is quite good. This means that the total number of observed protons and calculated protons are in good agreement, but provides no check of the true nature of the proton LET spectrum and as is clear from Figure 7, which is a plot of the l x j(l) versus l, the lowest LET channel contributes most of the dose. This figure also shows very good general agreement between the dose calculations and observations.

It was also found that the observed LET spectrum before an MET of 1200 minutes is quite different from that observed after this time. A look at Figure 1 suggests a possible explanationof this behavior. At this time the HST was moved out of the payload bay and this changed the mass distribution at the location of the TEPC spectrometer, but more importantly, the Shuttle was pointed in two different orientations before and after this time period. As a result of east-west effect and pitch angle distribution, the expected proton fluxes seen in the two orientations will be different. A quantitative evaluation of this effect is difficult at this time; however, this is the most likely explanation.

CONCLUSION

A lightweight, very low power, tissue-equivalent proportional counter system has been flown in mixed radiation environment. The results show:

(i) The observed total dose is in good agreement with passive TLD measurement and in excellent agreement with calculations based on current models of trapped radiation belts, galactic radiation, and nuclear transport.

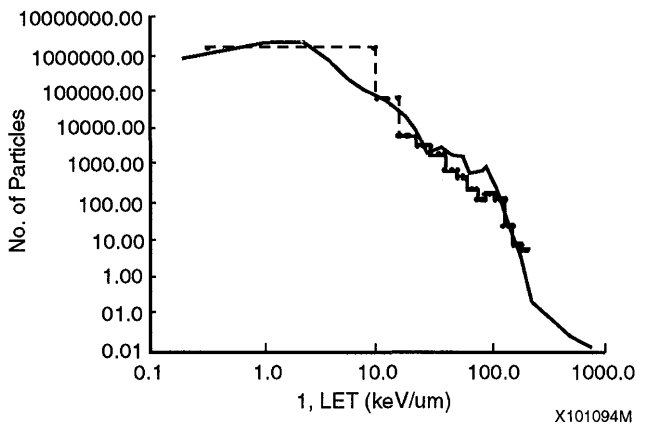

Figure 6. A comparison of the observed differential LET spectrum and that calculated using the trapped proton model, the galactic cosmic radiation model, and transport through the Shuttle mass distribution.

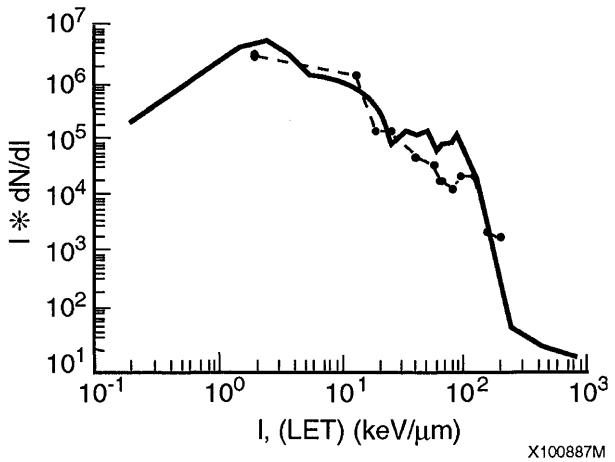

Figure 7. A comparison of the observed differential dose distribution as a function of LET with model calculations.

(ii) The observed LET spectrum is in excellent agreement with model calculations. This information can be used to provide LET dependent quality factor for better estimation of the dose-equivalent.

(iii) The measurements have indicated that for monitoring trapped protons, either additional channels should be added to the instruments or the distribution of the channels should be changed to make lower channels much narrower than in the current instrument.

(iv) The results clearly show that active dosimetry for crew health and safety is possible with these types of instruments.

ACKNOWLEDGMENTS

We greatly appreciate the help of Dr. Larry Brackenbush, Dr. Gordon Anderson, Dr. Tom Conroy, Mark Bowman, and Michael Golightly.

REFERENCES

Adams, J. H., Jr.; Silberberg, R.; Tsao, C. H. Cosmic Ray Effects on Microelectronics, Part I: The Near-Earth Particle Environment. NRL Memorandum Report 4506, 1981; August 25.

Braby, L. A. Portable Dose Equivalent Meter Based on Microdosimetric Techniques, Nuclear Instruments & Methods, B10/11: 910-914; 1985.

Katz, R.; Sharma, S. C.; Hamayoonfar, M. The structure of particle tracks. In: Attixs, F. H., ed. Topics in Radiation Dosimetry, Radiation Dosimetry, Supplement I. New York: Academic Press; 1972: pp. 317-383.

Kellerer, A. M. Analysis of Patterns of Energy Deposition. Proceedings of the Second Symposium on Microdosimetry. Stresa, Italy. Council on Economic Cooperation, Luxemberg, 1969: 107-134.

International Commission on Radiation Units and Measurements. ICRU Report Number 26, International Commission on Radiation Units and Measurements Publications, Bethesda, Maryland; 1977.

International Commission on Radiation Units and Measurements. ICRU Report Number 40, International Commision on Radiation Units and Measurements Publications, Bethesda, Maryland; 1986.

Richmond, R. G.; Badhwar, G. D.; Cash, B.; Atwell, W. A. Measurement of Differential Proton Spectra On Board The Space Shuttle using a Thermoluminescent Dosimetry System. Nuclear Instruments and Methods, A256: 393-397; 1987.

Sawyer, D. M.; Vette J. I. AP-8 Trapped Proton Environment for Solar Maximum and Solar Minimum, Report NSSDC/WDC-A-R&s 76-06, National Space Science Data Center, Goddard Space Flight Center, Greenbelt, Maryland; 1976.

Wilson, J. W.; Townsend, L. W.; Nealy, J. E.; Chun, S. Y.; Hong, B. S.; Buck, W. W.; Lamkin, S. L.; Ganpol, B. D.; Khan, F.; Cucinotta, F.A. BRYNTRN: A Baryon Transport Model. NASA TP-2887; 1989.

DSO 469C: Neutron Spectrum and Dose-Equivalent in Shuttle Flights During Solar Maximum

Investigators: James E. Keith, Ph.D.; Gautam D. Badhwar, Ph.D.; and David J. Lindstrom, Ph.D.

ABSTRACT

A set of passive detectors consisting of metal foils and Bonner spheres have been flown on three Shuttle flights during the solar maximum to measure, from thermal to about 10 MeV, neutron fluence as a function of energy, and their dose-equivalent. The differential energy spectrum in this energy range can be very well approximated by a power law, A x 10^4 $E^{-.765}$ neutrons/cm^2-day-MeV. This spectrum is well represented as a linear combination of the spectrum locally produced in Al using the HETC code and the albedo spectrum. Thus, above 10 MeV, the spectrum has been extrapolated using the HETC code. The most probable ratio of the neutron skin dose-equivalent to charged particle skin dose equivalent, using ICRP-51 neutron fluence-dose conversion tables, varies from 5 to 10% under approximately 2-3 g cm^{-2} of Al shielding. These values are considerably lower than the estimates obtained using fission foil or ^{6}Li-CR 39 techniques, both of which suffer from large and unknown proton contamination.

INTRODUCTION

The contribution of neutrons to the radiation exposure of astronauts has largely remained an ignored problem. Neutron spectra have never been measured on spacecraft. Neutrons inside the spacecraft arise from the interactions of the galactic cosmic radiation and trapped protons with the spacecraft material. In addition, albedo neutrons from the atmosphere are present. There are a number of theoretical estimates of the albedo spectrum and their dose contribution (Wilson et al., 1989). Measurements of the albedo neutrons above about 2 MeV have been made (Bhatt, 1976; Lockwood, 1976). Recently Feldman et al. (1990) have reported measurements of 0.5 - 20 MeV albedo neutrons using active detectors aboard the LACE spacecraft. There are hardly any calculations or predictions that take into account these three neutron sources and transport through the spacecraft shielding distributions.

The problem of detecting neutrons in space is made very difficult by their small flux in the overwhelming presence of protons. A few attempts to measure this flux have been made using passive detector systems (Frank and Benton, 1987). Their technique for the detection of thermal and resonance neutrons is based on the high neutron capture cross-section of ^{6}Li. The reaction ^{6}Li(n,T)^{4}He, when ^{6}Li TLDs are used provides a very low energy alpha particle which is detected by CR-39 plastic track detector (Benton and Henke, 1983). The thermal and resonance neutrons are separated by using thin Gd foils. Keith and Clark (1973), Keith and Richmond (1987), Fishman (1974) and Haskin et al. (1990) have used a variety of metal foils, e.g., Au, Ir, Ta, Sc, and Co, with and without Gd cover, to measure the thermal and resonance neutron fluences. Based on ICRP (1987) or NCRP (1971) fluence-to-dose conversion factors, these measurements show that, in the absence of on-board neutron-emitting power sources, thermal and resonance neutrons make a negligible contribution to the total radiation dose or dose-equivalent.

Calculations such as those of Armstrong et al. (1990) clearly show that the higher energy neutrons provide the bulk of neutron dose. The track techniques for the detection of higher energy neutrons (> 1 MeV) are based on fission-track detector system of ^{238}U/mica, ^{232}Th/mica, ^{209}Bi/mica, and ^{181}Ta/mica. Due to competing proton-induced fission reactions, these techniques require large corrections due to protons whose spectral shape and intensity must be assumed, since they have never been measured simultaneously with fission-track detectors. Dudkin et al. (1990) have developed a technique that looks at the recoil proton from elastic scattering of neutrons from hydrogen in BYa-type nuclear emulsion. The authors claim that this technique provides flux measurements accurate to about 20% in the 1-15 MeV region. They have reported high dose-equivalent contribution from neutrons on various cosmos satellites.

Accepted for publ. by *Nucl. Tracks Radiat. Meas.*

Neutron bubble detectors have now been flown on bio-cosmos satellites (Ing, 1990). However, the sensitivity of these detectors to charged particles remains to be determined. These passive neutron measurements, in various Soviet and US spacecraft, under a variety of orbital and solar activity conditions, have indicated that the neutron contribution to the skin dose-equivalent can vary from a few to as high as 38%.

The importance of neutrons to the total crew radiation exposure is only likely to increase. Townsend and Wilson (1990) have estimated that during solar minimum the neutron dose-equivalent is about 45% of the total dose-equivalent under the lunar regolith shielding currently being considered for lunar base. The manned Mars mission is likely to need large amounts of shielding, and the irradiation of this shielding by cosmic rays and solar particles will furnish a steady source of neutrons. Thus, because of the current uncertainty in measurements, widely varying dose-equivalent estimates of high energy neutrons, and their increasing importance for future manned missions, it is necessary to (i) measure the neutron spectrum in spacecraft under realistic conditions, and (ii) develop an active detector system, perhaps similar to the detectors used by Feldman et al. (1990), that can provide accurate measurements of the spectrum in the crucial 1-100 MeV range.

This report presents the results from an attempt to measure, for the first time, the neutron spectrum from thermal to about 10 MeV using a passive system of metal foils, with and without Gd covers, and Au foils inside Bonner spheres of different sizes, in a variety of orbits during solar maximum. This technique does not require a correction factor for proton-induced activity and thus represents a "clean" measurement.

PROCEDURES

Description of Experiment

The experimental package was divided into two parts: one to study the thermal and epithermal neutrons, and the other to study neutrons of higher energy.

The first part of the experimental package consisted of 2" x 2" thin foils (2-5 mil) of Sc, Co, Ta, Ir, and Au (bare and with 0.005 cm Gd wrapping). The reason for choosing these elements is that the radiative capture cross-section for these nuclei is quite large, and the radionuclide either cannot be produced by protons or their proton-induced reaction cross-section is very small. The foils were held without overlap in Velcro-backed envelopes made from Nomex cloth.

The second package consisted of four Bonner spheres with Au foils at the center. These polyethylene spheres had external diameters of 5.08, 7.62, 12.70, and 20.32 cm with central detector cavity 1.27 cm in diameter. The detector consisted of high purity Au discs (1.27 cm diameter x 0.0508 mm). Both the Au discs, metal foils, and four background monitor discs and foils were transported by aircraft to and from launch site in a 1.7 mm thick Cd box. The Au discs were inserted into the Bonner sphere cavities just before launch.

Both packages were stowed in the middeck locker of the Shuttle. They were taken out of the locker and deployed on the starboard side in flight. They were again stowed in the locker before entry. This package was flown on three Space Shuttle flights, STS-28, STS-36, and STS-31. The first two flights were high inclination low altitude flights and predominantly sampled the galactic cosmic radiation, whereas the third flight was in a lower inclination high altitude flight and sampled trapped proton radiation. Table 4 gives the orbital parameters and exposure times for each flight. All of the foils were immediately recovered at landing and brought to the Radiation Counting Laboratory, Houston. This 60-foot underground laboratory has dunite-filled steel-lined walls and is one of the lowest background radioactivity-measurement laboratories in the world.

Measurements

All of the foils were counted on large intrinsic Ge detectors. The 296, 308, 316, and 468 keV gamma rays from Ir foils and the 68, 1121, 1189 and 1231 keV gamma rays from the Ta foils were found to be abundant enough to measure easily. In addition, attempts were made to isolate the effect of particular resonances, one using Co and Gd-covered Co foils and one each using an Au and an Ir sandwich (several layers of the same foil bound together with the expectation that the outer layer would absorb all the neutrons whose energy corresponds to large capture resonances). The attempts produced no activation attributable to the resonances. The results of the foil measurements are given in Table 1. The data were corrected for the background seen in the monitor foils. Although it is possible to produce ^{192}Ir from

TABLE 1. DETAILS OF FOIL COUNTING

STS-28	Ir	Ir	Ir	Ir	Remarks
X-Ray Energy	296	308	316	467	keV
Bare Activity	88.1	83.6	97.7	44.4	/day
Gd Activity	79.6	92.0	39.4		/day
Background	46.1	46.9	45.4	20.0	/day
Bare Do	1.11±.17				/min $\chi\nu$=1.37
Gd cover Do	.594±.09				/min $\chi\nu$=0.14
STS-28	**Ta**	**Ta**	**Ta**	**Ta**	
X-Ray Energy	68	1121	1189	1231	/keV
Bare Activity	257	10.8	4.57	5.50	/day
Gd Activity	247	8.92	4.54	4.77	/day
Background	206	8.71	3.53	3.53	/day
Bare Do	.764±.139				/min $\chi\nu$=7.5
Gd cover Do	.450±.112				/min $\chi\nu$=7.1
STS-28	**Sc**	**Sc**			
X-Ray Energy	889	1120			keV
Bare Activity	10.6	10.4			/day
Gd Activity	7.56	9.00			/day
Background	5.84	8.16			/day
Bare Do	2.4±.1				/min $\chi\nu$=0.78
Gd cover Do	.067±.038				/min $\chi\nu$=0.12
STS-31	**Au**				
X-Ray Energy	412				keV
Bare Activity	3242				/day
Gd Activity	1834				/day
Background	86				/day
Bare Do	18.09±.96				/min $\chi\nu$=0.13
Gd cover Do	10.10±.91				/min $\chi\nu$=0.07

^{193}Ir by the (p,pn) reaction, this correction is negligible. By integrating over the calculated STS-28 proton spectrum at the location of the foil and the production cross-section of ^{192}Ir (Bertini et al., 1986), the upper limit to the disintegrationrate was calculated to be 1.2 x 10^{-7} dpm/cm^2. This is six orders of magnitude smaller than the measured activity.

The response function, R(E), of Bonner spheres using Au foils as detectors was calculated by Sanna (1973) and is shown in Figure 1. The measured disintegration rate, D_i^o, of ^{198}Au (half-life 2.7 days) is proportional to the integral

$$D_o^i \sim \int_{th}^{400} R_i(E)\, J(E)\, dE \qquad \text{(Eq. 1)}$$

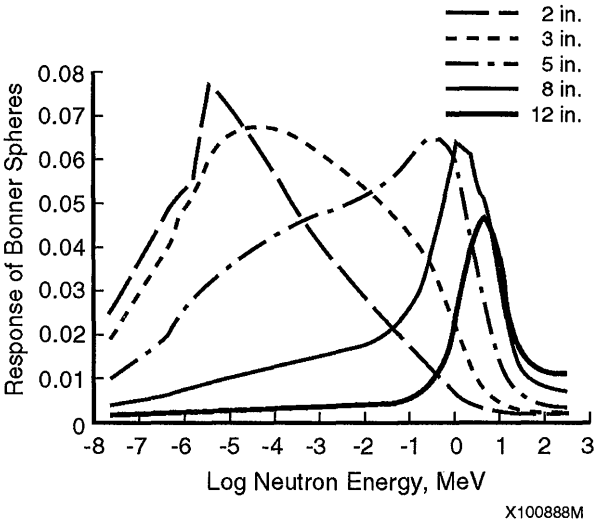

Figure 1. Response function for activity in Au at the center of Bonner spheres as a function of neutron energy.

where J(E) is differential neutron spectrum incident onthe polyethylene spheres, and "i" is the index for each of the spheres. Each Au disc was counted twice oneach of the two large intrinsic Ge detectors for a total of about 4000 minutes. The activities of the Au discs were derived from the measured spectra by the usual methods and corrected for the counting periods being an appreciable fraction of the half-life. The raw data were examined for consistency by statistical methods, both within and between detectors. The weighted (by inverse of the variance) averages of the decay-corrected activities and their standard deviations were computed. The data were corrected for the background rate, which in the region of the ^{198}Au photopeak was about 0.063/minute. The measured photopeak efficiency of these detectors for ^{198}Au gamma ray (412 keV) was 13%. The correctionfor self-absorption is negligible, and the correction for self-shadowing is included (Sanna, 1973) in the response function. The results of these measurements are given in Table 2. These results along with equation (1) form the basis of further analysis of the neutron spectrum in the Space Shuttle.

TABLE 2. SATURATED DISINTEGRATION RATE OF ^{198}AU FROM BONNER SPHERES

Sphere Diameter (cm)	STS-28 Do (dpm)	STS-36 Do (dpm)	STS-31 Do (dpm)
5.08	1.07±0.69	0.63±0.11	5.63±0.13
7.62	1.89±0.15	1.29±0.14	9.64±0.25
12.70	2.93±0.17	2.22±0.16	15.62±0.31
20.32	3.15±0.15	2.06±0.16	15.92±0.31

The correction for the production of neutrons in the Bonner spheres must be considered. Based on calculated charged particle flux from the AP8MAX (Vette and Sawyer, 1970) model, the CREME model (Adams et al., 1980) of galactic cosmic radiation model, and the production cross-section of neutrons in polyethylene, the upper limits to this correction are estimated to be 0.36, 1.8, 6.2, and 9% for the 2", 3", 5", and 8" spheres respectively. As these corrections are small compared to other uncertainties, they have not been applied to this data set.

Analysis

The problem of estimating the differential neutron spectrum, J(E), from the saturated disintegration rates, D_O, is simply that of inverting the integral Equation 1, given the known response function R(E), which is continuous square-integrable function of E. A number of techniques for inverting this integral equation are available in literature and, with a limited number of measurements, require some smoothing approximation to the form of the spectrum, J(E) (Routti, 1969). Based on the calculations of Armstrong et al. (1990), the fact that the slowing down neutron spectrum varies as E^{-1} suggests that the neutron spectrum be approximated as a power law, $E^{-\gamma}$, over the limited energy range of interest in these flights. The value of g was estimated by minimizing the merit function, defined as the ratio of saturation disintegration rate to the integral of equation (1) for each sphere. Table 3 and Figure 2 give the results of this calculation. The best fit was found to be g = 0.765±0.035 for all three flights. A somewhat better fit can perhaps be made, particularly for STS-31, by choosing a more complicated form of J(E) but is not warranted by this small a data set. Using Table 2, we thus have $J(E) = (1.24 \pm .04) \times 10^4 E^{-.765}$ for STS-28, $(0.85 \pm .04) \times 10^4 E^{-.765}$ for STS-36, and $J(E) = (6.50+0.27) \times 10^4 E^{-.765}$ neutrons/cm^2-day-MeV for STS-31 respectively.

The measured neutron spectrum is a combination of the neutrons produced in the Shuttle shielding and the atmospheric albedo neutrons. The production spectrum of neutrons in 1 g cm^{-2} of Al, as given by Armstrong et al. (1990), can be well approximated by $1.5 \times 10^5 \exp(-E/4.75)$ neutrons/cm^2-day-MeV from thermal energies to about 20 MeV, and by $5.3 \times 10^6 E^{-2.6}$ neutron/cm^2-day-MeV from 20 to 400 MeV. Their calculations also show that for moderate increases in the Al thickness, the flux of neutron above 20 MeV will increase linearly, and for neutrons below 20 MeV it will remain essentially a constant. The albedo spectrum can be well represented by a E^{-1} for E < 10 MeV and as exp(-E/100) for E > 10 MeV (Armstrong et al., 1990, Wilson et al., 1989). However, for this study we have approximated it by a power law, $5 \times 10^3 E^{-1}$ neutrons/cm^2-day-MeV as shown by the solid line in Figure 3 which gives a good description of the data. Based on this representation of the calculated neutron spectrum, it is found that a linear combination of 23% locally produced neutrons and 77% atmospherically produced albedo neutrons produces an energy spectrum that can be extremely well represented by the observed power law index of 0.765 in

TABLE 3. THE RATIO OF SATURATION DISINTEGRATION RATES OF ^{198}AU FOILS TO THE INTEGRALS OF THE NEUTRON SPECTRUM WEIGHTED BY THE RESPONSE FUNCTION OF BONNER SPHERES

Sphere Diameter (cm)	Integral $\gamma = 0.765$	STS-28 Ratio	STS-36 Ratio	STS-31 Ratio**
5.08	0.108	9.88±0.81	5.88±1.03	52.10±1.24
7.62	0.224	8.46±0.66	5.77±0.61	43.06±1.13
12.70	0.364	8.06±0.46	6.09±0.45	42.96±0.86
20.32	0.353	8.83±0.42	5.83±0.46	45.14±0.89
Weighted Average		8.63±0.27	5.92±0.27	45.12±1.89*
Reduced Chi-square	1.40	0.01	13.75	

* Adjusted by $\chi\nu$

** Ratio $= \dfrac{D_o}{\int E^{-\gamma} R(E)\, DE}$

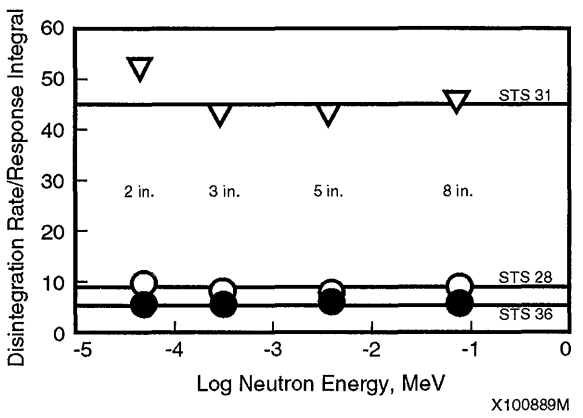

Figure 2. A plot of the ratio of saturation disintegration rate in Au foils to the calculated using equation (2) for J(E) = constant x E^{-8} plotted as a function $\log_{10} E$ of neutron energy.

the thermal energies to about 10 MeV region. Integrating over the energy range, these results give the relative integral flux of 65% as locally produced (from 1 g cm^{-2} of Al) and 35% as albedo neutrons. The shielding distribution function at the location of the Bonner spheres (assuming an isotropic flux) is highly skewed toward high thickness values, with a most probable value of about 2-3 g cm^{-2} and an average of about 16.5 g cm^{-2} of Al. In the Soviet (Dudkin et al., 1990) experiments using nuclear emulsions, the albedo contribution to the integral flux in the thermal energies to about 15 MeV range was about 50% of the total neutron flux. They also report dose-equivalent from 1.8 to 4.5 mrem/day with standard deviations of about 50% from a variety of Cosmos flights from 1977-1987. This amounts to 20-30% of the charged particle dose-equivalent. Although the actual shielding distribution from their flights is not available, the experiments were under about 5 g cm^{-2} to 50 g cm^{-2} of Al shielding. Thus they will see a higher locally produced neutron component and correspondingly smaller fraction of the albedo component than our measurements. Considering the large errors and much higher inclination of the flights, their measurements are not in disagreement with our results.

Thus by appropriately normalizing the calculations to the observed data in the limited energy range, the measurements can be extrapolated to much higher energies with a certain degree of confidence. In the following the differential energy spectrum from thermal energies to 10 MeV is taken to be a power law, $E^{-0.765}$, and above 10 MeV the form suggested by Armstrong et al. (1990), properly normalized to the flux at 10 MeV.

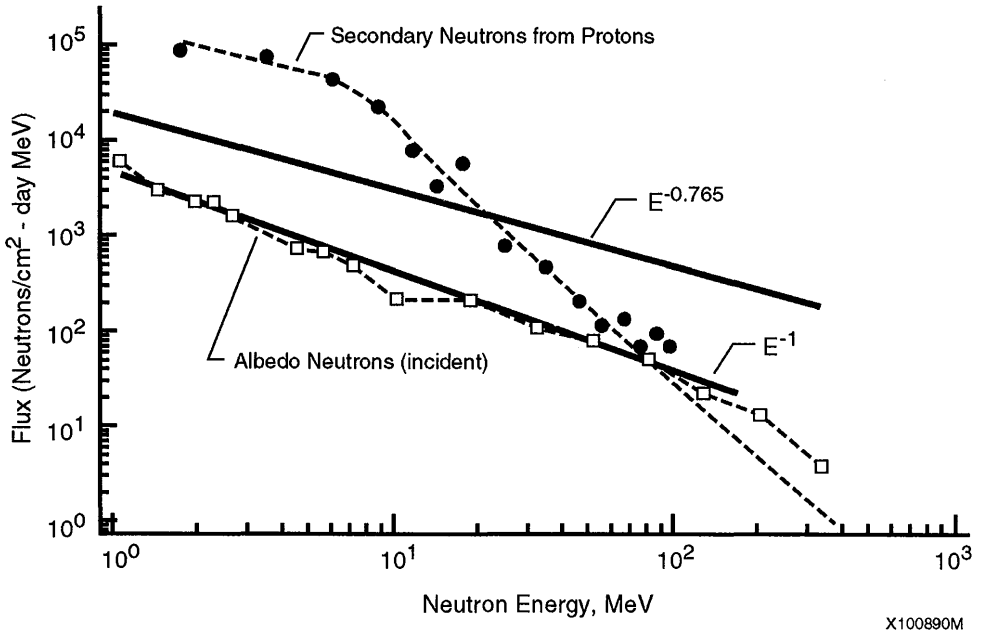

Figure 3. A plot of the calculated neutron spectrum from 1 g cm^{-2} Al, albedo neutrons, and the best linear combination that leads to the estimated power law, $E^{-0.765}$.

Dose-Equivalent From Neutrons

The quality factor of neutrons in MeV region is much higher than most of the charged particles in the space environment. The quality factors for thermal, epithermal, and high energy (> 1 MeV) have typically been taken as 2, 6.4, and 10 respectively (NCRP, 1971). Recent revisions have lead to an average quality factor that is about twice these values (ICRP, 1987). In converting fluence measurements to dose-equivalent, we have followed the recommendation of ICRP (1987). The dose-equivalent, H, is given by the integral

$$H = \int_{th}^{400} F(E)\, J(E)\, dE \qquad \text{(Eq. 2)}$$

where F(E) is the ICRP recommended fluence-to-dose equivalent factor. Table 4 gives a summary of our results where we have included the data of Keith and Richmond (1987) from STS-61A and STS-34. STS-34 carried an RTG on board and thus shows much higher thermal and epithermal neutron flux values than all the other flights. It is interesting to note that the ratio of the epithermal to thermal flux for high inclination flights (about 22%) is higher than for lower inclination flights (about 15%). Two sets of dose-equivalent calculations are presented: (i) assuming that the spectral index of the neutron spectrum remains as 0.765 from thermal to 400 MeV, and (ii) the spectral shape above 10 MeV is the shape calculated by Armstrong et al. (1990). The first case provides an absolute upper limit to the dose-equivalent because physical considerations suggest that the spectral index cannot remain constant, and the second case provides the most probable dose value.

Table 4 also gives the measured skin charged particle absorbed dose in these flights. These measurements can be converted to the charged particle dose-equivalent using the quality factor of 1.4 for STS-31 and 1.9 for STS-28 and STS-36. The most probable ratio of neutron dose-equivalent to charged particle dose-equivalent is calculated to be 5.1%, 9.5%, and 9.8% for STS-31, STS-36, and STS-28 respectively. The dose-equivalent contributions amount to 82% from locally produced (from 1 g cm$^{2)}$ and 18% from albedo neutrons respectively.

Table 5 gives a comparison of our measurements with other measurements reported in the literature (Benton and Parnell, 1987, and references therein). The ratio of neutron to charged particle dose-equivalent in these reports varies from a low of 14.6% to a high of 38.2% and is typically a factor of 2 to 7 higher than our calculations, even though NCRP (1971) fluence-to-dose-equivalent conversion factors were used. As the new ICRP (1987) recommendations lead to about

TABLE 4. NEUTRON FLUXES FOR VARIOUS FLIGHTS DETERMINED BY FOIL AND BONNER SPHERE MEASUREMENTS

	STS 61A	STS 28	STS 34	STS 36	STS 31
Launched	30 Oct 85	8 Aug 89	18 Oct 89	28 Feb 90	24 Apr 90
Duration (days)	7.03	5.08	4.99	4.43	5.05
Altitude (km)	324	306	306	246	617
Inclination (°)	57	57	34.3	62	28.5
Bare/Gd Foil Fluxes (neutrons/cm² min)					
Thermal	2.36±0.18	4.99±1.25	81.9±5.2		15.9±2.6
Epithermal	0.512±0.046	1.09±0.016	7.10±0.45		2.39±0.22
Bonner Sphere Measurements					
Integral Response/ Disintegration Rate		8.63±1.4		5.92±0.27	45.1±1.89
Integral Fluxes and Dose for Two Model Spectra					
IntFlux th-400 (neutrons/cm² sec) $E^{-0.765}$ spectrum		2.49±0.77		1.71±0.79	13.0±0.55
Dose Equiv (mRem) $E^{-0.765}$ spectrum		33.4±1.0		20.0±0.93	174±5.2
IntFlux th-400 (neutrons/cm² sec) Extrpolates above 10 MeV		1.46±0.45		1.00±0.46	7.62±0.32
Dose Equiv (mRem) Extrapolates above 10 MeV		11.4±0.35		6.80±0.32	59.2±1.8
Dose crew avg. charged particle (mRad)	121	61	40	37.7	830

twice the dose-equivalent for the same fluence, we believe that these high values, some of which are higher than our absolute upper limits, arise due to the difficulty already discussed of subtracting the proton-induced activity using such techniques. Dudkin et al. (1990) have reported dose-equivalent from 1.8 to 4.5 mrem/day with standard deviations of about 50% from a variety of Cosmos flights from 1977-1987. This amounts to 20-30% of the charged particle dose-equivalent. The disagreement in measurements with those of Dudkin et al. (1990), however, is much less, considering that their measurements were carried out under 2.5-10 times higher shielding than our measurements.

TABLE 5. COMPARISON OF DOSE RATES DUE TO CHARGED PARTICLES AND NEUTRONS FOR VARIOUS FLIGHTS

Flight	Flight Duration (days)	Inclin. (°)	Altitude (km)	Charged Particle Dose (mRad/d)	Neutron Dose (mRem/d)	Measr. Techn.
Cosmos 936	18.5	62.8	322	25.6	7.1	FFtrack
Cosmos 1129	18.56	62.8	310	18.0	7.2	FFtrack
STS-2	2.26	38	240	4.9	1.1	LiF/FF
STS-3	8.0	40.3	280	5.9	1.3	"
STS-4	7.0	28.5	297	5.4	2.2	"
STS-5	5.1	28.5	297	4.3	2.3	"
STS-6	5.0	28.5	284	4.8	1.3	LiF/FF
STS-28	5.1	57	306	12	2.2	BB
STS-36	4.4	62	246	8.9	1.5	"
STS-31	5.0	28.5	617	166	11.8	BB

Neutron Measurement Technique Key:

FFtrack = Fission foil tracks recorded in mica from fission induced in Th and/or Ta by fast neutrons. DIFFICULTY: slightly more energetic protons also induce fission and are much more abundant.

LiF/FF = Fission foils as described above and alpha particle tracks recorded in plastic from the Li6 (n, alpha) reaction. The LiF technique is most sensitive to thermal and medium energy neutrons. DIFFICULTY: again, slightly more energetic protons also produce comparable alpha particles by the Li^6 (p, alpha), Li^7 (p, alpha) and F^{19} (p, alpha) reactions. In both techniques, the corrections are at least as large as the signal and depend on the proton flux and spectrum, which are poorly known.

BB = Bonner spheres

The rather small contribution of neutrons to the total skin dose-equivalent in Shuttle flights suggests that neutrons do not pose a significant additional radiation risk for both the Shuttle and Space Station crews. If, onthe other hand, heavily shielded habitats are being considered, the role of neutrons as a potential radiation risk must be considered much more seriously.

RESULTS

A set of passive detector systems has provided the first clean measurements of the neutron spectrum in a spacecraft. These measurements do not require a correction due to confounding effects of proton-induced reactions. These results show that the contribution of thermal and epithermal neutron to the skin dose is negligible. Neutrons contribute only about 5-10% of the skin dose charged particle dose-equivalent and pose no significant additional burden onthe crew risk. The situation for the Space Station is likely to be similar. However, neutrons have the potential of being a serious problem for both the lunar base and manned Mars flights. There remains a clear need for developing active, space qualified, neutron detector systems that will span an energy region of about 1-100 MeV.

ACKNOWLEDGMENTS

The flight of Bonner spheres to study neutrons in space was initiated during the tenure of late Dr. Stuart Nachtwey as part of Johnson Space Center's overall radiation risk assessment effort. Mark Bowman, KRUG Life Sciences, was instrumental in many of the logistics that are necessarily a part of any flight experiment. We are very appreciative of all he has done and particularly in ensuring that the Au foils were returned to Houstonimmediately after the Shuttle had landed. Dr. J. Wacker, Battelle Pacific Northwest Laboratory, WA, counted some of other metal foils. Mr. Alva Hardy and Bill Atwell helped in providing the expected charged particle energy spectrum at the location of the Bonner spheres, the measured skin dose, and dose-equivalent values.

REFERENCES

Adams, J. H. Jr.; Silberberg, R.; Tsao, C. H. Cosmic Ray Effects on Microelectronics, Part I: The Near-Earth Particle Environment, NRL Memorandum Report 4506; August 25, 1981.

Armstrong, T. W. Comments Related to: IRS06 Susceptibility Limit for Albedo Neutrons, Space Station Freedom Ionizing Radiation Working Group Meeting, NASA Marshall Space Flight Center, Huntsville, AL; March 20-22, 1990.

Benton, E. V.; Parnell, T. A. Space Radiation Dosimetry on U.S. and Soviet Manned Missions, Terrestrial Space Radiation and its Biological Effects, NATO Advanced Study Institute, Corfu, Greece; October 11-25, 1987.

Benton, E. V. ; Henke, R. P. Radiation exposures during space flight and their measurements. Adv. Space Res. 3(8), 171. Bertini; 1983.

Bhatt V. L. Neutron high-energy spectra at 5 mbar near the geomagnetic equator. J. Geophys. Res. 81, 4603; 1976.

Dudkin, V. E.; Potapov, Yu. V.; Akopova, A. B.; Melkumyan, L. V.; Benton, E. V.; Frank, A. L. Differential Neutron Energy Spectra Measured on Spacecraft in Low Earth Orbit, Nucl. Tracks. Radiat. Meas., Vol 17, No. 2, pp. 87-91; 1990.

Feldman, W. C.; Auchampaugh, G. F.; Shunk, E. R. Initial Results of the Army Background Experiment, Los Alamos National Laboratory, Los Alamos, NM 87545 (Preprint); 1990.

Fishman, G. J. Neutron and proton activation measurements from Skylab, AIAA Paper No. 74-1227. AIAA/AGD Conf. Scient. Experiments Skylab, Huntsville, Alabama.; October 1974.

Guthrie, H. W.; Pickell, M. P.; Bishop, E. H., B.L, Literature Survey of Radiochemical Cross-section Data below 425 MeV, ORNL-3884, Oak Ridge National Laboratory, Knoxville, TN.; 1966.

Haskins, P. S.; McKission, J. E.; Ely, D. W.; Weisenberger, Piercy R. B.; Dyer, C. S.; Rammayya, A. V.; Camp, D. C. Effects of Increased Shielding on amounts of gamma radiation, COSPAR, The Hague, The Netherlands; June 25- July 6, 1990.

ICRP 51: Data for use in Protection Against External Radiation. The International Commission on Radiological Protection, Pergamon Press, Adopted by the Commission, March, 1987, p 32, Table 17, Column

headed ROT extended beyond 14 MeV using Table 23, p 39, column headed "Max"; 1987.

Keith, J. E. ; Clark, R. S. NASA Memorandum to J. Vernon Bailey; August 1, 1973.

Keith, J. E.; Richmond, R. G. Neutrons in Space: Measurements Aboard the Space Shuttle. Proceedings of the Topical Conference on Theory and Practices in Radiation Protection and Shielding, Knoxville, TN, April 22-24, 1987, American Nuclear Society ISBN 0-89448-132-0 Vol. 1, pp 281-286; 1987.

Ing, H. Neutron Bubble Detector Measurements on Cosmos, February meeting in Moscow; 1990.

Lockwood, J. A.; Chen, C.; Frilling, L. A.; St. Onge, R. N. Energy Spectrum and flux of high energy neutrons at balloon altitudes, J. Geophys. Res., 81(34), 6711; 1986.

National Council on Radiation Protection , Report 38, Protection Against Neutron Radiation, National Council on Radiation Protection and Measurements, Bethesda, MD 20814; 1971.

Routti, J. T. High-Energy Neutron Spectroscopy with Activation Detectors, Incorporating New Methods for the Analysis of Ge(Li) Gamma-Ray Spectra and the Solution of Fredholm Integral Equations. Berkeley, CA: University of California; 1969. Thesis. Available from University Microfilms, Inc., Ann Arbor MI. See also - Rindi, A. Unfolding Neutron Spectra: Louhi for Pedestrians. Berkeley, CA: Lawerence Berkeley Laboratory; LBL-6413; 1977.

Sanna, R. S. Thirty-one Group Response Matrices for the Multisphere Neutron Spectrometer over the Energy Range Thermal to 400 MeV, HASL-267, Health and Safety Laboratory, U.S. Atomic Energy Commission; March, 1973.

Sawyer, D. M.; Vette J. I. AP-8 Trapped Proton Environment for Solar Maximum and Solar Minimum, Report NSSDC/WDC-A-R&S 76-06, National Space Science Data Center, Goddard Space Flight Center, Greenbelt, Maryland; 1976.

Townsend, L. W. ; Wilson, J. W. Interaction of Space Radiation with Matter, IAF/IAA-90-543, 40th Congress of the International Astronautical Federation, Dresden, Germany; October 6-12, 1990.

Wilson, J. W.; Townsend, L. W.; Farhat, H. Cosmic-Ray Neutron Albedo Dose in Low-Earth Orbits, Health Physics, vol 57, no. 4, pp 665-668; 1989.

Vikhrov, A. I.; Dudkin, V. E.; Kovalev, E. E.; Komochkov, M. M.; Lebedev V.N.; Litinova E. G.; Mitricas V. G.; Potapov Yu. V.; Potemkin E. L.; Sichov B. S.; Frolov V. V. Atlas of Dose Characteristics of External Ionizing Radiation (Edited by Kovalev E. E.). Atomizdat, Moscow; 1978.

Appendixes

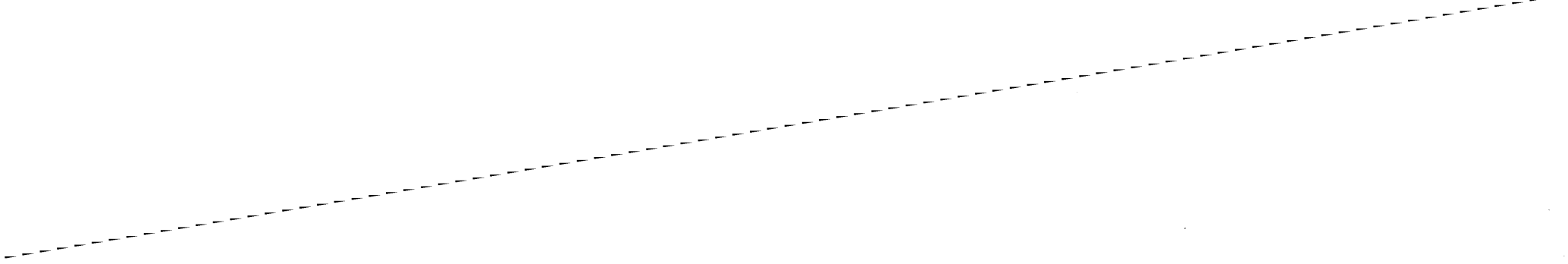

Appendix A: DSO Status as of January 31, 1991

DSO	TITLE	INVESTIGATOR(S)	COMPLETION STATUS	RESULTS/REMARKS
401	Validation of Predictive Tests and Countermeasures for Space Motion Sickness	J. L. Homick, Ph.D.	Complete: 58 subjects	Predicting susceptibility to SMS by using ground-based test results is difficult, due to the variability between the responses to and incidences of terrestrial versus space motion sickness. Reporting of SMS symptoms is now SOP on all Shuttle flights. There does not appear to be a direct correlation using current measures.
402	Cardiovascular Deconditioning Countermeasure Assessment	M. W. Bungo, M.D. P. C. Johnson, Jr., M.D.	Complete: 46 subjects	Pre-landing "fluid loading" is an effective countermeasure for orthostatic intolerance. Fluid loading prior to entry is now standard operating procedure on all Shuttle flights.
403	Head and Eye Motion During Ascent and Entry	W. E. Thornton, M.D.	Complete: 5 subjects	No abnormalities were seen with or without SMS.
404	On-Orbit Head and Eye Tracking Tasks	W. E. Thornton, M.D.	Complete: 16 subjects	No evidence of disordered end organs or of increased CNS pressure. Visual horizontal, vestibulo-ocular reflex, and VOR suppression gain were normal with and without SMS.
405	Acceleration Detection Sensitivity	W. E. Thornton, M.D.	Complete: 2 subjects	Hardware performance was inadequate; undesired angular oscillations made detection of linear motion questionable.
406	Kinesthetic Ability	W. E. Thornton, M.D.	Complete: 3 subjects	Wrist, elbow, and shoulder static and dynamic kinesthetic performance was measured in flight, with and without 1-g equivalent force loads. Kinesthetic ability did not appear to be significantly changed from preflight levels.

DSO	TITLE	INVESTIGATOR(S)	COMPLETION STATUS	RESULTS/REMARKS
407	Photographic Documentation of Body Fluid Shift	W. E. Thornton, M.D.	Complete: 7 subjects	Photographs are adequate; however, direct measurement is less complex and more accurate with less costly reduction and analysis.
408	Near Vision Acuity and Contrast Sensitivity	A. Ginsberg, Ph.D. J. M. Vanderploeg, M.D.	Complete: 32 subjects	Some changes in contrast sensitivity were observed; changes in acuity were insignificant. These changes should not cause major visual performance increases or decreases.
409	Microbial Screening	D. L. Pierson, Ph.D.	Complete: 4 flights	A drop in microorganisms appeared early in flight, but later in the missions a rise in airborne contaminants was observed. A number of potentially pathogenic fungi was identified.
410	Audiometry	W. E. Thornton, M.D.	Complete: 13 subjects	Procedures worked well, but differences in mission noise levels confounded results by causing threshold shifts. No evidence of increased intralabyrinthine pressure was found.
411	Simple Mass Measurement	W. E. Thornton. M.D.	Complete: 1 subject	Concept is valid, but balance time constant was too long for accurate measurements in limited acceleration space available.
412	Treadmill Operation	W. E. Thornton, M.D.	Complete: 2 subjects	Data showed expected variation in aspects of locomotor activity, but no major distortions. A properly loaded treadmill is one of the countermeasure devices for protection from adaptation to weightlessness.
413	Cell Attachment in Microgravity	D. R. Morrison, M.D.	Complete: 1 flight	Cells can attach to a growth surface in microgravity at ambient cabin temperature. (This study continued with an incubator as DSO 432.)
414	Ophthalmoscopy	E. L. Shulman, M.D.	Complete: 4 subjects	No indication of increased intracranial pressure.

DSO Status

DSO	TITLE	INVESTIGATOR(S)	COMPLETION STATUS	RESULTS/REMARKS
415	Tissue Pressure Tonometry	W. E. Thornton, M.D.	Complete: 5 subjects	Data were nominally obtained with significant individual variation.
416	Ambulatory Monitoring	W. E. Thornton, M.D.	Complete: 12 subjects	Bowel sounds were inversely related to presence of SMS and appeared to be the single best indicator of this syndrome. Sounds are now routinely used as an indicator.
417	In-flight Countermeasures for SMS	W. E. Thornton, M.D.	Terminated: 1 subject	Longitudinal loading of subject with equivalent body weight had no effect.
418	Eye-Hand Coordination	W. E. Thornton, M.D.	Complete: 5 subjects	Weightlessness and SMS had no effect on eye-hand tracking of periodic and aperiodic signals.
419	Evaluation of Food Flavor Perception in Zero Gravity	R. L. Sauer	Inactive: Never Flown	
420	Evaluation of Taste Acuity in Zero-g	R. L. Sauer	Inactive: Never Flown	
421	Animal Enclosure Module In-flight Test	M. C. Smith, Jr., D.V.M. P. C. Johnson, M.D. A. LeBlanc, Ph.D.	Complete: 1 flight	Six rats were kept in the AEM without compromising the crew's safety.
422	Anatomical Observation	W. E. Thornton, M.D.	Complete: 5 subjects	Many changes were noted using auscultation and palpation; percussion was not possible.
423	Study of In-flight Fluid Changes	W. E. Thornton, M.D. C. S. Leach, Ph.D.	Complete: 1 subject	This was the first "high resolution" fluid intake output study. A number of still unexplained findings were made including a delayed diuresis, diuresis in presence of increased ADH and increased urinary calcium within 24 hrs.

DSO Status

DSO	TITLE	INVESTIGATOR(S)	COMPLETION STATUS	RESULTS/REMARKS
424	Evoked Potentials	W. E. Thornton, M.D.	Complete: 5 subjects	No change in short and mid-latency audio-evoked potentials was found, with or without SMS. One visual evoked potential study showed no change.
425	Intraocular Pressure	S. L. Pool, M.D.	Complete: 1 subject	Results would be inconsistent with significant change in intralabyrinthine or intracranial pressure change.
426	Denitrogenation Procedures Validation	J. M. Waligora D. J. Horrigan	Withdrawn	
427	Soft Contact Lens Application Test	W. E. Thornton, M.D. L. R. Young, Ph.D.	Complete: 1 subject	Lens would not adhere using the prescribed procedure.
428	Unassigned			
429	Unassigned			
430	Unassigned			
431	Unassigned			
432	Engineering Test of Carry-on Incubator and Cell Attachment in Microgravity	D. R. Morrison, Ph.D. A. Cogoli, Ph.D.	Complete: 1 flight	Cell attachment in flight was greater than in ground control samples and much improved over DSO 413 results.
433	Preflight and Postflight Parallel Swing Tests	D. E. Parker, Ph.D. M. Reschke, Ph.D.	Complete: 5 subjects (incl those obtained as part of DSO 449).	Findings support the Otolith Tilt-Translation Reinterpretation Hypothesis that the brain reinterprets all otolith signals as indicating linear transaltion. Was renamed DSO 449 before STS-51D.

DSO Status

DSO	TITLE	INVESTIGATOR(S)	COMPLETION STATUS	RESULTS/REMARKS
434	Unassigned			
435	Unassigned			
436	In-flight Monitoring as a Reflection of Cardiovascular Deconditioning	M. W. Bungo, M.D.	Withdrawn	
437	Microbial Monitoring	D. L. Pierson, Ph.D.	Active: data has been collected on 1 flight and is to be collected on all flights with animals.	Adherence to the Specific Pathogen Free criteria for animals protected the crew when the Research Animal Holding Facility failed.
438	Unassigned			
439	Documentation of the Action of Metoclopramide	W. E. Thornton, M.D.	Complete: 9 subjects	SMS causes cessation of bowel activity. Metaclapromide, oral or injected, is an ineffective treatment to restore bowel activity or relieve symptoms of SMS.
440	Crew Visual Performance	Lt. Col. L. V. Genco H. L. Task, Ph.D.	Complete: 10 subjects	There was a minor decrease in acuity and a relatively large increase in stereo acuity. All values tend toward norms on return.
441	Blood Pressure Monitoring During Reentry	W. E. Thornton, M.D. T. P. Moore, M.D.	Inactive: 9 subjects	Blood pressure and heart rate showed modest increases with onset of g-loads and seat egress, but no evidence of hypotension or expected tachycardia in 3 subjects with apparent orthostatis.
442	Autogenic Feedback Training (AFT)	P. S. Cowings, Ph.D.	Complete: 1 subject	Provided valuable suggestions for improvement of hardware and procedures for the AFT experiment on Spacelab 3.

DSO Status

DSO	TITLE	INVESTIGATOR(S)	COMPLETION STATUS	RESULTS/REMARKS
443	Segmental Fluid Shift	J. S. Logan, M.D. R. J. Luciani L. D. Montgomery G. R. Coulter	Inactive	
444	Unassigned			
445	Thoracic Impedance Measurements	T. P. Moore, M.D. W. E. Thornton, M.D.	Inactive: 1 subject	There was evidence of slightly increased stroke volume and cardiac output.
446	Leg Plethysmography	T. P. Moore, M.D. W. E. Thornton, M.D.	Complete: 9 subjects (including those obtained as part of DSO 461).	There is typically a 1 to 1.5 liter volume change in each leg, largely due to shifts in body fluids. The shift occurs exponentially in the first 6-10 hours after launch. Postflight return is rapid (tens of minutes), but a decrement persists. Data were consistent with earlier Skylab data and provided the basis for understanding postflight orthostatis.
447	Causative Agents During SMS	W. E. Thornton, M.D.		Was incorporated into DSO 453 and flown under that designation.
448	Echocardiographic Evaluation of Cardiovascular Deconditioning	M. W. Bungo, M.D.		Resubmitted as a Form 100 Experiment (American Flight Echo).
449	Preflight and Postflight Parallel Swing Tests	D. E. Parker, Ph.D. M. Reschke, Ph.D.	Complete: 5 subjects (incl those obtained as part of DSO 433).	Findings support the Otolith Tilt-Translation Reinterpretation Hypothesis (see also DSO 433 remarks) is and provide the basis for proposing a Preflight Adaptation Trainer (PAT).
450	Salivary Cortisol During Acute Phases of Space Flight	N. M. Cintron, Ph.D.	Complete: 6 subjects	Space flight did not appear to affect the magnitude of cortisol levels. Saliva collection proved to be a better means of cortisol measurement than serum cortisol. The complete report begins on page 51.

DSO Status

DSO	TITLE	INVESTIGATOR(S)	COMPLETION STATUS	RESULTS/REMARKS
451	Eye-Hand Coordination During SMS	W. E. Thornton, M.D. T. P. Moore, M.D.	Inactive: 5 subjects	This DSO was a continuation of earlier electromechanical tracking tasks except used electronic generation and storage. Results were consistent with previous study.
452	Leg Volume Changes	T. P. Moore, M.D. W. E. Thornton, M.D.	Inactive	
453	Combined Blood Investigations	W. E. Thornton, M.D. C. Leach-Huntoon, Ph.D. H. J. Schneider, Ph.D. N. M. Cintron, Ph.D. R. Landry	Complete: 6 subjects	Some hypotheses about physiologic changes during space flight need additional study; new evidence indicates additional factors should be studied.
454	Clinical Characterization of SMS	W. E. Thornton, M.D. J. M. Vanderploeg, M.D.		Redesignated as DSO 455 before flight. See DSO 455 results.
455	Clinical Characterization of SMS	W. E. Thornton, M.D. J. M. Vanderploeg, M.D.	Inactive: 7 subjects	See DSO 456.
456	Medical Tests and Measurements for the STS-51D Payload Specialist	W. E. Thornton, M.D. T. P. Moore, M.D. J.M.Vanderploeg, M.D. S. L. Pool, M.D. N. M. Cintron, Ph.D. J. B. Charles, Ph.D. L. D. Inners, Ph.D. M. F. Reschke, Ph.D. D. E. Parker, Ph.D.	Complete: 1 subject	This study used protocols and hardware previously flown on DSOs 416, 424, 441, 446, 449, 451, 455, 458, and 460, and included studies of electroencephalograms (EEG) and electrocardiograms (ECG).
457	Salivary Pharmacokinetics of Scop-Dex	N. M. Cintron. Ph.D. L. Putcha, Ph.D.	Complete: 12 subjects	Results were inconclusive and inadequate for analysis. Confounding variables suggest that scopalomine and dextroamphetamine be evaluated separately for bioavailability.

DSO Status

DSO	TITLE	INVESTIGATOR(S)	COMPLETION STATUS	RESULTS/REMARKS
458	Salivary Acetaminophen Pharmacokinetics	N. M. Cintron, Ph.D. L. Putcha, Ph.D.	Complete: 13 subjects	A significant, perhaps progressive decrease in absorption rate has been noted in the disposition of acetaminophen taken in flight. The complete report begins on page 55.
459	Otolith Tilt-Translation Reinterpretation	M. Reschke, Ph.D. D. E. Parker, Ph.D.	Complete: 6 subjects	Pitch motion immediately after entry was perceived as translation. Ocular counterrolling was observed in flight, but of a lower magnitude than preflight. These data will be of great help in designing a Preflight Adaptation Trainer (PAT). Subjective accounts of sensory perceptions were elicited in interviews. The complete report begins on page 33.
460	Changes in Total Body Water During Space Flight	C. S. Leach, Ph.D. L. D. Inners, Ph.D. J. B. Charles, Ph.D.	Complete: 5 subjects	Within 22-24 hours of exposure to 0-g, total body water decreases are highly variable; thereafter, TBW remains stable. The complete report begins on page 1.
461	Leg Plethysmography	T. P. Moore, M.D. W. E. Thornton, M.D.	Complete: 9 subjects (incl those obtained as part of DSO 446).	See DSO 446.
462	Noninvasive Estimation of Central Venous Pressure	J. B. Charles, Ph.D. M. W. Bungo, M.D.	Active: 9 subjects	The technique is viable and produced good results. CVP decreased over the first 3 flight days, then remained at a constant value.

DSO Status

DSO	TITLE	INVESTIGATOR(S)	COMPLETION STATUS	RESULTS/REMARKS
463	In-flight Holter Monitoring	M. W. Bungo, M.D. J. B. Charles, Ph.D.	Complete: 1 subject	No increase in dysrhythmias was seen in this crewmember in contrast to the increase in dysrythmias seen during EVA's on previous STS flights.
464	In-flight Assessment of Renal Stone Risk Factor	N. M. Cintron, Ph.D.	On hold: 1 subject	Urine volume did not appear changed from preflight. A trend to increased excretion of calcium, phosphate, magnesium, and uric acid was present.
465	Preflight and Postflight Echocardiography	J. B. Charles, Ph.D. M. W. Bungo, M.D.	Supplanted by DSO 466	Due to a last-minute change of landing site, no postflight data were collected. DSO 466 replaced 465 when flights resumed.
466*	Pre- and Postflight Cardiovascular Assessment	J. B. Charles, Ph.D. M. W. Bungo, M.D. S. L. Mulvagh, M.D.	Active: 39 subjects on missions of <7 days; 24 additional subjects required on missions >7 days.	Data obtained thus far indicate that exposure to 0-g for short (4-5 day) missions result in diminished cardiac volumes which are compensated for by elevated heart rates on return to 1-g and resolve witin 2 days after landing. The complete report begins on page 9.
467*	Influence of Weightlessness on Baroreflex Function	D. L. Eckberg, M.D. J. M. Fritsch, M.S. J. B. Charles, Ph.D. M. W. Bungo, M.D.	Complete: 16 subjects	Subtle changes occurred in vagal control of the heart, even in subjects who were asymptomatic. The complete report begins on page 21.
468	Preflight Adaptation Training	M. F. Reschke, Ph.D. D. L. Harm, Ph.D. D. E. Parker, Ph.D.	Complete: 5 subjects.	Supplanted by DSO 604.

DSO Status

(*) Extended Duration Orbiter (EDO) Medical Program

DSO	TITLE	INVESTIGATOR(S)	COMPLETION STATUS	RESULTS/REMARKS
469	In-flight Radiation Dose Distribution	G. D. Badhwar, Ph.D. A. Konradi, Ph.D. J. Keith, Ph.D.	Active: 3 missions	The highlights of results to date are 1) neutrons do not pose a significant additional radiation hazard in space; 2) the currently used model for describing galactic cosmic radiation is deficient and needs to be improved; 3) active, time-resolved dosimetry can be performed on the Shuttle; and 4) no absorbed dose hot spots occurred in the Phantom Head portion of the study. Complete reports begin on pages 59, 65, and 75.
470	The Relationship of Space Adaptation Syndrome to Middle Cerebral Artery Blood Velocity Measured in Flight by Doppler	P. Hackett, M.D. J. P. Bagian, M.D.	Complete: 10 subjects	The objectives of this DSO are to document changes in cerebral and reginal blood flow in the microgravity environment and to correlate these changes with the onset and severity of the Space Adaptation Syndrome. Results will be available in early 1991.
471	Characterization of Respirable Airborne Particulate Matter in Shuttle Atmosphere	D. Russo, Ph.D. D. Pierson, Ph.D. B. Liu, Ph.D.	Active: 1 mission	The Airborne Particulate Sampler is used to characterize the type and amount of debris in the Shuttle cabin atmosphere.
472	Intraocular Pressure	LTC. T. H. Mader, M.D. R. T. Meehan, M.D. J. P. Bagian, M.D. J. B. Charles, Ph.D. G. R. Taylor, Ph.D.	Active: 5 subjects	A hand-held tonometer is used to measure intraocular pressures during microgravity in order to (1) establish a data base of changes in pressures that can be used to evaluate crew health and (2) provide a quantitative measure of cephalad fluid shifts.
473	Delayed-Type Hypersensitivity	G. R. Taylor, Ph.D.	Complete: 12 subjects	This investigation will validate alterations in cell-mediated immunity and provide insight into the mechanisms and the time course of changes in immune function resulting from space flight.

DSO Status

DSO	TITLE	INVESTIGATOR(S)	COMPLETION STATUS	RESULTS/REMARKS
474	Retinal Photography	R. T. Meehan, M.D. G. R. Taylor, Ph.D. S. S. Hayreh, M.D. LTC. T. Mader, M.D. S. L. Pool, M.D. P. Montague, C.R.A.	Active: 4 subjects	Retinal photography is a noninvasive method of detecting changes in intracranial pressure through changes in the retinal blood vessels and elevation of the optic disc.
475	Muscle Biopsy	V. R. Edgerton, Ph.D. M. L. Carter, M.D.	Complete: 8 subjects	Pre- and postflight muscle biopsies were taken in order to define the morphologic and biochemical effects of space flight on skeletal muscle fibers.
476*	In-flight Aerobic Exercise	J. B. Charles, Ph.D. M. W. Bungo, M.D.	Active: 7 subjects	Daily in-flight aerobic exercise will be evaluated as a means to inhibit the decrease in cardiac dimensions observed during space flight, improve postflight orthostatic tolerance, and minimize the loss of aerobic capacity after flight.
477	Muscle Performance	J. C. Hayes, M.S. B. A. Harris, Jr., M.D.	Active: 15 subjects	Atrophy of skeletal muscles occurs in response to chronic disuse and insufficient functional loading. The purpose of this study is to gather specific information concerning muscle atrophy in weightlessness for developing appropriate exercise modalities and prescriptions for countermeasures.
478*	LBNP Countermeasure to Reduce Post-Space Flight Orthostatic Intolerance	J. B. Charles, Ph.D. M. W. Bungo, M.D. L. F. Dietlein, M.D. S. M. Fortney, Ph.D.	Active: 2 subjects	This DSO will determine whether fluid loading via ingestion of salt tablets and water in association with lower body negative pressure treatment will protect tolerance to orthostatis (simulated in flight by LBNP).

DSO Status

(*) Extended Duration Orbiter (EDO) Medical Program

DSO	TITLE	INVESTIGATOR(S)	COMPLETION STATUS	RESULTS/REMARKS
479*	Hyperosmotic Fluid Countermeasure	M. A. B. Frey, Ph.D. J. B. Charles, Ph.D. M. W. Bungo, M.D. N. M. Cintron, Ph.D. S. Fortney, Ph.D.	Active: 5 subjects	Previous research has established the usefulness of consuming salt and water equivalent to isotonic saline as a countermeasure to orthostatic tolerance. This countermeasure will be tested for the capability to provide protection following longer flights.
480	Heavy Isotope Enrichment of Shuttle Galley Water	C. L. Huntoon, Ph.D. L. D. Inners, Ph.D. J. B. Charles, Ph.D.	Active: 1 subject	Samples will be collected of galley water, which is believed to be enriched in the heavy isotopes of oxygen and hydrogen. As studies using water labeled with these isotopes are planned for future Spacelab missions, a baseline level needs to be determined in order to facilitate data analysis.
316*	Bioreactor/Flow and Particle Trajectory in Microgravity	G. Spaulding, Ph.D.	Active: 1 mission requested	This equipment test will assist in the study of cell growth as an indicator for toxic conditions by permitting comparison of actual microgravity particle trajectories in the vessel with calculated trajectories.
	Extended Duration Orbiter (EDO) Medical Program DSOs			
601	Changes in Baroreceptor Reflex Function	J. B. Charles, Ph.D. B. S. Bennett, M.S. J. Fritsch, M.S. D. L. Eckberg, M.D. D. E. Houston, Ph.D.	Active: 11 subjects	In this study, a commercial neck-cuff device is used to measure baroreflex adaptations associated with space flight. An improved understanding of the mechanisms underlying postflight orthostatic intolerance is particularly important to safe postflight egress, especially in emergency situations.
602	Blood Pressure and Heart Rate Variability During Space Flight	J. B. Charles, Ph.D. M. A. Frey, Ph.D. M. M. Jones	Active: 3 subjects	An automatic blood pressure monitor and a heart rate monitor are worn for 24 hours in flight to determine whether arterial blood pressure and heart rate exhibit less variability in flight and if so, to determine whether reduced variability correlates with the baroreflex attenuation measured postflight.

DSO Status

(*) Extended Duration Orbiter (EDO) Medical Program

DSO	TITLE	INVESTIGATOR(S)	COMPLETION STATUS	RESULTS/REMARKS
603	Orthostatic Function During Entry, Landing, and Egress	J. B. Charles, Ph.D. M. A. B. Frey, Ph.D. J. P. Bagian, M.D. D. E. Houston, Ph.D. M. M. Jones	Active: 2 subjects	Heart rate and rhythm, blood pressure, cardiac output, and peripheral resistance will be monitored during entry, landing, and egress in order to develop and assess countermeasures designed to improve orthostatic tolerance upon return to Earth.
604	Visual Vestibular Integration as a Function of Adaptation	M. F. Reschke, Ph.D. J. J. Bloomberg, Ph.D. F. E. Guedry, Jr., Ph.D. D. L. Harm, Ph.D. D. E. Parker, Ph.D.	Active: 1 subject	Examination will be made of the perceived effects of head movements made on orbit. Paradoxical illusions that occur during the readaptation period pose a potential threat to crew safety during entry, landing, and egress following extended duration missions.
605	Postural Equilibrium Control During Landing/Egress	M. F. Reschke, Ph.D. W. H. Paloski, Ph.D. D. L. Harm, Ph.D.	Active: 8 subjects	Postural control as a function of mission duration will be assessed using a Posture Platform Test performed pre- and postflight only.
606	Muscle Size and Lipids (MRI/MRS)	M. Jaweed, Ph.D. P. Narayana, Ph.D. I. Butler, M.D. J. Slopis, M.D.	Active: 5 subjects	This study will quantitate in a noninvasive way the muscle size, water, and lipid changes that occur in the postural muscles as a result of space flight, and relate them to fatigue and recovery of strength. Magnetic Resonance Imaging (MRI) and Magnetic Resonance Spectroscopy (MRS) will be performed pre- and postflight.
607	Lower Body Negative Pressure Following Space Flight	S. M. Fortney, Ph.D. M. W. Bungo, M.D. J. B. Charles, Ph.D. N. M. Cintron, Ph.D. M. A. Frey, Ph.D. J. Buckey, M.D. S. Mulvagh, M.D.	Active	LBNP testing will be performed before and immediately following Shuttle flights of varying durations to determine whether additional countermeasures for orthostatic intolerance are required during longer flights.

DSO	TITLE	INVESTIGATOR(S)	COMPLETION STATUS	RESULTS/REMARKS
608	Effects of Space Flight on Aerobic and Anaerobic Metabolism	S. F. Siconolfi, Ph.D. H. W. Lane, Ph.D. A. D. Moore, Ph.D. B. A. Harris, Jr., M.D.	Active	The purpose of this study is to quantify the changes in aerobic and anaerobic metabolism during graded treadmill exercise performed pre- and postflight, and to relate those changes to alterations in body composition and fluid volume intake.
609	Unassigned			
610	In-flight Assessment of Renal Stone Risk	N. M. Cintron, Ph.D. C. Y. Pak, Ph.D.	Active	This DSO will determine whether space flight missions increase the crew's risk of forming renal stones and, if so, determine whether the risk increases with mission length.
611	Air Monitoring Instrument Evaluation and Atmosphere Characterization	D. Pierson, Ph.D. J. James, Ph.D. T. Limero, Ph.D.	Active	In order to ensure proper function and operation in flight, air monitoring equipment will be evaluated and verified. These instruments will also collect data on contaminant levels during missions of varying lengths to be used to establish baseline levels and to evaluate potential risks to crew health and safety.
612	Energy Utilization	H. W. Lane, Ph.D. L. Putcha, Ph.D. N. Cintron, Ph.D. E. Gibson, Ph.D. D. Schoeller, Ph.D.	Active	This DSO seeks to determine in-flight energy utilization during normal flight activity and during exercise in order to develop dietary countermeasures that prevent muscle loss.
613	Changes in the Endocrine Regulation of Orthostatic Tolerance following Space Flight	N. M. Cintron, Ph.D. J. B. Charles, Ph.D. P. A. Whitson, Ph.D. S. M. Fortney, Ph.D. S. F. Siconolfi, Ph.D.	Active	This study examines the body's ability to release catecholamines following space flight. Catecholamines are hormones such as adrenaline which provide a surge of energy to cope with emergency situations.

DSO Status

DSO	TITLE	INVESTIGATOR(S)	COMPLETION STATUS	RESULTS/REMARKS
614	The Effect of Prolonged Space Flight on Head and Gaze Stability during Locomotion	M. F. Reschke, Ph.D. J. J. Bloomberg, Ph.D. D. L. Harm, Ph.D. W. H. Paloski, Ph.D.	Active	This DSO will characterize pre- and postflight head and body movement along with gaze stability during walking, running, and jumping, all of which are relevant to egress from the Shuttle. In-flight head and gaze stability will be evaluated during scheduled exercise periods using a visual acuity chart.
		Development Test Objectives		
623*	Cabin Air Monitoring	D. L. Pierson, Ph.D.	Active	This DSO will use the solid sorbent sampler (SSS) to continuously sample the Orbiter atmosphere throughout the flight. The SSS is to be flown on first flight of a new vehicle, first flight of a vehicle after extensive refurbishment in the cabin, and on all Spacelab manned module flights.
635*	Eyewash Demonstration	J. Schulz, M.D. K. Fuhrmann	Active	The Shuttle Emergency Eyewash is designed to rinse an individual's eyes with large volumes of water in the event of exposure to toxic chemicals or irritants.
640*	Hydrazine Monitoring	J. James, Ph.D.	Active	The hydrazine monitor will sample the Shuttle air to detect the presence of hydrazine or monomethyl-hydrazine in order to ensure the safety of the crew after completion of an EVA.
645*	Combustion Products Analyzer	J. James, Ph.D.	Active	The CPA will continuously sample the air throughout a mission to detect the presence of targeted compounds indicative of thermodegradation event.

DSO Status

(*) Extended Duration Orbiter (EDO) Medical Program

DSO	TITLE	INVESTIGATOR(S)	COMPLETION STATUS	RESULTS/REMARKS
646*	Automated Microbic System II Filler Module Operational Test	S. K. Mishra, Ph.D. R. L. Fortune J. L. Staples	Active	The AMS II is capable of performing microbial identification and susceptibility tests, and this DTO will evaluate the filler module of this system, which consists of an automatic vacuum pump, a filling chamber, and a compartment for camera assembly stowage.
651*	Cycle Ergometer Hardware Evaluation	M. E. Greenisen, Ph.D.	Active	The EDO Cycle Ergometer will be evaluated for ease of setup/stowage, restraint comfort/effectiveness, performance with individuals of varying anthropometry, heart rate responses to submaximal workloads, and vibration effects.
652*	Vibration Recordings on the Shuttle Treadmill Using an Accelerometer	Sheila W. Boettcher, M.Ed. Glenn K. Klute, M.S.	Active	The concern regarding treadmill exercies and its vibration impact on Shuttle mission objectives has necessitated using an accelerometer to quantify the frequency and magnitude of vibration during treadmill exercise.

DSO Status

(*) Extended Duration Orbiter (EDO) Medical Program

Appendix B: DSOs Listed by Discipline

DISCIPLINE	DSO	SHORT TITLE	INVESTIGATOR(S)
Air Monitoring	623^	Cabin Air Monitoring	D. L. Pierson, Ph.D.
	640^	Hydrazine Monitoring	J. James, Ph.D.
	645^	Combustion Products Analyzer	J. James, Ph.D.
Biomedical Physiology	450	Salivary Cortisol During Spaceflight	C. S. Leach, Ph.D. et al.
	453	Combined Blood Investigations	W. E. Thornton, M.D. et al.
	456	Medical Tests and Measurements (STS-51D P/S)	J. M. Vanderploeg, M.D. et al.
	457	Salivary Pharmacokinetics of Scop-Dex	N. M. Cintron, Ph.D.; L. Putcha, Ph.D.
	458	Salivary Acetaminophen Pharmacokinetics	N. M. Cintron, Ph.D.; L. Putcha, Ph.D.
	464	In-flight Assessment of Renal Stone Risk Factor	N. M. Cintron, Ph.D.
	480	Heavy Isotope Enrichment of Shuttle Galley Water	C. L. Huntoon, Ph.D. et al.
	610*	In-flight Assessment of Renal Stone Risk Factor	N. M. Cintron, Ph.D.; C. Y. Pak, Ph.D.
	612*	Energy Utilization	H. W. Lane, Ph.D. et al.
	613*	Endocrine Regulation	N. M. Cintron, Ph.D.
Cardiovascular Physiology	402	Cardiovascular Deconditioning Countermeasures	M. W. Bungo, M.D.; P. C. Johnson, Jr., M.D.
	407	Photographic Documentation of Body Fluid Shift	W. E. Thornton, M.D.
	412	Treadmill Operation	W. E. Thornton, M.D.
	415	Tissure Pressure Tonometry	W. E. Thornton, M.D.
	423	Study of In-flight Fluid Changes	W. E. Thornton, M.D.; C. S. Leach, Ph.D.
	441	Blood Pressure Monitoring During Re-entry	W. E. Thornton, M.D.; T. P. Moore, M.D.
	445	Thoracic Impedance Measurements	T. P. Moore, M.D.; W. E. Thornton, M.D.
	446	Leg Plethysmography	T. P. Moore, M.D.; W. E. Thornton, M.D.
	456	Medical Tests and Measurements (STS-51D P/S)	W. E. Thornton, M.D., et al.
	460	Changes in Total Body Water During Space Flight	C. S. Leach, Ph.D. et al.
	461	Leg Plethysmography	T. P. Moore, M.D.; W. E. Thornton, M.D.
	462	Estimation of Central Venous Pressure	M. W. Bungo, M.D.; J. B. Charles, Ph.D.
		Cardiovascular DSOs continued on next page...	

DISCIPLINE	DSO	SHORT TITLE	INVESTIGATOR(S)
Cardiovascular Physiology *(cont'd)*	463	In-flight Holter Monitoring	M. W. Bungo, M.D.; J. B. Charles, Ph.D.
	465	Pre- and Postflight Echocardiography	M. W. Bungo, M.D.; J. B. Charles, Ph.D.
	466*	Pre- and Postflight Cardiovascular Assessment	M. W. Bungo, M.D.; J. B. Charles, Ph.D.
	467*	Influence of Weightlessness on Baroreflex Function	D. L. Eckberg, M.D. et al.
	476*	In-flight Aerobic Exercise	J. B. Charles, Ph.D.; M. W. Bungo, M.D.
	478*	In-flight LBNP	J. B. Charles, Ph.D. et al.
	479*	Hyperosmotic Fluid Countermeasure	M. A. B. Frey, Ph.D. et al.
	601*	Changes in Baroreceptor Reflex Function	J. B. Charles, Ph.D. et al.
	602*	Blood Pressure Variability During Space Flight	J. B. Charles, Ph.D. et al.
	603*	Orthostatic Function During Entry, Landing, and Egress	J. B. Charles, Ph.D. et al.
	607*	LBNP following Space Flight	S. M. Fortney, Ph.D. et al.
Equipment Testing and Experiment Verification	316	Bioreactor/Flow and Particle Trajectory in 0-g	G. Spaulding, Ph.D.
	411	Simple Mass Measurement	W. E. Thornton, M.D.
	421	Animal Enclosure Module In-flight Test	M. C. Smith, Jr., D.V.M.
	442	Autogenic Feedback Training (AFT)	P. S. Cowings, Ph.D.
	611*	Air Monitoring Instrument Evaluation	D. L. Pierson, Ph.D. et al.
	635^	Eyewash Demonstration	J. Schulz, M.D.; K. Fuhrmann
	646^	AMS II Filler Module Operational Test	S. K. Mishra, Ph.D. et al.
Exercise Physiology	475	Muscle Biopsy	V. R. Edgerton, Ph.D.; M. L. Carter, M.D.
	606*	Muscle Size and Lipids (MRI/MRS)	M. Jaweed, Ph.D. et al.
	608*	Aerobic and Anaerobic Metabolism in Space	S. F. Siconolfi, Ph.D. et al.
Microbiology	409	Microbial Screening	D. L. Pierson, Ph.D.
	413	Cell Attachment in Microgravity	D. R. Morrison, Ph.D.
	432	Carry-on Incubator/Cell Attachment in Micro-G	D. R. Morrison, Ph.D.; A. Cogoli, M.D.
	437	Microbial Monitoring	D. L. Pierson, Ph.D.

DSOs by Discipline

DISCIPLINE	DSO	SHORT TITLE	INVESTIGATOR(S)
Neurophysiology	401	Predictive Tests and Countermeasures for SMS	J. L. Homick, Ph.D.
	403	Head and Eye Motion During Re-entry	W. E. Thornton, M.D.
	404	On-Orbit Head and Eye Tracking Tasks	W. E. Thornton, M.D.
	405	Acceleration Detection Sensitivity	W. E. Thornton, M.D.
	417	In-flight Countermeasures for SAS	W. E. Thornton, M.D.
	418	Eye-Hand Coordination	W. E. Thornton, M.D.
	459	Otolith Tilt-Translation Reinterpretation	M. F. Reschke, Ph.D.; D. E. Parker, Ph.D.
	468	Preflight Adaptation Training	M. F. Reschke, Ph.D. et al.
	604*	Visual Vestibular Integration and Adaptation	M. F. Reschke, Ph.D. et al.
	605*	Postural Equilibrium Control	M. F. Reschke, Ph.D. et al.
	614*	Head and Gaze Stability	M. F. Reschke, Ph.D. et al.
Space Motion Sickness and Space Adaptation Studies	406	Kinesthetic Ability	W. E. Thornton, M.D.
	410	Audiometry	W. E. Thornton, M.D.
	414	Ophthalmoscopy	E. L. Shulman, M.D.
	416	Ambulatory Monitoring	W. E. Thornton, M.D.
	422	Anatomical Observation	W. E. Thornton, M.D.
	424	Evoked Potentials	W. E. Thornton, M.D.
	425	Intraocular Pressure	S. L. Pool, M.D.
	427	Soft Contact Lens Applications Test	W. E. Thornton, M.D.; L. R. Young, Ph.D.
	433	Pre- and Postflight Parallel Swing Tests	D. E. Parker, Ph.D.; M. L. Reschke, Ph.D.
	439	Documentation of the Action of Metoclopramide	W. E. Thornton, M.D.
	447	Causative Agents During SMS	W. E. Thornton, M.D.
	449	Pre- and Postflight Parallel Swing Tests	D. E. Parker, Ph.D.; M. L. Reschke, Ph.D.
	451	Eye-Hand Coordination During SMS	W. E. Thornton, M.D., T. P. Moore, M.D.
	454/455	Clinical Characterization of SMS	W. E. Thornton, M.D.; J.Vanderploeg, M.D.
	456	Medical Tests and Measurements (STS-51D P/S)	W. E. Thornton, M.D. et al.
	470	Space Adaptation/Doppler In Flight	P. Hackett, M.D.; J. Bagian, M.D.
Vision	408	Near Vision Acuity and Contrast Sensitivity	A. Ginsberg, Ph.D.; J. M. Vanderploeg, M.D.
	440	Crew Visual Performance Testing	LTC L. V. Genco; H. L. Task, Ph.D.
	472	Intraocular Pressure	LTC T. H. Mader, M.D. et al.
	473	Delayed-Type Hypersensitivity	G. R. Taylor, Ph.D.
	474	Retinal Photography	R. T. Meehan, M.D. et al.

DSOs by Discipline

(*) Extended Duration Orbiter (EDO) Medical Program

(^) Development Test Objectives

Appendix C: DSOs Listed by Investigator

INVESTIGATOR	ORG CODE	DSO NUMBER	SHORT TITLE
G. D. Badhwar, Ph.D.	SN	469	In-flight Radiation Dose Distribution
J. P. Bagian, M.D.	CB	470	In-flight Doppler
J. J. Bloomberg, Ph.D.	SD5	614	Head and Gaze Stability
M. W. Bungo, M.D.	SD1	402	Cardiovascular Deconditioning Countermeasures
		462	Estimation of Central Venous Pressure
		463	In-flight Holter Monitoring
		465	Pre- and Postflight Echocardiography
		466	Pre- and Postflight Cardiovascular Assessment
		476	In-flight Aerobic Exercise
M. L. Carter, M.D.	CB	475	Muscle Biopsy
J. B. Charles, Ph.D.	SD5	462	Estimation of Central Venous Pressure
		463	In-flight Holter Monitoring
		465	Pre- and Postflight Echocardiography
		466	Pre- and Postflight Cardiovascular Assessment
		467	Influence of Weightlessness on Baroreflex Function
		476	In-flight Aerobic Exercise
		478	In-flight LBNP
		479	Hyperosmotic Fluid Countermeasure
		601	Changes in Baroreceptor Reflex Function
		602	Blood Pressure Variability During Space Flight
		603	Orthostatic Function During Entry/Landing/Egress
		607	LBNP Following Space Flight
		613	Endocrine Regulation Following Space Flight

(*) Included as a part of DSO 456 "Medical Tests and Measurements (STS-51D P/S)"

INVESTIGATOR	ORG CODE	DSO NUMBER	SHORT TITLE
N. Cintron, Ph.D.	SD4	450	Salivary Cortisol During Spaceflight
		453	Combined Blood Investigations
		457	Salivary Pharmacokinetics of Scop-Dex
		458*	Salivary Acetaminophen Pharmacokinetics
		464	In-flight Assessment of Renal Stone Risk Factor
		607	LBNP Following Space Flight
		610	In-flight Assessment of Renal Stone Risk
		612	Energy Utilization
		613	Endocrine Regulation Following Space Flight
P. S. Cowings, Ph.D.	ARC	442	Autogenic Feedback Training (AFT)
D. L. Eckberg, M.D.		467	Influence of Weightlessness on Baroreflex Function
V. R. Edgerton, Ph.D.		475	Muscle Biopsy
S. M. Fortney, Ph.D.	SD5	478	In-flight LBNP
		607	LBNP Following Space Flight
M. A. B. Frey, Ph.D.		479	Hyperosmotic Fluid Countermeasure
LTC. L. V. Genco		440	Crew Visual Performance Testing
A. Ginsberg, Ph.D.		408	Near Vision Acuity (Contrast Sensitivity)
P. Hackett, M.D.		470	In-flight Doppler
D. L. Harm, Ph.D.	SD5	468	Preflight Adaptation Training
		604	Visual Vestibular Integration
		605	Postural Equilibrium
B. A. Harris, Jr., M.D.	CB	477	Muscle Performance

DSOs by Investigator

(*) Included as a part of DSO 456 "Medical Tests and Measurements (STS-51D P/S)"

INVESTIGATOR	ORG CODE	DSO NUMBER	SHORT TITLE
J. C. Hayes, M.S.	SD5/KRUG	477	Muscle Performance
J. L. Homick, Ph.D.	SD	401	Predictive Tests and Countermeasures for SMS
L. D. Inners, Ph.D.	SD5/KRUG	460* 480	Total Body Water Heavy Isotope Enrichment of Galley Water
J. T. James, Ph.D.	SD4	611	Air Monitoring Instrument Evaluation
M. Jaweed, Ph.D.	SD4	606	Muscle Size and Lipids (MRI/MRS)
P. C. Johnson, Jr. , M.D.	SD	402	Cardiovascular Deconditioning Countermeasures
J. E. Keith, Ph.D.	SN	469	In-flight Radiation Dose Distribution
A. Konradi, Ph.D.	SN3	469	In-flight Radiation Dose Distribution
H. W. Lane, Ph.D.	SD4	608 612	Aerobic and Anaerobic Metabolism Energy Utilization
C. S. Leach-Huntoon, Ph.D.	SA	423 453 460* 480	Study of In-flight Fluid Changes Combined Blood Investigations Total Body Water Heavy Isotope Enrichment of Galley Water
LTC. T. H. Mader, M.D.		472	Intraocular Pressure
R. T. Meehan, M.D.		472 474	Intraocular Pressure Retinal Photography
T. P. Moore, M.D.	SD5	441* 446/461* 451*	Blood Pressure Monitoring During Reentry Leg Plethysmography Eye-Hand Coordination During SMS

DSOs by Investigator

(*) Included as a part of DSO 456 "Medical Tests and Measurements (STS-51D P/S)"

INVESTIGATOR	ORG CODE	DSO NUMBER	SHORT TITLE
D. R. Morrison, Ph.D.	SD4	413	Cell Attachment in Microgravity
		432	Carry-on Incubator/Cell Attachment in Microgravity
C. Y. Pak, Ph.D.		610	In-flight Assessment of Renal Stone Risk
W. H. Paloski, Ph.D.	SD5	605	Postural Equilibrium
D. E. Parker, Ph.D.	SD5	433/449*	Pre- and Postflight Parallel Swing
		459	Otolith Tilt-Translation Reinterpretation
D. L. Pierson, Ph.D.	SD4	409	Microbial Screening
		437	Microbial Monitoring
		611	Air Monitoring Instrument Evaluation
S. L. Pool, M.D.	SD	425	Intraocular Pressure
L. Putcha, Ph.D.	SD4	457	Salivary Pharmacokinetics of Scop-Dex
		458*	Salivary Acetaminophen Pharmacokinetics
M. F. Reschke, Ph.D.	SD5	433/449*	Pre- and Postflight Parallel Swing
		459	Otolith Tilt-Translation Reinterpretation
		468	Preflight Adaptation Training
		604	Visual Vestibular Integration
		605	Postural Equilibrium
		614	Head and Gaze Stability
D. Russo, Ph.D.	SD4	471	Particulate Matter in Shuttle Atmosphere
E. L. Shulman, M.D.	CB	414	Opthalmoscopy
S. F. Siconolfi, Ph.D.	SD5	608	Aerobic and Anaerobic Metabolism

DSOs by Investigator

(*) Included as a part of DSO 456 "Medical Tests and Measurements (STS-51D P/S)"

INVESTIGATOR	ORG CODE	DSO NUMBER	SHORT TITLE
M. C. Smith, Jr., D.V.M.		421	Animal Enclosure Module In-flight Test
G. Spaulding, Ph.D.	SD4	316	Bioreactor
H. L. Task, Ph.D.		440	Crew Visual Performance
G. R. Taylor, Ph.D.	SD5	472	Intraocular Pressure
		473	Delayed-Type Hypersensivity
		474	Retinal Photography
W. E. Thornton, M.D.	CB	403	Head and Eye Motion During Re-entry
		404	On-Orbit Head and Eye Tracking Tasks
		405	Acceleration Detection Sensitivity
		406	Kinesthetic Ability
		407	Photographic Documentation of Body Fluid Shift
		410	Audiometry
		411	Simple Mass Measurement
		412	Treadmill Operation
		415	Tissue Pressure Tonometry
		416	Ambulatory Monitoring
		417	In-flight Countermeasures for SAS
		418	Eye-Hand Coordination
		422	Anatomical Observation
		423	Study of In-flight Fluid Changes
		424	Evoked Potentials
		427	Soft Contact Lens Application
		439*	Documentation of the Action of Metoclopramide
		441*	Blood Pressure Monitoring During Re-entry
		446/461*	Leg Plethysmography
		447	Causative Agents During SMS
		451*	Eye-Hand Coordination During SMS
		454/455	Clinical Characterization of SMS
		456	Medical Tests and Measurements (STS-51D P/S)

DSOs by Investigator

(*) Included as a part of DSO 456 "Medical Tests and Measurements (STS-51D P/S)"

INVESTIGATOR	ORG CODE	DSO NUMBER	SHORT TITLE
J. M. Vanderploeg, M.D.	SB/KRUG	408 454/455 456	Near Vision Acuity (Contrast Sensitivity) Clinical Characterization of SMS Medical Tests and Measurements (STS-51D P/S)
P. A. Whitson, Ph.D.	SD4	613	Endocrine Regulation
L. R. Young, Ph.D.		427	Soft Contact Lens Application Test

(*) Included as a part of DSO 456 "Medical Tests and Measurements (STS-51D P/S)"

Note:

AC, CB, SB, SD, SD3, SD4, and SD5 are NASA JSC mail codes.
ARC = NASA Ames Research Center

DSOs by Investigator

Appendix D: STS Flight History

FLIGHT #/ VEHICLE	LAUNCH/ LANDING/ LOCATION	DURATION (DAYS)	CREWMEMBERS	PRIMARY PAYLOAD	MEDICAL DSO'S	COMMENTS
STS-1 Columbia	4-12-81 4-14-81 EAFB	2.25	John W. Young Robert L. Crippen	DFI	401 402	First Orbital Flight Test (OFT) of the Space Shuttle System.
STS-2 Columbia	11-12-81 11-14-81 EAFB	2.25	Joe H. Engle Richard H. Truly	DFI OSTA-1 ACIP	401 402	Second OFT; first test of Remote Manipulator System (RMS); mission cut to 2 days by fuel cell failure.
STS-3 Columbia	3-22-82 3-30-82 US Army, White Sands, NM	8.00	Jack Lousma C. Gordon Fullerton	DFI OSS-1 ACIP GAS EEVY MLR PDP	401 402	Third OFT; student experiments; test of hardware for electrophoresis operations (EEVT); landing site changed to Northrop Strip (White Sands, NM) due to water on lake bed at EAFB; landing delayed 1 day due to bad weather at the alternate landing site.
STS-4 Columbia	6-27-82 7-04-82 EAFB	7.04	Thomas K. Mattingly Henry Hartsfield	DFI IECM MLR NOSL CFES ACIP GAS	401 402	Final OFT; included a DOD; first flight of Continuous Flow Electrophoresis System (CFES).
STS-5 Columbia	11-11-82 11-16-82 EAFB	5.08	Vance D. Brand Robert Overmyer William Lenoir Joseph Allen	TELESAT-E SBS-C	401 405 402 406 403 408 404	First operational flight; first deployment of satellites.

FLIGHT #/ VEHICLE	LAUNCH/ LANDING/ LOCATION	DURATION (DAYS)	CREWMEMBERS	PRIMARY PAYLOAD	MEDICAL DSO'S	COMMENTS
STS-6 Challenger	4-04-83 4-09-83 EAFB	5.00	Paul J. Weitz Karol J. Bobko Donald H. Peterson F. Story Musgrave	TDRS-A CFES MLR NOSL GAS	401 406 402 407 403 408 404 409 405 410	First flight of Challenger; first Shuttle EVA (Peterson, Musgrave); TDRS failed to reach geosynchronous orbit due to UIS guidance failure.
STS-7 Challenger	6-18-83 6-24-83 EAFB	6.08	Robert L. Crippen Frederick H . Hauk Sally K. Ride John M. Fabian Norman E. Thagard	TELESAT PALAPA B-1 SPAS-01 OSTA-2 CFES	401-410 412-417	Physician crewmember (Thagard) to study SMS; use of RMS to deploy and retrieve the Shuttle Pallet Satellite (SPAS-1); EAFB landing due to bad weather wave-off at KSC.
STS-8 Challenger	8-30-83 9-05-83 EAFB	6.04	Richard H. Truly Daniel C. Brandenstein Guion S. Bluford Dale A. Gardner William E. Thornton	INSAT 1-B PFTA	401-412 414-418 421-425 427, 432 433, 441	First Shuttle night launch and landing; physician crewmember (Thornton) made use of DSO's to continue in-flight study of SMS.
STS-9 Columbia	11-28-83 12-08-83 EAFB	10.32	John W. Young Brewster H. Shaw Robert a. Parker Owen K. Garriott Byron Lichtenberg Ulf Merbold	SPACELAB 1	401 402 409	Two shifts, 24 hr/day operations; astronomy, physics, materials sciences, and biomedical research (neurovestibular, cardiovascular, hematological, immunological, and psychological adaptation to space flight); first non-US crewmember (Merbold-Germany).
STS-41B Challenger	2-03-84 2-11-84 KSC	7.97	Vance D. Brand Robert L. Gibson Bruce McCandless II Robert L. Stewart Ronald R. McNair	SPAS-01A PALAPA B-2 WESTAR-VI		First test of MMU; first KSC landing; both satellites failed to reach geosynchronous orbit due to PAM failure.

STS Flight History

FLIGHT #/ VEHICLE	LAUNCH/ LANDING/ LOCATION	DURATION (DAYS)	CREWMEMBERS	PRIMARY PAYLOAD	MEDICAL DSO'S	COMMENTS
STS-41C Challenger	4-06-84 4-13-84 EAFB	6.99	Robert L. Crippen Francis R. Scobee Terry J. Hart James D. van Hoften George D. Nelson	LDEF-1	401 402 408	Rendezvous, repair, and redeploy of Solar Max satellite; student experiment (bees); highest STS altitude to date (269 naut. miles).
STS-41D Discovery	8-30-84 9-05-84 EAFB	6.04	Henry W. Hartsfield Michael L. Coats Richard M. Mullane Stephen A. Hawley Judith A. Resnik Charles D. Walker	OAST-1 SBS-D TELSTAR 3C SYNCOM IV-1 CFES	401 402 408 439 440 441	Evaluation of the deployable solar array (OAST-1); first "frisbee" type satellite deployment (SYNCOM); first commercial payload specialist (Walker).
STS-41G Challenger	10-05-84 10-13-84 KSC	8.23	Robert L. Crippen Jon A. McBride David D. Leestma Sally K. Ride Kathryn D. Sullivan Paul D. Scully-Power Marc Garneau	OSTA-3 LFC/ORS ERBS IMAX GAS (8)	401 408 439 440 441 450	First US woman to perform an EVA (Sullivan); first 7-person crew; first US orbital fuel transfer; first Canadian crewmember (Garneau).
STS-51A Discovery	11-08-84 11-16-84 KSC	7.99	Frederick H. Hauck David M. Walker Dale A. Gardner Joseph P. Allen Anna L. Fisher	MSL-1 SYNCOM IV-2 TELESAT	401	Two EVAs for retrieval of PALAPA B-2 and WESTAR VI satellites from STS-11 launch.
STS-51C Discovery	1-24-85 1-27-85 KSC	3.06	Thomas K. Mattingly Loren J. Shriver Ellison S. Onizuka James F. Buchli Gary E. Payton	DOD	401 440 408 441 439 442	First dedicated DOD mission; test of hardware for SL-3; Autogenic Feedback Experiment (DSO 442).

STS Flight History

FLIGHT #/ VEHICLE	LAUNCH/ LANDING/ LOCATION	DURATION (DAYS)	CREWMEMBERS	PRIMARY PAYLOAD	MEDICAL DSO'S	COMMENTS
STS-51D Discovery	4-12-85 4-19-85 KSC	7.00	Karol J. Bobko Donald E. Williams M. Rhea Seddon Jeffrey A. Hoffman S. David Griggs Charles D. Walker E. J. "Jake" Garn	SYNCOM IV-3 TELESAT-I CFES	401 456	SYNCOM failed to activate after deployment; unscheduled EVA to attach "fly swatters" to RMS for attempt to trip the activation switch; American Flight Echocardiograph (AFE) provided first US heart images in-flight; US Senator Garn was payload specialist.
STS-51B Challenger	4-29-85 5-06-85 EAFB	6.96	Robert F. Overmyer Frederick D. Gregory Don L. Lind Norman E. Thagard William E. Thornton L. van den Berg Taylor G. Wang	SPACELAB 3 NUSAT GLOMR	437 451 439 453 441 462	Crystal growth and materials science experiments; auroral photography; test of Research Animal Holding Facility (failure caused contamination); test of Autogenic Feedback Training for effectiveness in combatting SMS.
STS-51G Discovery	6-17-85 6-24-85 EAFB	7.07	Daniel C. Brandenstein John O. Creighton Shannon W. Lucid John M. Fabian Steven R. Nagel Patrick Baudry Sultan S. A. Al-Saud	ARABSAT-A TELSTAR-3D SPARTAN 101/MPESS MORELOS-A	455	The French Echocardiograph Experiment (FEE) and French Posture Experiment (FPE) provided data on physiological adaptation to space flight.
STS 51-F Challenger	7-29-85 8-06-85 EAFB	7.95	C. Gordon Fullerton Roy D. Bridges F. Story Musgrave Anthony W. England Karl G. Henize Loren W. Acton John-David Bartoe	Spacelab-2	441 453	Around-the-clock astronomy studies, including extensive solar observation; blood collection for vitamin D metabolites; plant growth.

STS Flight History

FLIGHT #/ VEHICLE	LAUNCH/ LANDING/ LOCATION	DURATION (DAYS)	CREWMEMBERS	PRIMARY PAYLOAD	MEDICAL DSO'S	COMMENTS
STS 51-I Discovery	8-27-85 9-03-85 EAFB	7.10	Joe H. Engle Richard O. Covey James Van Hoften John M. Lounge William F. Fisher	SYNCOM IV-4 ASC-1 AUSSAT-1 MSL-2 CFES	455 458	Rendezvous with failed SYNCOM from mission 51-D; EVA for capture and repair redeploy.
STS 51-J Atlantis	10-03-85 10-07-85 EAFB	4.07	Karol J. Bobko Ronald J. Grabe Robert C. Stewart David C. Hilmers William A. Pailes	DOD	451 461	Second dedicated DOD mission; first flight of Atlantis.
STS 61-A Challenger	10-30-85 11-06-85 EAFB	7.00	Henry W. Hartsfield Steven R. Nagel Bonnie J. Dunbar Guion S. Bluford James F. Buckli Reinhard Furrer Wubbo Ockels Ernst Messerschmid	Spacelab D-1 GLOMR	---	First eight-person crew; first foreign dedicated Spacelab (West Germany); life sciences experiments (neurovestibular, cardiovascular, immulogical) and materials sciences.
STS 61-B Atlantis	11-26-85 12-03-85 EAFB	6.87	Brewster H. Shaw Bryan D. O'Connor Mary L. Cleave Sherwood C. Spring Jerry L. Ross Charles D. Walker Rudolfo Neri-Vela	MORELOS-B SATCOM Ku-2 AUSSAT-1 EASE/ACCESS CFES IMAX	455 457 458 461	Two EVAs for assembly of EASE and ACCESS truss structures to evaluate Space Station construction techniques.
STS 61-C Columbia	1-12-86 1-18-86 EAFB	5.09	Robert L. Gibson Charles F. Bolden Franklin Chang-Diaz George D. Nelson Steven A. Hawley Bill Nelson Robert J. Cenker	SATCOM Ku-1 MSL-2 GAS Bridge	451 461 455 462 457 463 458 464 459 465 460	U. S. Congressman (B. Nelson) payload specialist performed 10 biomedical DSOs; landing at EAFB delayed two days after bad weather wave-off at KSC.

STS Flight History

FLIGHT #/ VEHICLE	LAUNCH/ LANDING/ LOCATION	DURATION (DAYS)	CREWMEMBERS	PRIMARY PAYLOAD	MEDICAL DSO'S	COMMENTS
STS 51-L Challenger	1-28-86	---	Francis R. Scobee Michael J. Smith Judith A. Resnik Ellison S. Onizuka Ronald E. McNair Gregory Jarvis Sharon C. McAuliffe	TDRS-B SPARTAN-Halley	450 455 459	Explosion claims crew and orbiter at 73 seconds into the flight.
STS-26 Discovery	9-29-88 10-03-88 EAFB	4.04	Frederick (Rick) Hauck Richard O. Covey John M. Lounge George (Pinky) D. Nelson David C. Hilmers	TDRS-C OASIS	457 458 459 460 466	Return to flight; protein crystal growth experiment; biomedical (cardiovascular, neuro-vestibular, pharmacokinetic, and total body water).
STS-27 Atlantis	12-02-88 12-06-88 EAFB	4.38	Robert L. Gibson Guy S. Gardner Richard M. Mullane Jerry L. Ross William M. Shepherd	DOD	450 458 466 467	Pharmacokinetic studies; pre- and postflight echocardiography and baroreflex testing.
STS-29 Discovery	3-13-89 3-18-89 EAFB	4.99	Michael L. Coats John E. Blaha James P. Bagian James F. Buchli Robert C. Springer	TDRS-D; Life Sciences Experiments	457 458 462 468 470 466 467	"Chicks-in-space" student experiment; first flight for Transcranial Doppler (470).
STS-30 Atlantis	5-04-89 5-08-89 EAFB	4.04	David M. Walker Ronald J. Grabe Norman E. Thagard Mary L. Cleave Mark C. Lee	Magellan	457 462 463 466 467	First planetary probe deployed from Shuttle.

STS Flight History

FLIGHT #/ VEHICLE	LAUNCH/ LANDING/ LOCATION	DURATION (DAYS)	CREWMEMBERS	PRIMARY PAYLOAD	MEDICAL DSO'S	COMMENTS
STS-28 Columbia	8-08-89 8-13-89 EAFB	5.04	Brewster H. Shaw Richard N. Richards James C. Adamson David C. Leestma Mark N. Brown	DOD	457 469 458 466 459 467	
STS-34 Atlantis	10-18-89 10-23-89 EAFB	4.99	Donald E. Williams Michael L. McCulley Franklin Chang-Diaz Shannon Lucid Ellen S. Baker	Galileo	457 475 470 477 474 466	Jupiter probe becomes second planetary probe deployed from Shuttle.
STS-33 Discovery	11-22-89 11-27-89 EAFB	5.0	Frederick D. Gregory John E. Blaha F. Story Musgrave Manley (Sonny) Carter Kathryn C. Thornton	DOD	450 466 462 467 463 475 468 474	
STS-32 Columbia	1-09-90 1-20-90 EAFB	10.8	Daniel C. Brandenstein James D. Wetherbee Bonnie J. Dunbar G. David Low Marsha S. Ivins	SYNCOM IV-5 AFE CNCR FEA L3 MLE PCG	457 467 471 475 472 477 473 476 478 466	Retrieval of LDEF. First EDO flight is Shuttle program's longest.
STS-36 Atlantis	2-28-90 3-04-90 EAFB	4.43	John O. Creighton John H. Casper Richard M. Mullane David C. Hilmers Pierre J. Thuot	DOD	463 468 469 473 479 466	

STS Flight History

FLIGHT #/ VEHICLE	LAUNCH/ LANDING/ LOCATION	DURATION (DAYS)	CREWMEMBERS	PRIMARY PAYLOAD	MEDICAL DSO'S	COMMENTS
STS-31 Discovery	4-24-90 4-29-90 EAFB	5.06	Loren J. Shriver Charles F. Bolden Steve A. Hawley Bruce McCandless II Kathryn D. Sullivan	HST IMAX-04	462 466 469 467 472 473 479	Launch of Hubble Space Telescope.
STS-41 Discovery	10-06-90 10-10-90 EAFB	4.09	Richard N. Richards Robert D. Cabana William M Shepherd Bruce E. Melnick Thomas D. Akers	Ulysses SSBUV-02 SSCE-01 CHROMEX-02 VC-CCTV OCTW-01 SE-81-09	472 474 602 603 604 601 605	Third and final planetary probe planned on Shuttle.
STS-38 Atlantis	11-15-90 11-20-90 KSC	4.91	Richard O. Covey Frank L. Culbertson Robert C. Springer Carl J. Meade Charles D. (Sam) Gemar	DOD	473 477 613	Seventh dedicated DOD flight; Fifth night launch of STS; DFRF waveoff and bad winds second day lead to EOM at KSC.
STS-35 Columbia	12-2-90 12-10-90 EAFB	8.96	Vance D. Brand Guy S. Gardner Jeffrey A. Hoffman John M. Lounge Robert A.R. Parker Samuel T. Durrance Ronald A. Parise	ASTRO-01 BBXRT-01 SAREXII-01 AMOS-06	468 466 476 477 480 601 602 605 603 606	Sixth night launch; fourth non-daylight landing.

STS Flight History